HUNGARIAN AGRICULTURAL ENGINEERING

41/2022

MAGYAR · TUDOMÁNYOS · AKADÉMIA
1825

HUNGARIAN ACADEMY OF SCIENCES

Hungarian Agricultural Engineering

N° 41/2022

PERIODICAL OF THE COMMITTEE OF AGRICULTURAL AND BIOSYSTEM ENGINEERING OF THE HUNGARIAN ACADEMY OF SCIENCES

Published by
Hungarian University of Agriculture and Life Sciences
Institute of Technology
H-2103 Gödöllő, Páter K. u. 1.

HUNGARIAN UNIVERSITY OF AGRICULTURE AND LIFE SCIENCES
Institute of Technology

Gödöllő
2022

Published online: http://hae-journals.org
HU ISSN 0864-7410 (Print)
HU ISSN 2415-9751(Online)

PREFACE

In the name of the Committee of Agricultural and Biosystem Engineering of the Hungarian Academy of Sciences we would like to welcome everyone who is interested in reading our journal. The Hungarian Agricultural Engineering (HAE) journal was published 34 years ago for the very first time with an aim to introduce the most valuable and internationally recognized Hungarian studies about mechanisation in the field of agriculture and environmental protection.

In the year of 2014 the drafting committee decide to spread it also in electronic (on-line and DOI) edition and make it entirely international. From this year exclusively the Hungarian University of Agriculture and Life Science's Institute of Technology (former Szent István University's Faculty of Mechanical Engineering) took the responsibility to publish the paper twice a year in cooperation with the Hungarian Academy of Sciences.

Our goal is to occasionally report the most recent researches regarding mechanisation in agricultural sciences (agricultural and environmental technology and chemistry, livestock, crop production, feed and food processing, agricultural and environmental economics, energy production, engineering and management) with the help of several authors. The drafting committee has been established with the involvement of outstanding Hungarian and international researches who are recognised on international level as well. All papers are selected by our editorial board and a triple blind review process by prominent experts which process could give the highest guarantee for the best scientific quality.

We hope that our journal provides accurate information for the international scientific community and serves the aim of the Hungarian agricultural and environmental engineering research.

Gödöllő, 20.11.2022.

Dr. István SZABÓ
editor in chief

Dr. László TÓTH
editor in chief

IN MEMORIAM

Dr. Csaba Fogarassy

(3.5.1971. – 28.9.2022.)

Csaba Fogarassy PhD. born in Fehérgyarmat, graduated from the University of Agricultural Science, School of Environmental and Landscape Management in Gödöllő in 1996 in the field of Environmental Management Engineer.
He was a Full Professor and Director of Institute of Agricultural and Food Economics and Director of the Climate Change Economics Research Centre at Hungarian University of Agriculture and Life Sciences. Founding member and secretary of the Interdepartmental Committee of the Circular Economy of the Hungarian Academy of Sciences. He obtained his PhD in 2000 on the study of energy crop cultivation and then, in 2014, in the field of business management, dealing with game theory modelling of sustainability in his second PhD dissertation. He was working on the design of material and energy-saving business models for the circular economy. He has carried out numerous sectoral surveys in recent years on linear circular transformation processes. He is committed to helping develop circular economic plans for developing countries.
Csaba was obsessed with Rubik's cube and poetry, having so far published three volumes of his own poems. He also played a significant role in charity programs, being the Governor of Hungary's Lions Club in 2021/2022.

He was a Managing Editor of the Scientific Journal Hungarian Agricultural Engineering from 2012. Through his sacrificial work, with numerous publications and his tireless organisational activity, he was determining person of the Journal. We have lost a part of our personal and professional lives with him, and we have lost a person for whom research and publications was a life's work.

Csaba was both our colleague and a friend. We will never forget him!

Rest in peace!

Dr. László Tóth
Editor in Chief

Dr. László Magó
Secretary of the Editorial Board

HUNGARIAN AGRICULTURAL ENGINEERING
No 41/2022 5-10
Published online: http://hae-journals.org/
HU ISSN 0864-7410 (Print)
HU ISSN 2415-9751(Online)
DOI: 10.17676/HAE.2022.41.5
Received: 25.02.2022 - Accepted: 26.03.2022

PERIODICAL
OF THE COMMITTEE OF AGRICULTURAL AND BIOSYSTEM ENGINEERING OF THE HUNGARIAN ACADEMY OF SCIENCES
and
HUNGARIAN UNIVERSITY OF AGRICULTURE AND LIFE SCIENCES
INSTITUTE OF TECHNOLOGY

THE INFLUENCE OF STORAGE TEMPERATURE ON THE WEIGHT OF GOLDEN DELICIOUS APPLES

Author(s):
S. Kassebi [1], P. Korzenszky [2]

Affiliation:
[1] Doctoral School of Mechanical Engineering – Hungarian University of Agriculture and Life Sciences, 2100 Gödöllő, Páter Károly u. 1., Hungary;
[2] Institute of Technology – Hungarian University of Agriculture and Life Sciences, 2100 Gödöllő, Páter Károly u. 1., Hungary;

Email address:
kassebi.salma@phd.uni-mate.hu; korzenszky.peter.emod@uni-mate.hu

Abstract: The great majority of customers choose nutritious, fresh fruit with a distinct color for human ingestion. The Golden Delicious apple is a popular yellow-colored, delicate, sweetish, somewhat acidic, crisp-fleshed, juicy, fragrant, and aromatic apple. Apples, like other fruits, are stressed throughout their development and growth in the field, as well as during harvest and the postharvest environment (processing, storage, transportation). The refrigerated system enables bulk processing of food goods from harvest to market, guaranteeing that freshness and integrity are preserved for a prolonged time through precise temperature and humidity regulation. This study looked at the effects of three months of storage on the weight loss of Golden Delicious apples, both under refrigerated settings at 5±0.5°C and 82% relative humidity and in controlled ambient conditions at 25±0.5°C relative humidity and 60% relative humidity. The results showed that the weight loss in the two groups of apples was different. Apples held in cold storage lost 3.31g to 4.59g of weight; meanwhile, apples stored at room temperature lost 23.29g to 31.76g of weight.

Keywords: Golden Delicious apples, storage, weight loss, shelf life, temperature

1. Introduction

Unlike other perishable foods such as meat, fruits and vegetables are living tissues that continue to breathe and transpire even after being separated from the plant [1]. Sugars, salts, organic acids, minerals, water-soluble dyes, vitamins, and nondigestible carbohydrates are essential to fruit components of a balanced human diet [2]–[4].

Water makes around 75–90% of the total bulk of fruits. The ultimate water content of fruits and vegetables is generally determined by structural variations [5]. Substrate and water losses in the parent plant are compensated by a continuous flow of photosynthates, minerals, and water before harvest; however, these losses are not restored in the postharvest channel [6]. As a result, these foods begin to degrade and finally spoil, diminishing their shelf life and quality.

Various factors determined the percentage of deterioration, most of which are internal, such as internal tissue conditions, which can be affected by different mechanical interactions during harvest or transportation [7]. The external factors are also important, such as temperature and relative humidity during storage (RH%) [8].

The apple is among the world's most fleeting and significant fruits, primarily cultivated in temperate climates. There are around 7500 apple varieties, although only a few are famous worldwide. Golden Delicious is a popular variety that is grown throughout the world. It is a significant crop with an annual production of 83 million tonnes [9]. Apples are one of the most consumed fruits in Europe. In 2021, the apple production in Europe was 11.735,000 T. Golden Delicious production was 2.120.000 T. Apple is one of the main fruits available in Hungary for fresh consumption and postharvest storage. In 2021 the total production of apples was 520.000 T, for Golden Delicious was 50.000 T [10]. Only a small percentage of apples are consumed right after harvesting, and consumers must conserve a significant part of them for a long time to ensure their preservation for future consumption [11].

Apple seems like one of those fruits for which the quality degrades fast over time while storing, resulting in a wide range of customer satisfaction. Consumers dislike fruits that are low in weight, colourless, and withered [12]. Apples are collected and processed in late summer and fall; however, they are readily accessible pretty much all season.

The most significant environmental element impacting the degradation of harvested and stored fruit is temperature [13]. The temperature has a considerable impact on how other internal and external variables influence the fruit and its shelf life [14]. As a result, it is essential to maintain constant control over this component [15]. While lower storage temperatures might cause cold damage, higher temperatures can significantly decrease the product's shelf life. Many studies have been carried out to investigate the effect of storage temperature on fruit quality and shelf life [16]–[20]. The results show that temperature has a substantial impact on postharvest fruit quality.

Cold storage is the foundation for preserving fruit quality over long periods [21]. Using cold storage helps to reduce the respiration rate of fruits and vegetables and extends the shelf life. Previously, people generally consumed fruits completely at their production site; but, technological improvements in postharvest and commercialization technology have permitted shipping fruits to be sent to distant locations and consumed within a few to several days of collection. This approach emphasizes the need to retain natural characteristics and freshness from farm to remote customer.

The objective of this study was to determine the effects of storage temperature on the postharvest weight change of apple (Golden Delicious) fruit, which is an essential aspect of quality conditions.

2. Materials and Methods

Apple fruit "Golden Delicious" were collected directly from the same farm, "Kecskemét," located in Hungary. The fruit sample average weight was 160 ±60 g.

Apples have been subjected to a screening and selection operation to remove any damaged fruit. Samples were divided into two groups; each one was composed of 12 apples with identification: the first group, named AO: Apple Outside cold storage, was stored in the laboratory at an ambient environment (T_o=25±0.5°C, with the relative humidity of φ=60RH%). The second group was placed in a cold storage refrigerator. The storage temperature was set at T_i=5±0.5°C with relative humidity of 82 %, and the identification was AI: Apples Inside cold storage.

The following materials were used to experiment: Cold storage room' FRIGOR-BOX' with nominal 3.7m^3 capacity and a precision scale type KERN PCB (3500±0.01g). (Figure 1)

Figure 1. KERN PCB-type laboratory balance for measuring weight loss

All apples were weighed before, during, and after the storage period in 3 replicates. The same samples were evaluated for weight loss once a week for 3 months.

Weight loss (Δm) was determined as follows: $\Delta m = m_0 - m_i$ [g], where m_0 indicates the initial fruit weight [g] at harvest and mi shows the fruit weight [g] during storage. Weight loss was calculated by the difference in the weight before and after storage, results given in gram. The measurements were performed in the Food Technology Laboratory at the Hungarian University of Agriculture and Life Sciences. Weight measurement was performed 3 times on each apple. We calculated the mathematical average of the results. For the average data of each week, we used a linear regression function to look for trends. The difference between the equations shows the clear distinction between the two processes.

3. Results and Discussion

The Golden Delicious apples used in the experiment were kept at room temperature, and we tracked weight loss week by week. The highest measured weight of the apples at the start was between 138 and 220g using a calibrated scale.

The 12 apples of various weights were weighed and averaged in triplicate once a week. The results are presented in the figure. The effect of storage at room temperature on apple weight loss during 3 months is shown in Figure 2.

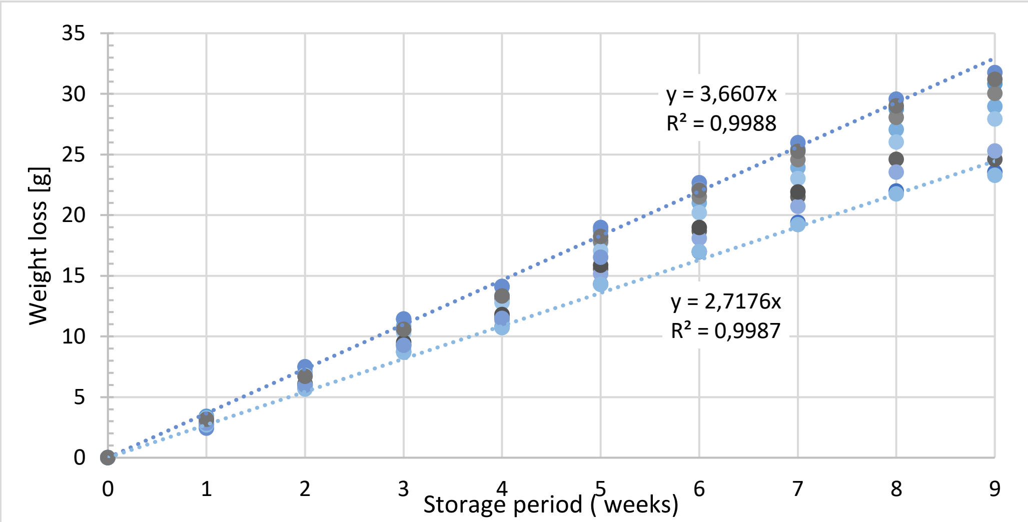

Figure 2. Weight loss of apples stored at ambient temperature during 3 months

As a result of this study, a trend line was fitted to the average price of the measurements over 9 weeks. The linear trend line with a coefficient of determination R^2= 0.99 faithfully, explained the variation in weight loss of the apples during storage.

The weight loss of apples varied between 23.29 g and 31.76g (Table 1). The mass of the fruit declined continuously. The first apple that began to shrink and perish was in week 6.

The other group of apples included in the experiment was stored in a refrigerated chamber for 3 months. (Ti=5±0.5°C; φ=82RH%). The measured weight of the apples at the start was between 135±1 and 187±1 g using a calibrated scale.

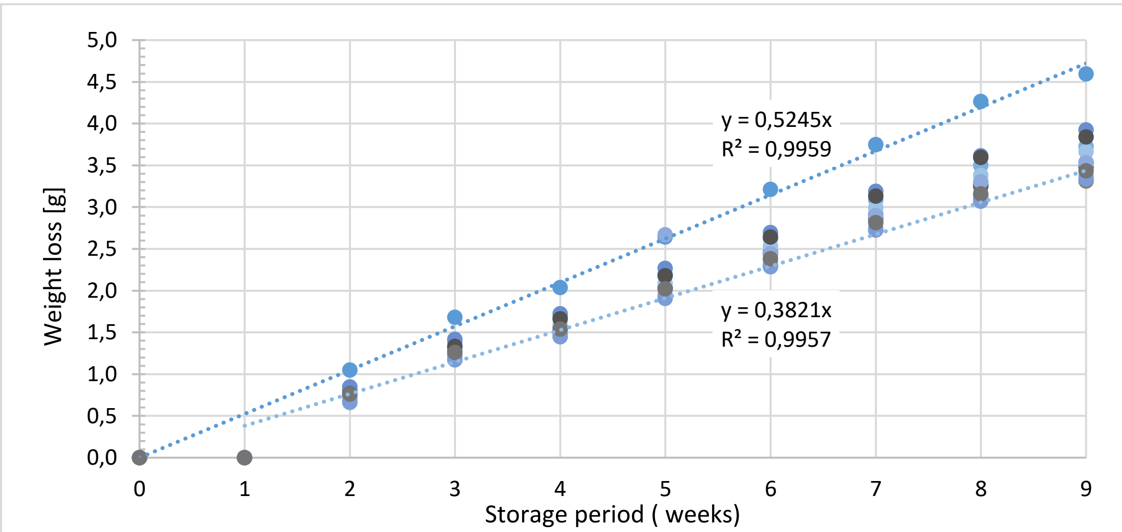

Figure 3. Weight loss of apples stored at 5±0.5°C during 3 months

The results shown in Figure 3 revealed that the mass of apples decreased between 3.31g and 4.59g after 9 weeks under cold storage. The variation in weight loss of the apples stored at 5±0.5 °C was faithfully explained by the linear trend line with a coefficient of determination R^2= 0.98.

The study showed that low-temperature treatment significantly inhibited the increase of weight loss, and 5±0.5 °C storage was best to the extent of the shelf life and inhibited weight loss of Golden Delicious apple.

The weight of the fruit reduced with time at both ambient and cold storage conditions. When compared to room temperature storage, cold storage exhibited significantly less change. (Table (1)).

Table1. The measured Weight loss of apples stored at 5±0.5°C and 25±0.5°C weekly

Apples stored at 25 ±0.5°C	**AO.1**	**AO.2**	**AO.3**	**AO.4**	**AO.5**	**AO.6**	**AO.7**	**AO.8**	**AO.9**	**AO.10**	**AO.11**	**AO.12**
Week 0	0	0	0	0	0	0	0	0	0	0	0	0
Week 1	3.41	2.68	2.76	3.29	2.43	3.10	3.24	2.78	2.90	2.69	2.85	3.18
Week 2	7.46	5.73	6.00	7.04	7.50	6.66	6.78	5.93	6.11	5.65	5.97	6.71
Week 3	11.43	8.75	9.28	10.84	11.44	10.51	10.31	9.16	9.50	8.69	9.27	10.59
Week 4	14.08	10.77	11.53	13.36	14.13	13.13	12.78	11.32	11.79	10.72	11.48	13.34
Week 5	18.71	14.30	15.57	17.73	18.97	17.88	17.06	15.16	15.85	14.29	16.51	18.25
Week 6	22.22	16.96	18.68	21.00	22.67	21.50	20.20	18.09	18.99	17.00	22.12	22.05
Week 7	25.42	19.40	21.50	23.92	25.96	24.57	23.02	20.72	21.90	19.22	rotten	25.27
Week 8	28.73	21.99	24.59	27.05	29.57	28.06	26.02	23.53	rotten	21.75	rotten	29.01
Week 9	30.83	23.55	24.59	28.94	**31.76**	30.04	27.94	25.29	rotten	**23.29**	rotten	31.19
Apples stored at 5±0.5°C	**AI.1**	**AI.2**	**AI.3**	**AI.4**	**AI.5**	**AI.6**	**AI.7**	**AI.8**	**AI.9**	**AI.10**	**AI.11**	**AI.12**
Week 1	0	0	0	0	0	0	0	0	0	0	0	0
Week 2	1.05	0.77	0.81	0.85	0.85	0.74	0.76	0.70	0.77	0.66	0.67	0.76
Week 3	1.68	1.28	1.30	1.39	1.42	1.22	1.29	1.22	1.33	1.17	1.17	1.26
Week 4	2.04	1.56	1.58	1.70	1.72	1.49	1.59	1.52	1.66	1.45	1.45	1.54
Week 5	2.64	2.03	2.03	2.19	2.27	1.94	2.09	2.67	2.18	1.93	1.91	2.02
Week 6	3.21	2.46	2.43	2.62	2.70	2.30	2.53	2.44	2.64	2.33	2.29	2.38
Week 7	3.75	2.91	2.86	3.09	3.19	2.73	2.99	2.90	3.13	2.75	2.73	2.81
Week 8	4.27	3.27	3.25	3.50	3.61	3.11	3.38	3.30	3.60	3.13	3.07	3.16
Week 9	**4.59**	3.53	3.48	3.72	3.92	**3.31**	3.66	3.53	3.84	3.37	3.34	3.43

Apples held in cold storage lost between 3.31g and 4.59g of weight; meanwhile, apples stored at room temperature lost between 23.29 g and 31.76g of weight.

Storage at the two different temperatures significantly impacted the weight of the fruit. Fruit that has lost weight generally appears shrivelled and unappealing. There were significant alterations in the weight loss of apples placed at ambient temperature.

4. Conclusions

When picked at its height of ripeness, the fruit is a tasty, healthy, and colourful part of the daily diet, as it is generally attractive and very healthy, however, an apple continues to live and breathe even after being picked, which led to quality changes. Although it is impossible to stop respiration completely, postharvest cooling aims to slow down the process and thus increase shelf life.

This paper studied the changes in weight loss of Golden Delicious apple fruits during storage at room temperature and cold storage. The weight loss of cold-stored samples was inhibited, indicating that the internal transpiration of the apples mainly influenced the weight loss.

Fruits respond to postharvest conditions with desirable changes if proper protocols are applied, but otherwise, they may develop negative and unacceptable characteristics due to physiological disorders. In further studies, we will investigate the effect of different storage conditions on the variation of measurable parameters of fruit.

Acknowledgement

The study was supported by the Stipendium Hungaricum Program and the Doctoral School of Mechanical Engineering, The Hungarian University of Agriculture and Life Sciences, Gödöllő, Hungary.

References

[1] **Zhang, W., Jiang, H., Cao, J., Jiang, W.** (2021). Advances in biochemical mechanisms and control technologies to treat chilling injury in postharvest fruits and vegetables. *Trends in Food Science and Technology*, vol. 113, p. 355-365, doi: 10.1016/j.tifs.2021.05.009.

[2] **Anklam, E., Belitz, H.-D., Grosch, W., Schieberle P.** (2005). Food Chemistry. *Third Edition, Analytical and Bioanalytical Chemistry*, vol. 382, no. 1, p. 10–11, May 2005, doi: 10.1007/s00216-004-3036-9.

[3] **Rickman, J. C., Barrett, D. M., Bruhn, C. M.** (2007). Nutritional comparison of fresh, frozen and canned fruits and vegetables. Part 1. Vitamins C and B and phenolic compounds. *Journal of the Science of Food and Agriculture*, vol. 87, no. 6, p. 930–944, doi: 10.1002/jsfa.2825.

[4] **Pajk, T., Rezar, V., Levart, A., Salobir , J**. (2006) .Efficiency of apples, strawberries, and tomatoes for reduction of oxidative stress in pigs as a model for humans. *Nutrition* ,vol. 22, p. 376–84, doi: 10.1016/j.nut.2005.08.010.

[5] **Vicente, A. R., Manganaris, G. A., Sozzi, G. O., Crisosto, C. H.** (2009). Nutritional quality of fruits and vegetables. Postharvest Handling. *A Systems Approach, Elsevier Academic Press, Cambridge, MA, USA, 2nd edition*. doi: 10.13140/2.1.3302.4960.

[6] **Paul, D. R., Clarke, R.**(2002). Modeling of modified atmosphere packaging based on designs with a membrane and perforations. *Journal of Membrane Science*, vol. 208, p. 269–283, doi: 10.1016/S0376-7388(02)00303-4.

[7] **Farkas, Cs., Fenyvesi, L., Petróczki, K.** (2019). Multiple linear regression model of Golden apple's failure characteristics under repeated compressive load. *Potravinarstvo Slovak Journal of Food Sciences*, vol. 13, no. 1, Art. no. 1, doi: 10.5219/1168.

[8] **Hussen, A.** (2021). Impact of temperature and relative humidity in quality and shelf life of mango fruit. *International Journal of Horticulture and Food Science*, vol.3(1), p. 46-50

[9] "FAOSTAT." https://www.fao.org/faostat/en/#home (accessed Feb. 28, 2022).

[10] "WAPA - The World Apple and Pear Association." http://www.wapa-association.org/asp/index.asp (accessed Mar. 11, 2022).

[11] **Kovač, A., Skendrović Babojelić, M., Pavičić, N., Voća, S., Voća, N., Dobričević, N., Jagatić, A.M., Šindrak, Z.** (2010). Influence of harvest time and storage duration on '"Cripps Pink"' apple cultivar (Malus × domestica Borkh) quality parameters. *Ciencia y Tecnologia Alimentaria*, vol. 8, p. 1–6.

[12] **Opara, U. L., Pathare, P. B.** (2014). Bruise damage measurement and analysis of fresh horticultural produce—A review. *Postharvest Biology and Technology*, vol. 91, p. 9–24, doi:10.1016/j.postharvbio.2013.12.009.

[13] **Ghabour, R., Kassebi, S., Korzenszky, P.** (2021). Simulation and experiment of apple fruits in domestic fridge. *Hungarian Agricultural Research*. vol. 30, p. 11.

[14] **Khorshidi, J.** (2019). Storage temperature effects on the postharvest quality of apple (Malus domestica Borkh. cv. Red Delicious). *New York Science Journal*, Vol.3(3), p.67-70.

[15] **Lee, S. K., Kader, A. A.** (2000). Preharvest and postharvest factors influencing vitamin C content of horticultural crops. *Postharvest Biology and Technology*, vol. 20, no. 3, p. 207–220, doi: 10.1016/S0925-5214(00)00133-2.

[16] **Biolatto, A., Vazquez, D. E., Sancho, A. M., Carduza, F. J., Pensel**, **N. A.** (2005). Effect of commercial conditioning and cold quarantine storage treatments on fruit quality of 'Rouge La Toma' grapefruit (Citrus paradisi Macf.). *Postharvest Biology and Technology*, vol. 35, no. 2, p. 167–176, doi: 10.1016/j.postharvbio.2004.08.002.

[17] **Marcilla, A., Zarzo, M., Río**,**M. A.** (2006). Effect of storage temperature on the flavour of citrus fruit. *Spanish Journal of Agricultural Research*, vol. 4, p. 336, doi: 10.5424/sjar/2006044-210.

[18] **Tembo, L., Chiteka, Z., Kadzere, I., Akinnifesi, F., Tagwira, F.** (2008). Storage temperature affects fruit quality attributes of Ber (Ziziphus mauritiana Lamk.) in Zimbabwe. *African Journal of Biotechnology*, vol. 7, p. 3092–3099.

[19] **Militaru, M., Butac, M., Cristian, P., Costinel, B. L., Cosmina, S.** (2016). Influența duratei de păstrare asupra calității merelor influence of storage duration on apple fruit quality. *Fruit Growing Research*, Vol. XXXII, p. 7.

[20] **Jan, I., Rab, A.** (2012). Influence of storage duration on physico-chemical changes in fruit of apple cultivars. *Journal of Animal and Plant Sciences*, vol. 22, p. 708–714.

[21] **Kassebi, S., Korzenszky, P.** (2021). The effect of post-harvest storage on the weight of Golden Delicious apples. *Science, Technology and Innovation*, vol. 13, p. 7–11, doi: 10.5604/01.3001.0015.5265.

HUNGARIAN AGRICULTURAL ENGINEERING
No 41/2022 11-16
Published online: http://hae-journals.org/
HU ISSN 0864-7410 (Print)
HU ISSN 2415-9751(Online)
DOI: 10.17676/HAE.2022.41.11
Received: 11.04.2022 - Accepted: 10.05.2022

PERIODICAL
OF THE COMMITTEE OF AGRICULTURAL AND BIOSYSTEM ENGINEERING OF THE HUNGARIAN ACADEMY OF SCIENCES
and
HUNGARIAN UNIVERSITY OF AGRICULTURE AND LIFE SCIENCES
INSTITUTE OF TECHNOLOGY

HUNGARIAN UNIVERSITY OF AGRICULTURE AND LIFE SCIENCES
Institute of Technology

CIRCULAR CHARACTERISTICS OF ORGANIC FOOD CONSUMPTION, NEW CONSUMPTION TRENDS IN HUNGARY

Author(s):
Cs. Fogarassy[1], E. Berecz[1]

Affiliation:
[1] Institute of Agriculture and Food Economics - Hungarian University of Agriculture and Life Sciences, 2100 Gödöllő, Páter Károly u. 1., Hungary;

Email address:
fogarassy.csaba@uni-mate.hu; edina.s.berecz@gmail.com

Abstract: Consumers have an important role to play in the transition to a circular economy by making more sustainable decisions and further supporting the functioning of value groups through their consumer choices. To this end, it is necessary to promote circular and sustainable policies and practices that can lead to the emergence of demonstration initiatives. From the theory of the circular economy and the sustainability literature, 10 groups of factors can be identified that can influence the acceptance of circular products and services for consumers. None of the aspects were specifically related to the consumption and recycling of organic food. Food supply systems are identified as a potential area for the implementation of circular concepts; however, these concepts focus mainly on food production and the recycling of surplus food. Current circular solutions place less emphasis on food-related consumption, separating it from production or waste streams. In the next study, we would like to demonstrate that consumption trends have surprisingly overlapped in recent years (during Covid), resulting in a generational change in the consumption of organic food. And the clear driving force of this change is circular thinking and gaining preferences.

Keywords: organic food, food consumption, circular economy, food supply, consumer behaviour

1. Introduction

Due to climate change and the need for an environmentally sustainable production system, circular economic characteristics have come to the fore in a number of studies. However, moving towards a circular value chain poses a lot of challenges for market participants. However, it is also undisputed that an analysis of consumer behaviour is essential because, without their commitment, circular systems do not work properly. In this paper, we examine the circular characteristics of the consumption habits of Hungarian consumers related to food purchases. Factor and cluster analysis was used for market segmentation. Our research question was as follows: "Is there a consumer segment in the Hungarian organic food market for which the use of circular economic solutions can be encouraged by marketing or state regulatory means?" According to our hypothesis, consumer segments are well defined and separable, so increased participation in the Hungarian circular value chain can be facilitated by business models. We believe that highly educated young people who are very conscious food consumers and have high incomes may have a good chance of future innovations in the circular innovations, healthy food production. These young consumers tend to buy organic food, are confident internet and software users, live in cities, and follow a healthy lifestyle. In the future, finding the right marketing tools to integrate consumers more effectively and build commitment to sustainable, circular systems is a key challenge. Gathering from various databases and continuously analyzing consumer feedback can be a huge step towards increasing sustainable consumption and avoiding food waste. The significance of our study is that we have found a dynamically growing consumer group that strongly expresses its acceptance of circular economic values and can thus be a target group for policies that integrate circular systems.

It should be emphasized that more and more studies have recently been carried out highlighting the importance of consumers and the nature of consumption in the further development of circular solutions. Consumers may also play different roles in circular systems, may be conscious buyers, sellers, distributors, storages, enhancers, collaborators, and may also act as waste disposers [1]. Some authors have pointed out that the active participation of consumers in achieving circular goals is at odds with current trends, which are characterized by a complete lack of consumer awareness [2]. There are researchers who suggest conducting analytical studies of the types of individuals or groups that are more likely to accept circular solutions [3] and examining policy strategies that influence acceptance in the context of them [4, 5]. This would make it possible to identify potential target groups among the relevant consumers. In order to identify groups with a commitment to circular principles, markets should be differentiated based on circular conceptual considerations, but we do not currently have adequate data for this [6; 7]. Therefore, researchers should use other indicators for their analysis.

These include the zero-kilometer food indicator (for locally produced, sold and consumed food), organic farming indicators, 'small amount of food and drink' followers who do not want to be obese) and confidence /confidence index are important aspects in a circular system [8]. The activities of target groups can be triggered by a combination of certain motives and characteristics of more sustainable products and services [9]. It is also a challenge for policies to initiate a change in consumption patterns, as many people believe that their food choices are a private matter and any government recommendations violate freedom of choice. Related to this is an interesting question about the role that the media can play in creating the conditions for the transition to a circular economy [10]. Many consumers are unaware of the whole food chain, the various actors involved and the moral implications of their decisions. The consumer environment in which people make routine decisions today does not support more sustainable consumption habits [11]. Research shows that young adults are primarily concerned with shopping and the environmentally friendly conditions of purchase, and are less interested in the process of sustainable use and disposal. The main obstacles in this process are the lack of information and the lack of knowledge and skills [12]. Other studies have shown that consumption patterns differ greatly in terms of gender, age, and income [13]. In addition, the results of some studies show that the sustainable consumption behaviour of young adults is less different than that of older adults. Regarding food consumption, when young adults (14-17 years old) buy food on their own, they want cheap and tasty products without considering the composition or the manufacturer. Some people prefer organic foods, but primarily for their own health rather than for ecological or environmental reasons [14]. Other research shows that young adults are in virtually constant contact with each other and actively communicate through social media. In doing so, they are basically able to find the missing information about healthy or harmful products, social work conditions, or waste management programs, and they can also share this information [15]. Regarding sustainable consumer behaviour, the results show that there were no significant differences in age, gender, and financial expenditures. In addition, eating habits are related to people's value orientation, emotions, personal and collective identity, traditions, and eating culture [16]. For example, meat consumption is also associated with certain masculinity and ethnicity [17].

2. Local practice vs. sustainable production

Consumers of organic products tend to accept circular economic values because the main motivations for consuming organic food in many countries are considerations of positive health effects, environmental protection, and animal welfare [18; 19; 20; 21; 22; 23]. Circular solutions require consumers to integrate new products, reuse existing infrastructures, or register in a completely different way, such as by introducing consumer service systems [24; 25;]. This will make it easier to involve consumers who are open and ready to apply innovative solutions. In organic farming, there are various innovative sourcing systems and direct sales forms that are used by an increasing number of consumers. Community purchasing groups and community-supported agricultural production are also operating successfully in different countries. It is clear to everyone that there are many opportunities to use sustainable assets in short supply chains if they meet specific economic, environmental and social conditions. However, Born and Purcell (2006) [26] emphasize the need to avoid 'local traps', which means that local systems should not automatically be declared 'good practice', as 'local food' is not always the same as 'sustainable food' [27]. Circular economic models are based on the prudent and balanced use of resources to reduce environmental burdens. This requires strong support from producers and a shift in consumers' food purchasing habits towards sustainability. Examples include the use of a low-carbon footprint, the promotion of zero-kilometer products, and conscious action to avoid food waste and reduce waste (food banking system). The potential positive effects of short supply chains on the circular economy and sustainability goals can be achieved by supporting local food and smallholders. This could lead to a significant reduction in waste and, among other things, to greater trust between producers and consumers.

3. Consumer trust and product labelling

Controlling production, the production of the product and its unquestionable confidence in its intrinsic value have long been central to the sale of organic products. In the case of indirect purchases through commercial partners and sales networks, consumers can only find out about the content value and place of origin of the product through the trademarks placed on the product. The display of this information is a mandatory element of the marketing of the product, but how reliable is this information for imported goods? Central to this is the practice of certification by certification bodies around the world and the presence of information to help consumers make a purchase! Whether healthy food is really healthy, or many claim it is based on the usual scheme, is "the same as traditional, only sprayed at night," so they don't even think about buying organic products, and it doesn't really matter what price they offer!

In this connection, it should be mentioned that, according to Csíkné (2014) [28], the most important influencing factors in the purchase of food for the average Hungarian consumer are price, freshness, food safety and choice. He found that the least influential factors were direct personal contact with farmers, knowledge of production methods and the reduction of pollution. In Hungary, organic production is very export-oriented: the majority (90-95%) of the main products (eg. maize, sunflower seeds, wheat, pumpkin seeds, rye, animal products) go abroad unprocessed. Organic food of Hungarian origin rarely appears in the retail trade, consumers can only buy imported products, sometimes of lower quality. In the organic market, there are problems on both the demand and supply side, products are marketed that are not needed and some desired products are missing [29].

Hungarian organic food stores focus mainly on vegan foods, and only a few of them deal with meat products, although this may be more appropriate for traditional eating habits [30]. Knowledge of the demand and supply characteristics of the market is contrary to the principle of a circular economy, ie. suppliers need to know demand and customers need to know reliable suppliers. This fact also underscores the role of a well-functioning label. A well-functioning label or trademark can build trust in the marketing of organic food. The results of a Chinese survey have shown that the information provided on the label of organic food plays a key role in encouraging consumers to turn to organic food with confidence [31]. Rácz (2013) [32] found that in many cases Hungarian consumers are unfamiliar with the objective meaning of food labels. This uncertainty can be caused by the number of labels, so consumers are unable to gather extensive information before making a purchase decision due to the lack of uniform sustainability labels and the use of several label formats [32]. The various domestic promotional campaigns, as well as the labelling of foods that are produced in Hungary or contain raw materials produced in Hungary, have been operating for years. However, the special marketing program for organic food produced in Hungary and the related labelling system do not work at all. The research question related to the above is how fast will the relationship system of traditional organic food consumption change in the near future?

4. Materials and Methods

The research related to the eco-market trends was conducted in February 2018, in the largest Hungarian organic farming market (Bioculture Ecoparket). After conducting five consumer test surveys, we evaluated the questionnaire and further developed it based on common expert suggestions. Interviewees had the opportunity to judge specific questions. We used the aspects discussed in the literature review from the survey to determine what circular values are available to Hungarian consumers. The focus of the survey was on the relationship between consumers and producers, consumer health awareness and the use of direct sales channels, which contribute to the development of producer-consumer interactions (loops), ie a structure that supports circular operation. There has been no similar study on the product lines of the Hungarian food industry so far, so we can analyze the current situation primarily from the consumer's point of view.

5. Results

The circular economy, which we refer to today as synonymous with sustainability, cannot function without commitment. Appropriate characteristics of consumer behaviour and attitudes are essential. Based on four clusters, in our survey we can distinguish two clusters, special groups, from the 1st youth (21–30 years) cluster and the 2nd mature adults (41–65 years) cluster, in which the opinions of the stakeholders are in line with the characteristic values of the circular economy (Figure 1.). Summarizing the characteristics of the different clusters, we can state that the members of clusters 1 and 2 think mainly in the local dimension, their attitude is the most appropriate for the circular economic values. Direct contacts with product chain actors are most preferred. Cluster 1 in particular is noteworthy for this study. Highly educated, young people who are very conscious consumers with good income conditions. They usually buy organic food and live in a big city. Finding the right marketing tools in the future to integrate into consumption systems and be committed to the concept of cyclical development can be a very important challenge in the future. for the introduction of circular systems. The amount of food wasted is significantly lower for more expensive and better quality foods than the linear (global) or traditional produce-consume-discard model.

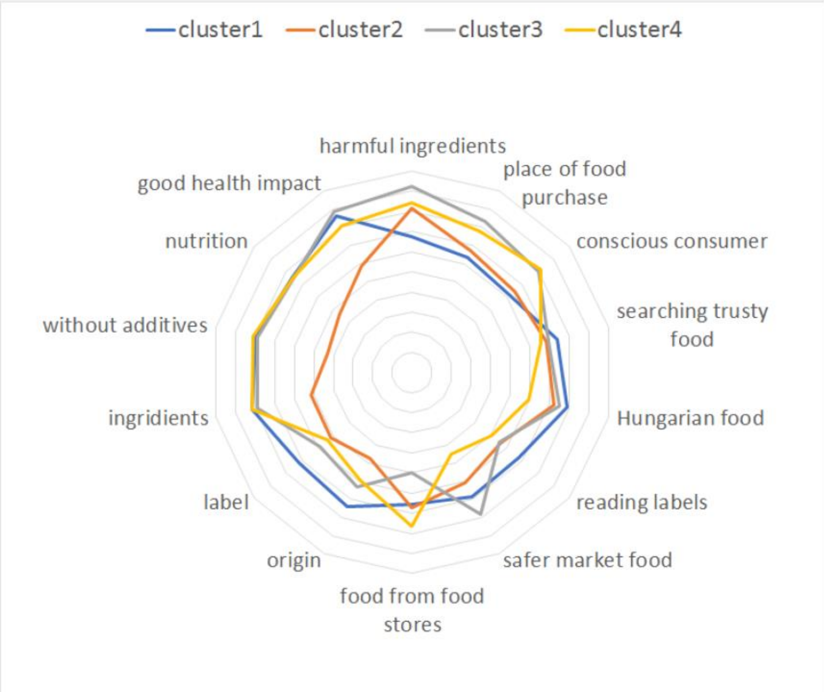

Figure 1. Images of each cluster (cluster 1, cluster 2, cluster 3, cluster 4)

Food waste can be significantly reduced by creating loops / cycles in a locally operated organic farm. The characteristics and speed of the process depend on consumer decisions, the basic building blocks of circular systems, such as the sharing of databases, the latest information available to all, the introduction of short supply chains, accurate and detailed knowledge of market players, and the customization of consumption. in consumer communities are more or less already known. However, the introduction of circular business models is still in a very early stage in the value creation processes of organic food. Current research findings may provide a starting point for future surveys and studies where we can make effective use of the experience gained. It would be interesting to get an accurate answer to the question of whether consumers of organic food can be committed to circular technologies and methods or clearly reject new, innovative, digital and value-based food supply systems. Trends show that the main consumers of organic food are changing significantly (younger and higher-income consumers may take the lead in the coming years) and the volume of consumption may increase significantly as a result of digitalisation. Our research has also found that the 41-65 age group, which today plays the most significant role in the consumption of organic and premium foods, is much more inflexible in the use of key elements of the circular value chain. The demand for local food is not as strong in them as it is for the conscious younger (and more digital) generation. The results of the research mainly show that a group of consumers with high incomes and relatively little information (mainly in the 21-30 age group) has appeared on the market of organic products.

6. Discussion and Conclusions

The circular economy, which we refer to today as synonymous with sustainability, cannot function without commitment. Appropriate characteristics of consumer behaviour and attitudes are essential. Based on our survey, we can distinguish two clusters, the cluster of young people (aged 21–30 years) and the cluster of mature adults (aged 41–65 years), in which the opinions of the stakeholders are in line with the typical values of the circular economy. Summarizing the characteristics of the different clusters, we can state that the members of clusters 1 and 2 think mainly in the local dimension, their attitude is the most appropriate for the circular economic values. Direct contacts with product chain actors are most preferred. Cluster 1 in particular is noteworthy for this study. Highly educated, young people who are very conscious consumers with good income conditions. They usually buy organic food and live in a big city. Finding the right marketing tools to integrate into consumption systems and be committed to the concept of cyclical development can be a very important challenge in the future. Together with other authors, I believe that clarifying the link between food consumption and food waste is a key area for the introduction of circular systems. The amount of food wasted is significantly lower for more expensive and higher quality foods than for the linear (global) or traditional product-discard model.

Food waste can be significantly reduced by creating loops / circuits in the locally operated bioeconomy. The characteristics and speed of the process depend on consumer decisions, the basic building blocks of circular systems, such as the sharing of databases, the latest information available to all, the introduction of short supply chains, accurate and detailed knowledge of market players, and the customization of consumption process in consumer communities is more or less already known. However, the introduction of circular business models is still in a very early stage in the value creation processes of organic food. Current research findings may provide a starting point for future surveys and studies where we can make effective use of the experience gained. It would be interesting to get an accurate answer to the question of whether consumers of organic food can be committed to circular technologies and methods or clearly reject new, innovative, digital and value-based food supply systems. Trends show that the main consumers of organic food are changing significantly (younger and higher-income consumers may take the lead in the coming years) and that the volume of consumption may increase significantly as a result of digitalisation.

Acknowledgement

Special thanks to the National Research, Development and Innovation Office – NKFIH (Program ID: OTKA 131925).

References

[1] **Maitre-Ekern, E. & Dalhammar, C.** (2019). Towards a hierarchy of consumption behaviour in the circular economy. Maastricht Journal of European and Comparative Law, 26, 394–420.

[2] **Kirchherr, J., Piscicelli, L., Bour, R., Kostense-Smit, E., Muller, J., Huibrechtse-Truijens, A. & Hekkert, M.** (2018). Barriers to the Circular Economy: Evidence From the European Union (EU). Ecological Economics, 150, 264–272.

[3] **Catulli, M., Lindley, J., Reed, N., Green, A., Kiri, S.P. & Hyseni, H.** (2013). What is Mine is NOT Yours: Further insight on what access-based consumption says about consumers. Consum. Cult. Theory 2013, 15, 185–208.

[4] **Mugge, R., Jockin, B. & Bocken, N.** (2017). How to sell refurbished smartphones? An investigation of different customer groups and appropriate incentives. Journal of Cleaner Production, 147, 284–296.

[5] **Hazen, B.T., Mollenkopf, D.A. & Wang, Y.** (2017). Remanufacturing for the Circular Economy: An Examination of Consumer Switching Behavior. Business Strategy and the Environment, 26, 451–464.

[6] **Sijtsema, S.J., Snoek, H.M., Van Haaster-de Winter, M.A. & Dagevos, H.** (2020). Let’s Talk about Circular Economy: A Qualitative Exploration of Consumer Perceptions. Sustainability, 12, 286.

[7] **Meemken, E.-M. & Qaim, M.** (2018) Organic Agriculture, Food Security, and the Environment. Annual Review of Resource Economics, 10, 39–63.

[8] **Kiss, K.. Ruszkai, C. & Takács-György, K.** (2019). Examination of Short Supply Chains Based on Circular Economy and Sustainability Aspects. Resources, 8, 161.

[9] **Xu, J., Deng, Y. & Yao, L.** (2014). Sustainable development-oriented industrial restructuring modeling and analysis: A case study in Leshan. Clean Technologies and Environmental Policy, 16, 267–279.

[10] **Camacho-Otero, J., Boks, C. & Pettersen, I.N.** (2018). Consumption in the Circular Economy: A Literature Review. Sustainability, 10, 2758.

[11] **Popp, J., Oláh, J., Kiss, A., Temesi, A., Fogarassy, C. & Lakner, Z.** (2019). The socioeconomic force field of the creation of short food supply chains in Europe. Journal of Food and Nutrition Research, 58, 31–41.

[12] **Kreuzer, C., Weber, S., Off, M., Hackenberg, T. & Birk, C.** (2019). Shedding Light on Realized

Sustainable Consumption Behavior and Perceived Barriers of Young Adults for Creating Stimulating Teaching–Learning Situations. Sustainability, 11, 2587.

[13] **Pinto, D.C., Herter, M.M., Rossi, P. & Borges, A.** (2014). Going green for self or for others? Gender and identity salience effects on sustainable consumption. International Journal of Consumer Studies, 38, 540–549.

[14] **Fischer, D., Böhme, T. & Geiger, S.M.** (2017). Measuring young consumers' sustainable consumption behavior: Development and validation of the YCSCB sca-le. Young Consum. 2017, 18, 312–326.

[15] **Kanchanapibul, M., Lacka, E., Wang, X. & Chan, H.K.** (2014). An empirical investigation of green purchase behaviour among the young generation. Journal of Cleaner Production, 66, 528–536.

[16] **Nagy-Pércsi, K. & Fogarassy, C.** (2019). Important Influencing and Decision Factors in Organic Food Purchasing in Hungary. Sustainability, 11, 6075.

[17] **Schösler, H., De Boer, J. & Boersema, J.J.** (2012). Can we cut out the meat of the dish? Constructing consumer-oriented pathways towards meat substitution. Appetite 2012, 58, 39–47.

[18] **Oroian, C.F., Safirescu, C.O., Harun, R., Chiciudean, G.O., Arion, F.H., Muresan, I.C. & Bordeanu, B.M.** (2017). Consumers' Attitudes towards Organic Products and Sustainable Development: A Case Study of Romania. Sustainability, 9, 1559.

[19] **Popa, I.D. & Dabija, D.C.** (2019). Developing the Romanian Organic Market: A Producer's Perspective. Sustainability, 11, 467.

[20] **Akhondan, H., Johnson-Carroll, K. & Rabolt, N.** (2015). Health consciousness and organic food consumption. J. Fam. Consum. Sci. 2015, 107, 27–32.

[21] **Yazdanpanah, M. & Forouzani, M.** (2015). Application of the Theory of Planned Behaviour to predict Iranian students' intention to purchase organic food. Jour-nal of Cleaner Production, 2015, 107, 342–352.

[22] **Vietoris, V., Kozelová, D., Mellen, M., Chreneková, M., Potclan, J.E., Fikselová, M., Kopkáš, P. & Horská, E.** (2016). Analysis of Consumer Preferences at Organic Food Purchase in Romania. Polish Journal of Food and Nutrition Sciences, 66, 139–146.

[23] **Bryła, P.** (2016). Organic food consumption in Poland: Motives and barriers. Appetite 2016, 105, 737–746.

[24] **Mont, O.K.** (2002). Clarifying the concept of product–service system. Journal of Cleaner Production, 10, 237–245.

[25] **Tukker, A.** (2015). Product services for a resource-efficient and circular economy—A review. Journal of Cleaner Production, 97, 76–91.

[26] **Born, B. & Purcell, M.** (2006). Avoiding the local trap: Scale and food systems in planning research. Journal of Planning Education and Research, 2006, 26, 195–207.

[27] **Deppermann, A., Havlík, P., Valin, H., Boere, E., Herrero, M., Vervoort, J. & Mat-hijs, E.** (2018). The market impacts of shortening feed supply chains in Europe. Food Security, 10, 1401–1410.

[28] **Csíkné M, E.** (2014). Direct Selling on the Market of Agricultural Product. Ph.D. Thesis, Szent István University, Gödöllő, Hungary, 2014. https://szie.hu/file/tti/archivum/Csikne_Macsai_Eva_thesis.pdf (accessed on 20 May 2022).

[29] **Szente, V., Torma, D. & Szendrő, K.** (2017). Organic and local food market – al-ternatives or cooperation possibility? International Journal of Multidisciplinarity in Business and Science 3: 3 p. 85-92.

[30] **The Canadian Trade Commissioner Service** (2011): Our Offices in Canada and Abroad 2010–2011. Monograph. http://publications.gc.ca/site/eng/382535/publication.html (accessed on 20 May 2022).

[31] **Ayyub, S., Wang, X., Asif, M. & Ayyub, R.M.** (2018). Antecedents of Trust in Orga-nic Foods: The Mediating Role of Food Related Personality Traits. Sustainability, 10, 3597.

[32] **Rácz, G.** (2013). The Effects of Value Transformation and Trend of Sustainable Development on the Domestic Food Consumption. Ph.D. Thesis, Szent István University Gödöllő, Gödöllő, Hungary, https://szie.hu/file/tti/archivum/Racz_Georgina_thesis.pdf (accessed on 20 May 2022).

HUNGARIAN AGRICULTURAL ENGINEERING
No 41/2022 17-23
Published online: http://hae-journals.org/
HU ISSN 0864-7410 (Print)
HU ISSN 2415-9751(Online)
DOI: 10.17676/HAE.2022.41.17
Received: 20.04.2022 - Accepted: 15.05.2022

PERIODICAL
OF THE COMMITTEE OF AGRICULTURAL AND BIOSYSTEM ENGINEERING OF THE HUNGARIAN ACADEMY OF SCIENCES
and
HUNGARIAN UNIVERSITY OF AGRICULTURE AND LIFE SCIENCES
INSTITUTE OF TECHNOLOGY

MODELING THE EFFECT OF WHEEL TRAVELING ON THE SOIL SURFACE ON THE LOAD OF BURIED STRUCTURE

Author(s):
I. Keppler

Affiliation:
Institute of Technology - Hungarian University of Agriculture and Life Sciences, 2100 Gödöllő, Páter Károly u. 1., Hungary;

Email address:
keppler.istvan@uni-mate.hu

Abstract: As a result of the technical development of agriculture, machines with very high axle loads appeared in the fields and on farm roads. As a result, subsurface soil pressure values will also increase, which will ultimately put increased stress on underground pipelines and other structures. In our paper, we show the possibility of modelling the problem using explicit dynamical methods by means of a simple example.

Keywords: discrete element method, soil pressure, underearth pipelines, axle loads, explicit dynamical method

1. Introduction

(Keller and Or 2022) demonstrated that while surface contact stresses remained nearly constant over the course of modern mechanization, subsoil stresses have propagated into deeper soil layers. It can be assumed that this will lead to an increase in the load on the subsurface structures.

Because of the complexity of the structure-soil interaction, buried underearth structures (i.e. pipes) and surrounding soils jointly bear external loads (Bildik and Laman, 2019). The simplified analytical model if the soil pressure considers the soil prism above the subsoil structure (Yu et. al. 2022), and by considering the soil density and "wall" friction the equilibrium of infinitesimal soil slices results a differential equation which has a solution giving the load on a pipe buried in depth H to be

$$\sigma_M = \frac{1 - e^{-\frac{2fK}{B}H}}{2fK}\gamma B$$

where σ_M is the vertical pressure, H is the cover depth, B is the trench width, γ is the unit weight of the backfill, f is the soil-soil friction coefficient and K is the Rankine active soil pressure coefficient. This model is not suitable for the determination of the pressure load arising from the wheel rolling on the surface of this soil-pipe structure.

Several experimental investigations were made for determining the pressure load of buried pipes. Shmulevich et al. (1986) carried out experimental studies and showed that soil pressures have approximately parabolic distribution. Talesnick and Frydman (2018) measured the soil pressure on a 0.8 m-diameter pipe during installation and varied traffic loading.

Several authors have worked on modelling this phenomenon using the finite element method. (Ahmed et al., 2015) evaluated the effect of geogrid on the soil pressure. (Wu et. al. 2021) made sensitivity study regarding the FE model of soil – pipe interaction. (Kang 2019) analysed the effect of imperfect trench installations. The effect of internal friction has been studied by (Whidden 2009). (Zamanian et. al. 2020) considered the influence of hydrostatic pressure on the yield strength and shear dilatancy of the soil.

Analytical solutions of this problem adequate for taking into account even the acceleration of the moving wheel do not exist, this is why our focus has turned towards the application of explicit dynamics modelling method. Instead of soil mechanics relations based on the results of classical continuum mechanics, explicit dynamical methods using the computational power of modern computing tools can provide a more accurate picture of the load conditions. For modelling the problem, we will use the so-called discrete element modelling method. The discrete element method was developed for rock mechanics in the late 1970s (Cundall and Strack, 1979). The method, which was later developed further, has now become suitable for modelling almost any problem where granular materials interact with their environment or with each other. Such a problem is the effect of soil pressure on underground structures. Using the potential of the new method, it is also possible to model the load variations caused by a moving wheel passing over the pipeline.

2. The discrete element method

For modelling the mechanical behaviour of the granular material, EDEM discrete element software was used. In the discrete element model the simulation evaluates the contact forces according to the "Hertz-Mindlin no slip" contact model: the material and interaction parameters have their effect on the normal- and tangential forces. These forces and moments acting between the interacting soil particles in the form of the following equations [2].

The normal force is calculated using

$$F_n = \frac{4}{3} E_0 \delta^{\frac{3}{2}} \sqrt{R_0} - 2\sqrt{\frac{5}{6}} \frac{\ln C_r}{\sqrt{\ln^2 C_r + \pi^2}} \sqrt{2E_0 \sqrt[4]{R_0 \delta}} \sqrt{m_0} v_{\mathrm{nrel}},$$

where $\frac{1}{E_0} = \frac{1-\nu_1^2}{E_1} + \frac{1-\nu_2^2}{E_2}$ is the equivalent Young modulus of the two interacting soil particles, δ is the overlap between these two soil particles. This normal overlap represents the normal deformation of a particle. The normal overlap δ between two particles i and j at positions x_i and x_j (where x is the distance measured on the line connecting the centres of the two overlapping particles) with radii R_i and R_j is defined as: $\delta = R_i + R_j - (x_j - x_i)$. $R_0 = \frac{R_1 R_2}{R_1 + R_2}$ is the equivalent radius, $\mathrm{m}_0 = \frac{\mathrm{m}_1 \mathrm{m}_2}{\mathrm{m}_1 + \mathrm{m}_2}$ is the equivalent mass and v_{nrel} is the normal component of the relative velocity of the soil particles.

The tangential force can be calculated as

$$F_t = -8G_0 \sqrt{R_0 \delta} \delta_t - 2\sqrt{\frac{5}{6}} \frac{\ln C_r}{\sqrt{\ln^2 C_r + \pi^2}} \sqrt{2G_0 \sqrt[4]{R_0 \delta}} \sqrt{m_0} v_{\mathrm{trel}},$$

where $\frac{1}{G_0} = \frac{2-\nu_1}{G_1} + \frac{2-\nu_2}{G_2}$ is the equivalent shear modulus of the two interacting soil particles, δ_t is the tangential overlap between the two particles and v_{trel} is the tangential component of the relative velocity of the soil particles. The tangential overlap is the tangential displacement of the contact point up to the point at which the contact ends or the particle begins to roll or slip. The tangential overlap represents the tangential deformation of a particle. The tangential force is limited by Coulomb friction $\mu_s F_n$, where μ_s is the coefficient of static friction.

The moment from rolling friction is $M_r = -\mu_r F_N R_i \omega_i$, where R_i is the distance of the contact point from the centre of the i-th soil particles and ω_i is the unit angular velocity vector, which is a dimensionless quantity representing only the direction of rotation of the i-th soil particle. μ_r is the coefficient of rolling friction. The tangential force also has moment on the particle: $M_t = F_t R_i$.

According to (Potyondy and Cundall, 2004), from $t > t_{\mathrm{bond}}$ (from the time, when bonding is "turned on") at contact points and at points which are closer to each other than a pre-defined distance (called bonded disk radius) particles are glued to each other by bonding bridges. Bonds of finite stiffness can exist at contacts, and these bonds carry load and can break. An applied macroscopic load is carried by the grain and "glue" skeleton in the form of force chains that propagate from one grain to the next across grain contacts, some of which may be filled with "glue". The forces arising in these bonding bridges can be calculated by taking into account their deformation and their material properties.

The bonding forces/moments acting on the particles are set to initial value zero, and are adjusted incrementally every time step:

$$\delta F_n = -v_n S_n A \delta t,$$

$$\delta F_t = -v_t S_t A \delta t,$$

$$\delta M_n = -\omega_n S_t J \delta t,$$

$$\delta M_t = -\omega_t S_n \frac{J}{2} \delta t,$$

where $A = R_B^2\pi$, $J = \frac{1}{2}R_B^4\pi$. R_B is the radius of the glue, $S_{n,t}$ are the normal and shear stiffness per unit area, $\delta t$is the timestep, $v_{n,t}$ are the normal and tangential velocities of the particles and $\omega_{n,t}$ are the normal and tangential components of the angular velocity vector.

The bond is broken when the normal or tangential stress exceeds some predefined value (the strength of the bonding bridges):

$$\sigma < -\frac{F_n}{A} + \frac{2M_t}{J} R_{Bmax} ,$$

$$\tau < -\frac{F_t}{A} + \frac{M_t}{J} R_{Bmax} .$$

These bonding forces/torques are in addition to the standard Hertz-Mindlin forces.

During the simulations, the linear- and angular momentum theorem is used to write the equation of motion for all the individual particles resulting multiple number of differential equations to be solved in a sufficiently large number of time steps. The used time step has a great impact on the stability of the numerical model. We selected for the simulation 25% of the Rayleigh-type time step:

$$\delta t = 0{,}25 T_R = 0{,}25 \cdot (0.1631\nu + 0{,}8766)^{-1} \pi R \left(\frac{\rho_p}{G_p}\right)^{\frac{1}{2}} .$$

It is important to consider that the quality of the obtainable solution could sensitively depend on the value of this time step used during the simulations. The same time step must be used during the calibration process of the discrete element model and during the simulations.

3. Materials and Methods

Among the possible explicit dynamic modelling procedures, the discrete element method was used to study the phenomenon. A very important advantage of the modelling procedure we have chosen is that it can also track the wheel separation under load conditions during wheel motion. This is not possible at all with analytical methods and is rather difficult with solutions based on the finite element method.

3.1. The discrete element model

The discrete element model of the soil-wheel-pipe structure can be seen on (Figure 1). The model consists of a *D*=420mm finned rigid wheel, approximately 45000soil particles and a radius *R*=100mm half pipe created from 10 segments to make it possible to determine the soil pressure distribution on its surface. The soil depth under the wheel was approximately 2000mm, which is quite small, but our goal was only to demonstrate the possibilities of DEM modelling.

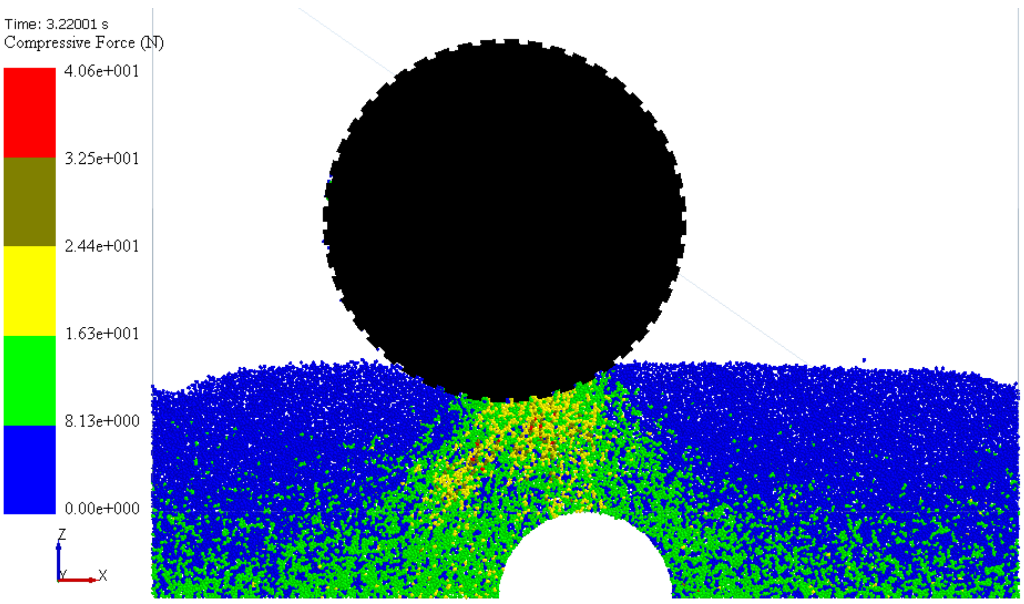

Figure 1. DEM model of the soil – wheel – pipe structure, particle-particle compressive force is shown

For the discrete element model of soil, we used the following calibrated (based on the modelling of the standard shear test) data from (Keppler et. al. 2015):

- Poisson's ratio $\nu_p = 0.25$, $\nu_t = 0.3$
- Shear modulus $G_p = 10^7$Pa, $G_t = 8 \cdot 10^9$ Pa,
- Density $\rho_p = 3000$ kgm^{-3}, $\rho_t = 7500$ kgm^{-3},
- Coefficient of restitution: $C_{r,p-p} = C_{r,t-p} = 0.5$,
- Coefficient of static friction $\mu_{p-p} = 0.9$, $\mu_{p-t} = 0.3$,
- Coefficient of rolling friction $\mu_{r,p-p} = 0.01$, $\mu_{r,p-t} = 0.01$.

And for the bonded soil model we used:

- Normal stiffness: $S_n = 10^9$ Nm^{-3},
- Shear stiffness $S_t = 10^9$ Nm^{-3},
- Critical normal stress $\sigma_{max} = 1.5 \cdot 10^6$ Pa,
- Critical shear test $\tau_{max} = 8 \cdot 10^5$ Pa,
- Bonded disk radius $R_B = 0.006$m.

Subscript *p* means particle, *t* means other structural elements in the model. The bulk material particles were created as a clump of two spheres having 2 mm radiuses and 1.5 mm distance between the two spherical surfaces resulting one clumped particle. The whole geometrical configuration involved periodic boundaries in *x* and *y* directions (see Figure 1.). This means quite similar "infinite" extent of the model to the direction perpendicular (*y*) direction of the figure and behaves like the plain strain model in classical continuum modelling. The kinematical parameters of the wheel were $v_0 = 0$ initial velocity and $a = 0.47\ \frac{\mathrm{m}}{\mathrm{s}^2}$ constant acceleration. This resulted the rolling of the wheel above the pipe without sliding. We used 25% of the Raileigh time step during the DEM modelling calculations.

3.2. Data analysis

After the running of the simulations, we analysed the pressure distribution arising on the surface of the pipe segments. On Figure 2. you see the pressure overload of the topmost horizontal segment of the pipe caused by the rolling wheel.

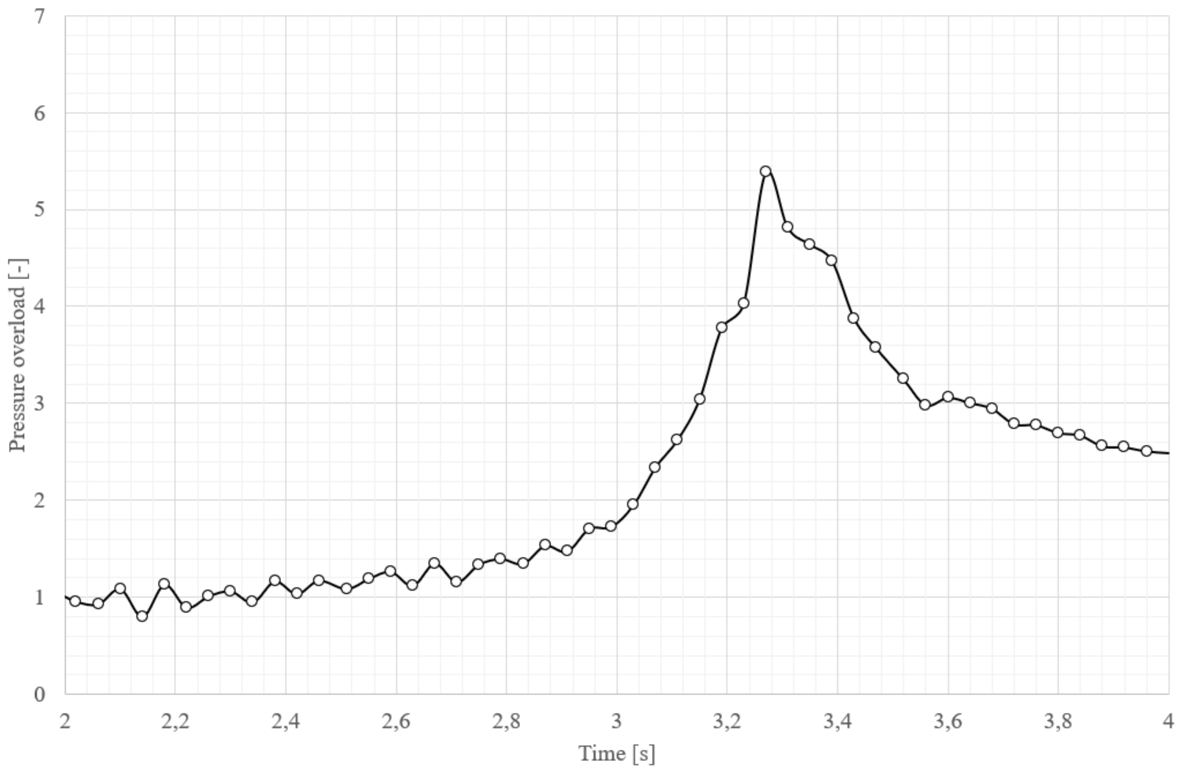

Figure 2. Pressure overload caused by the wheel rolling over the pipe

The pressure overload was calculated as the pressure arising from the soil resting above the pipe divided by the pressure caused by the rolling wheel. Of course, this value highly depends on the axle load (in our case it was 500N), but the goal of this article is to demonstrate the capabilities of the DEM modelling, so the concrete value is not so important for us. The cause of the pressure overload is the change in the force distribution between the soil particles (Figure 3.).

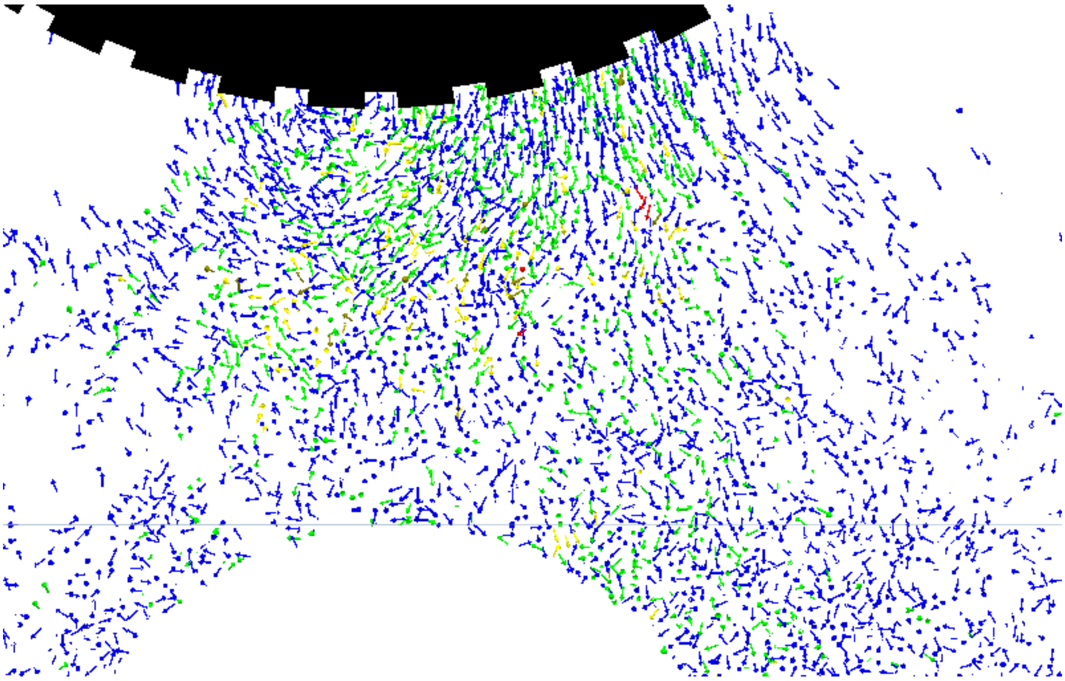

Figure 3. Particle force distribution vector field above the pipe segment

4. Results

Having all these data for all the pipe segments, we created the pipe wall overload diagram, by calculating the maximal pressure overload for all pipe segments. It is worth to note, that by using this method we have the chance to find the maximal overload values for all the separate pipe segments, although these quantities appear in different positions of the wheel for each segment.

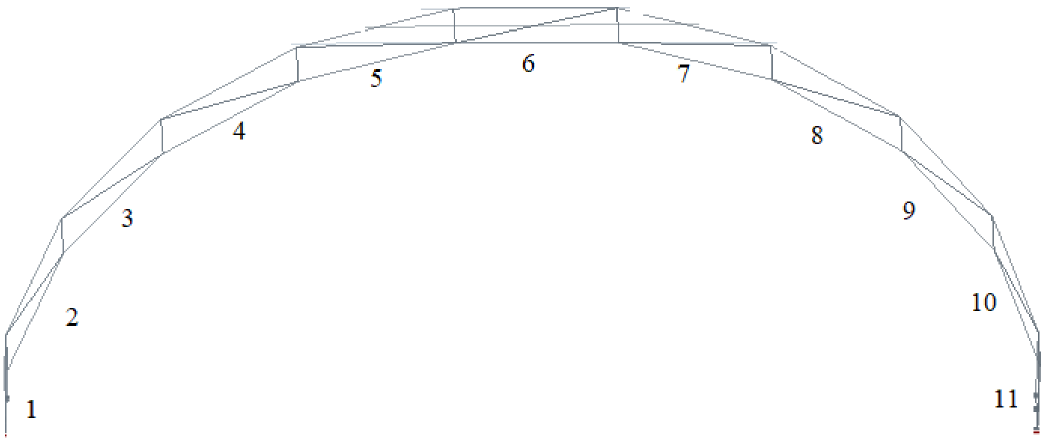

Figure 4. Pipe segments for pressure distribution data

Figure 5 shows the pressure overload values on all the pipe segments listen on Figure 4.

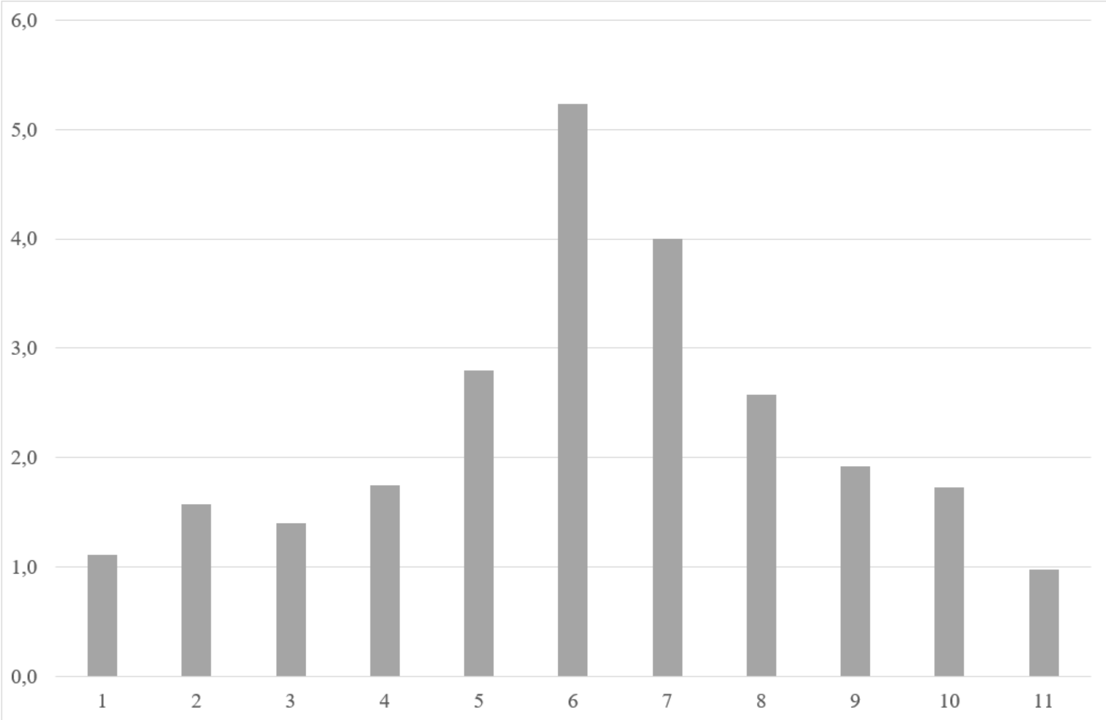

Figure 5. Pressure overload of the different pipe segments.

The results of the numerical simulation show that the highest overload is expected at the top of the pipe. This shows a good match between the results of the exercise and the "expected" physical behaviour as Zhou et al. (2011) and Li (2017) who studied the 0.61 diameter and 0.1 m-diameter pipes, respectively, and both depicted that the soil pressure is the largest at the pipe crown and has roughly parabola distribution.

5. Conclusions

What we found was that the side of the tube towards which the wheel was approaching was subjected to much higher loads than the other side, and the highest overload is expected at the top of the pipe.

The method presented here provides a more detailed picture of the mechanical processes occurring in the granular assemblies and about their interaction with the structures under investigation than the classical analytical solutions. Our primary objective in this article was to investigate the applicability of the DEM-based method. It follows that the results obtained can only be applied in practice after further experimental and numerical analysis. However, we have been able to demonstrate that the application of DEM-based methods can be realistic in the field of the present study. Of course, the applicability of the specific numerical results requires a number of further tests.

Acknowledgements

The research was funded by the project "Development of mobile mechatronic industrial applications using laser and structural stress measurement technologies" and "KFI 16-1-2017-0216".

References

[1] **Keller Thomas, Or Dani** (2022). Farm vehicles approaching weights of sauropods exceed safe mechanical limits for soil functioning, Proceedings of the National Academy of Sciences, 2022 Vol. 119 No. 21 e2117699119

[2] **Bildik, S., Laman, M.** (2019). Experimental investigation of soil-structure pipe interaction. KSCE J. Civ. Eng. 23 (9), 3753–3763.

[3] **Jin-Hong Yu, He-Gao Wu, Chang-Zheng Shi, Zhu Ma, Wen-Tao Xu** (2022). Behavior and innovative design model on soil pressure at the top of large-diameter buried steel pipes, Soils and Foundations 62 (2022) 101153.

[4] **Shmulevich, I., Galili, N., Foux, A. (**1986). Soil stress distribution around buried pipes. J. Transp. Eng. 112 (5), 481–494

[5] **Talesnick, M.L., Frydman, S.** (2018). Soil pressure and pipe deformation measurements for characterizing flexible pipe–soil systems under shallow cover. J. Pipeline Syst. Eng. Pract. 9 (1).

[6] **Ahmed, M.R., Tran, V.D.H., Meguid, M.A. (**2015). On the role of geogrid reinforcement in reducing earth pressure on buried pipes: experimental and numerical investigations. Soils Found. 55 (3), 588–599

[7] **Wu, H.G., Yu, J.H., Shi, C.Z., Ma, Z.** (2021). Pipe-soil interaction and sensitivity study of large-diameter buried steel pipes. KSCE J. Civ. Eng. 1 (12), 793–804.

[8] **Cundall, P.A. and Strack,** O.D.L. (1979). A discrete numerical model for granular assemblies, Geotechnique, Vol. 29 No. 1, pp. 47-65.

[9] **D.O. Potyondy, P.A. Cundall** (2004). A bonded-particle model for rock, International Journal of Rock Mechanics & Mining Sciences 41 1329–1364

[10] **Keppler I., Hudoba Z., Oldal I., Csatar A., Fenyvesi L.** (2015). Discrete element modeling of vibrating tillage tools, Engineering Computations, Volume 32, Issue 2, Pages 308-328.

[11] **Zhou, Z.F., Ling, J.M., Liang, B.** (2011). Analysis of earth pressure on oil pipe. Journal of Chongqing Jiaotong University. Natural Sci. 30 (4), 794–797.

[12] **Li, Y.G.** (2017). Experimental study on earth pressure distribution around buried pipeline. Henan University of Technology (in Chinese), Zhengzhou.

[13] **Kang, J.** (2019). Finite element analysis for deeply buried concrete pipes in proposed imperfect trench installations with expanded polystyrene (EPS) foams. Eng. Struct. 189, 286–295.

[14] **Whidden, W.R.** (2009). Buried flexible steel pipe: design and structural analysis. ASCE Manuals and Reports on Engineering Practice No 119, Reston, Virginia, USA.

[15] **Zamanian, S., Hur, J., Shafieezadeh, A.** (2020). A high-fidelity computational investigation of buried concrete sewer pipes exposed to truckloads and corrosion deterioration. Eng. Struct. 221

HUNGARIAN AGRICULTURAL ENGINEERING
No 41/2022 24-37
Published online: http://hae-journals.org/
HU ISSN 0864-7410 (Print)
HU ISSN 2415-9751(Online)
DOI: 10.17676/HAE.2022.41.24
Received: 30.04.2022 - Accepted: 25.05.2022

PERIODICAL
OF THE COMMITTEE OF AGRICULTURAL AND BIOSYSTEM ENGINEERING OF THE HUNGARIAN ACADEMY OF SCIENCES
and
HUNGARIAN UNIVERSITY OF AGRICULTURE AND LIFE SCIENCES
INSTITUTE OF TECHNOLOGY

DEHYDRATING USING COMBINED ENERGY INTAKE METHOD

Author(s):
V. Madár[1], J. Gubó[2], L. Tóth[3]

Affiliation:
[1] PYROWATT Co. Ltd.,6120 Kiskunmajsa, Vágóhid u. 91., Hungary;
[2] CSŐ-MONTAGE Co. Ltd.; 1103 Budapest, Gyömrői u 33., Hungary;
[3] Institute of Technology - Hungarian University of Agriculture and Life Sciences, 2100 Gödöllő, Páter Károly u. 1., Hungary;

Email address:
madar.viktor@pyrowatt.hu; Gubo.Janos@csomontage.hu; Toth.Laszlo.emeritus@uni-mate.hu

Abstract: Our paper introduces the research and development of a new, continuously operational food dehydrator, and the prototype of said machine. Conditions related to heating technology are required for dehydrators that prevent the vegetables and fruits from suffering too much damage to their internal components. In the new system, traditional convective heat transfer was combined with microwave dehydration, which is well-known for its better efficiency. The final goal is to create an industrial system that can satisfy both small works and industrial demands, while being more energy efficient than traditional solutions, and has faster dehydration potential. However, at the same time, due to dehydrating on lower temperature, it should end up in a gentler drying process. It is fundamental to keep the valuable components of the products intact. The system is continuously operational. The material is sent via conveyor belt through the canal, while magnetrons are operating, and low- heat and moisture airflow is moving above it. Materials dried with the machine were evaluated by the Institute of Horticulture, at the Hungarian University of Agriculture and Life Sciences s (MATE).

Keywords: fruit drying, low-impact drying, microwave, convective energy, energy conservation

1. Introduction

There is a wide array of positive feedback on various foodstuffs forums relating to the advantages of dried and dehydrated fruits and vegetables. Drying, or dehydration are similar processes physically, one of them is the oldest form of conservation (Radu et al., 2018). Both processes deal with the removal of the material's initial high moisture content. The moisture content related from drying is ~12-14% of the original, average moisture content, or even lower. For dehydration, the moisture content is somewhere between 18% and 22%. Fundamental processes have long-standing traditions, they may be extremely simple, or more complex variations.

Apart from conservation, dehydration's purpose is to keep taste- and aroma intact, meaning the enjoyment factor during consumption should remain. Drying and dehydration was done in direct sunlight, when weather conditions were favourable. Even to this day, many consider the dehydration using sunlight the most advantageous. In order to reach sufficient quality, several important factors are necessary: protection from dust, various insects, but damage may come from too strong a sunlight as well, f.e. overheated materials have their colours changed, and their surface hardens. The duration of dehydrating, and the state of the environment (temperature, airflow, air moisture content) where dehydrating is conducted, are also important. The applicable periods for fruits that ripen later are even less, especially in temperate climate, due to frequent and significant changes. As such, most recommend closed- or semi-closed dehydration processes, and dehydrators using electric heating. Removal of hydration can traditionally be done via two processes: convective and conductive heat transfer.

Both processes are known for starting the heating of material on the outside surface, and heat energy is transferring towards the inside (Beke, 1999). Airflow is advantageous for the drying method using sunlight as well, as water and moisture on the surface of the material is transferred through it, away from the material.

Therefore, water (vapour) expelled from the material by the conductive heat flowing into it is realised through a convective method (through airflow), which also makes the process faster. As an example, when conducting dehydration using an oven, it's often advised to slightly open the oven door. Through the opening, air filled with moisture and vapour can exit from the oven, helping and hastening the drying process.

In the earliest larger closed dehydrators, a convective and conductive combination process was used, usually by pouring in hot, dry air. For these processes, energy becomes a significant cost factor. Therefore, one of the goals of these processes is to reduce the energy committed to the process. This should be achieved in a way that doesn't impact the material quality of the end product.

2. Development goals

We have developed a process which aids both energy conservation and quality conservation (Aboltins-Palabinskis, 2018). To reach this goal, we implemented a combination of convective moisture extraction (could be called convective drying), and short wave energy transmission (heat transfer). Short wave heating and cooking has become mainstream nowadays, due to the massive popularity of the microwave oven. There were many debates on its effect on life, and even today, there are many against it. However, nobody could reliably prove that it causes any sort of sickness by itself. If we analyse the physics of the process, we can't find a phenomenon that could support these claims (Radu et al., 2018).

We have designed a machine in which the moisture within the materials is heated swiftly through applying microwaves, and expended in a shorter time towards the surface of the material. From there, the low temperature and vapour content airflow transfers it to the outside. The design of the system can be seen on Fig. 1.

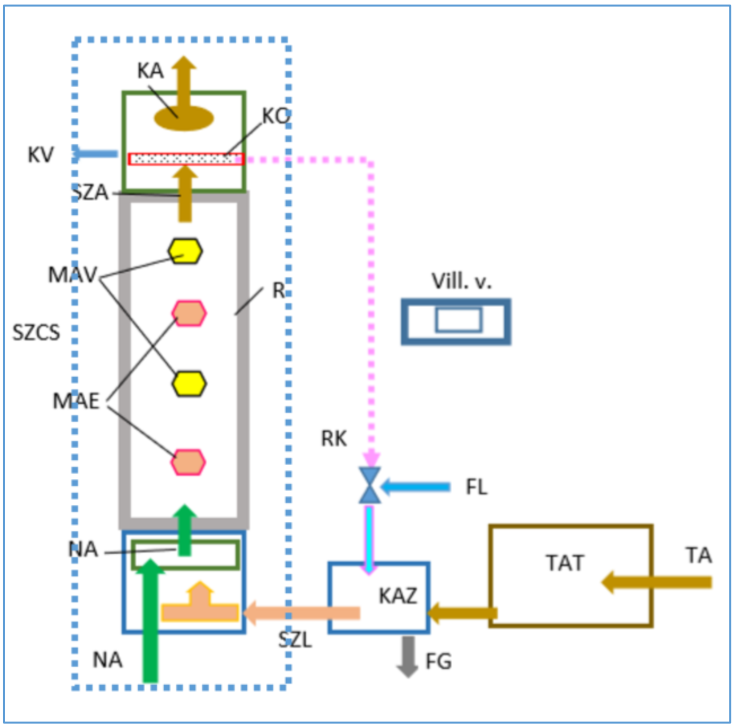

Explanation of abbreviations on the figure:
SZCS – drying channel,
MAV – magnetrons,
MAE – rectified magnetron,
NA – moist material input,
R – cavity resonator,
SZ – dry material,
KA – finished material,
KO – condensator,
KV – waste water,
SZL – dry air input,
KAZ – convection furnace
FG – waste gas,
RK – fresh recuperation air,
TAT – container space,
TA – fuel,
Vill.v – electric control.

Figure 1. Theoretical design of the experimental machine within the closed metal container.

We planned a so-called dehydration tunnel (drying channel) for the system, where the material transferred through perforated conveyor belt undergoes microwave treatment, while a low-temperature and vapour content airflow consistently remains in its direct proximity.

Air flows through the channel (tunnel) above the product on top of the conveyor belt, towards the open end (Fig. 2).

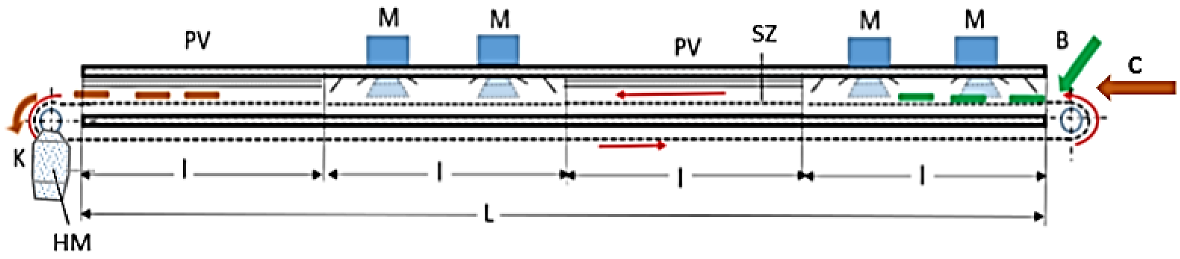

Figure 2. Structure of the tunnel

Explanation of abbreviations on the figure:
M – magnetrons, PV – polarised, high voltage areas, B – input of moist product, C – input of drying airflow, K – end product, measurement, SZ – conveyor belt using plastic belt, HM – engine motor operating the transport conveyor

3. Movement and role of the drying airflow

In convective drying, the most important function belongs to the low moisture/vapour content airflow, which transfers heat into the drying system, heats the materials to dry present within, and extracts the moisture content from the system. (Beke et al, 1999) The total pressure of this moist air (p) comes from the partial pressure of vapour (p_g) and dry air (p_1):

$$p = p_1 + p_g$$

Partial steam pressure:

$$p_g = p\frac{m_g R_g}{mR}$$

where: m_g – mass of the vapour
m – sum of dry air and vapour mass

$$m = m_1 + m_g$$

moisture content of the airflow:

$$x = \frac{m_g}{m_1}$$

Partial pressures can also be used to express the *moisture content of saturated airflow*:

$$x = 0{,}622\frac{p_g}{p - p_g}$$

Relative moisture content, from partial gas pressures:

$$\varphi = \frac{p_g}{p_{gt}}$$

where p_{gt} – gas pressure of saturated airflow.

Evaporation heat is necessary for the evaporation of the material's moisture content. It is only valid for specific moisture content and temperature, as partial gas pressure means the ratio between capillary water and free fluid evaporation. This means that it's *varied, depending on material types and moisture content.* It is always higher than one (Szabó, 2005). This shows that in order to remove capillary water from the materials, more energy is required than necessary for evaporating them from an open surface.

The goal is to affect the capillary water within the material using the microwave, since it is harder to remove (Beke- Mujumdar, 1997).

We mentioned that extracting the moisture from the material's surface is done using the airflow. Therefore, during the aerotechnical analysis, it's important to determine the moist air's enthalpy. In order to do this, Mollier's enthalpy moisture content, also known as i-x diagram is usable (Fig. 3).

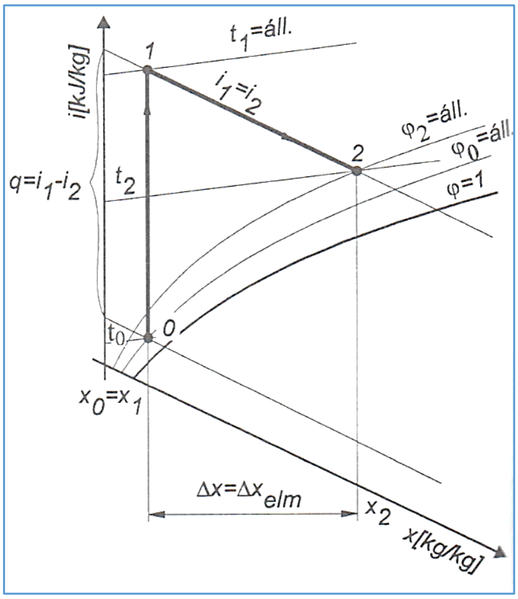

Figure 3. Drying process (Beke, 1997).

The machinery planned for manufacture will be a so-called cross-weighing system, continuously operating. Therefore, calculations have to take this into consideration (Chen et al., 2017), (Janowicz-Lenart, 2018).

During one unit of time, $G_1(kg/h)$ moist material enters the drying area, which has a moisture content of w_1, and a temperature of t_1'. At the end of the drying process, G_2 (kg/h) of dried material leaves the system at w_2 moisture content and t_2' temperature (Moreno et al., 2018), (Saravacos et al., 1999).

Mass flow of the dried material:

$$G_2 = G_1 \frac{1 - w_1}{1 - w_2} \quad (kg/h)$$

Material balance of evaporated and extracted vapour:

$$W = G_1 - G_2 \qquad (kg/h)$$

For both dry and moist materials:

$$W = G_1 \cdot \frac{w_1 - w_2}{100 - w_2}; \quad W = G_2 \cdot \frac{w_1 - w_2}{100 - w_1}$$

Dehydration potential of the drying airflow W (kg/h):

$$W = L \cdot \Delta x \qquad (kg/h)$$

Where: $\Delta x = (x_2 - x_1)$ g/kg, equals the airflow's moisture intake.
L = airflow volume (kg/h)

Necessary heating performance of the dehydrator Q (MJ/h):

$$Q = L \cdot \Delta i$$

Where: L – volume of drying airflow (kg/h)
$\Delta i = (i_2 - i_1)$ change in heat content (enthalpy) ($kJ/kg_{sz.lev.}$)

Necessary heat performance:

$$Q_h = G_{tü}\, H \qquad (MJ/h)$$

Where: $G_{tü}$ – fuel quantity (kg/h)
H – heat performance of fuel used for the heating process (MJ/kg)

Points of separation on the drying curve can be differentiated by A; B; C; D and E. (Fig. 4)

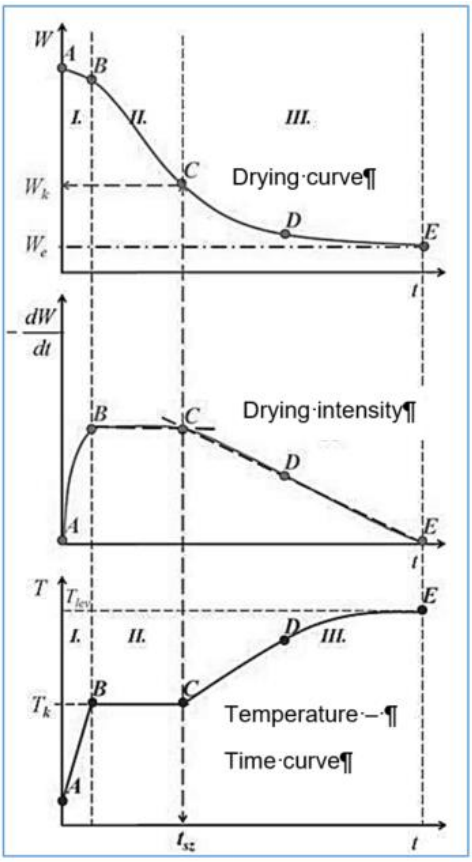

Figure 4. Specific phases of dry (Dévay, 2013)

Explanation of abbreviations on the figure:
I. warming phase; II. constant speed phase; III. decreasing speed phase.

According to experiences (and literature sources), the speed and temperature of the airflow has a significant impact on the colouring. This is why the effects of temperature and air velocity have to be considered. Preparation is necessary for making them variable (Beke, 1999), (Miller et al., 2012).

In general, even changes in the internal components is dependent on the level of heat transmission, since heat level affects various chemical reactions, which are f.e. causes for loss in internal component, and even *aroma*.

For example, the so-called convective drying (dehydration) using airflow, by increasing the speed of dehydrating fruits, loss in aroma also increases. In the case of vegetables and fruits, apart from aroma, proteins, sugars, vitamins, acids and carbohydrates are also damaged.

Nowadays' practice mostly considers the convective process (using airflow) to use for drying. Using the effect of the temperature-controlled airflow within the tunnel, so-called direct airflow drying is achieved. Therefore, at the same time of the progress of the materials to be dried, the flow of the hot air current is also managed. Due to the evaporation of moisture, the difference in partial gas pressures towards the end of the transport is lower, which also results in a decrease of drying speed. In the high frequency electric area, the drying material acts as a dielectric object, which results in a production of heat. This is added to the flowing air current, counter-balancing the heat extraction from evaporation. This causes the loss in temperature to be reduced towards the end of the tunnel.

4. Microwave part of the machine

During traditional heat transmission, contact heat transmission, convection and radiation are present, however, heat and energy within the material can only be led inside via heat transmission (Fig. 5).

Most biological materials are quite bad at heat transmission, which causes a significant loss in energy during heat transmission processes, and due to the imbalanced water content within the material, local overheating is possible (Chen et al., 2017.).

Finally, the relative moisture content of the drying context, its temperature, and the velocity of flow determines the speed of drying.

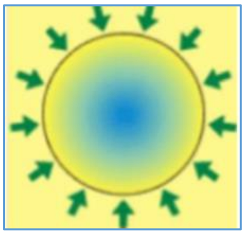

Figure 5. Flow happens from the outside towards the inside during convective heating

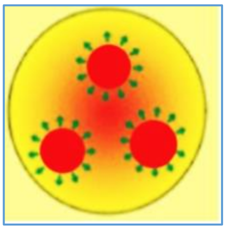

Figure 6. Microwave heats the entire mass of the material, both inside and outside

Most biological materials within an alternate current electric pressure field act as an electric agent with high loss coefficient. The (estimated) dielectric constant of the material is basically determined by the moisture content, meaning it depends on how much water there is in the material. However, ion structure is also important, which is determined by salt content. (Kurják-Bessenyei, 2014), (Kurják et al., 2012). The latter affects the specific heat of the base materials, as such, should be taken into consideration during microwave treatment as a special attribute. The energy of the microwave field affects the entire mass (Fig. 6), meaning the heat effect is higher for parts with greater internal moisture content (dielectric area), where it's the most intensive. Therefore, the effect of the microwave field is highly significant.

Sources have differing opinions on the non-thermic effects of microwaves. The theoretic explanation of non-thermic correlations is complicated, as microwave treatments are always followed by heat.

Heat transfer and moisture reduction for foodstuffs using microwave radiation is generally done at the ~2,5GHz frequency.

Due to the effects of the electromagnetic field, positive and negative potentials are biased (Fig. 7). Therefore, the effect of interaction between the electromagnetic field and the material is polarisation (Ludányi L. 2004), (Parviz, 2016).

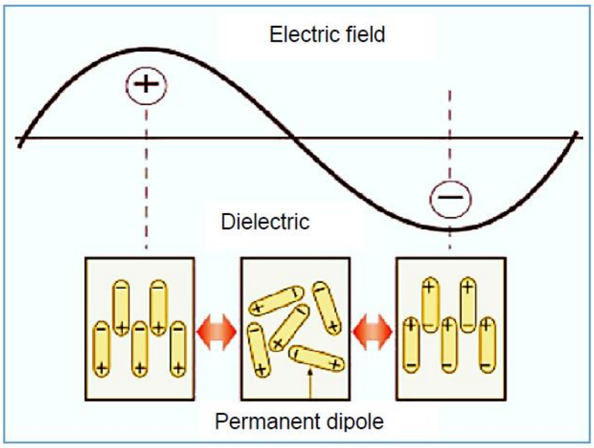

Figure 7. Molecule movements affected by shifting context

All parts of the material that became polarised seems as if one side became the positive pole, and the other became the negative pole. The electric field "organises" these dipoles, and deforms the molecule without the dipole's moment changing. In spite of the heat movement, they aim to rotate into the area. This also includes molecules which are equivalent, or have ion connection. Polar materials polarise not only by deforming, but also by orientation due to the effects of the electric field. The permittivity of dielectric agents (charge movement, rearrangement of dipoles) depends on frequency (Szabó 2005). We can calculate the transformation of microwave energy into heat within the material with relatively high precision:

$$P_D = 55{,}61 \cdot 10^{14} \cdot E^2 \cdot f' \cdot \varepsilon' \cdot tan\delta \quad (\text{W/cm}^2)$$

Where:

P_D – dissipated energy (consumed by material) [W/cm^2]
E – strength of electric field [V/cm]
f' – frequency [Hz]
ε' – dielectric constant
$\tan\delta$ – tangent of loss

Energy diffusion, and charge movement are affected by the penetration depth of the microwaves (taken for the material's sub-surface depth). Therefore, it has no effect where the energy is reduced to e^{-1} value when compared to penetration energy.

Magnetrons are the base units of microwave ovens. These transform injected direct current into microwaves with relatively high efficiency (Ludányi, 2004). The geometric shape of the wave generated within the cavity resonator affects the diffusion of the created electric field. Therefore, the structure and geometry of the handling area has to match the wavelength. Metal stirring fittings and reflective surfaces built into the handling area prevent static waves from being generated, which makes the diffusion of energy within the area more balanced (Ludányi, 2004).

Several literature sources show that microwave drying has significantly shorter duration when compared to convective drying (Kurják-Bessenyei, 2014.). Machines may be better utilised, since the amount of dried material created in one unit of time is much larger (Fig. 8).

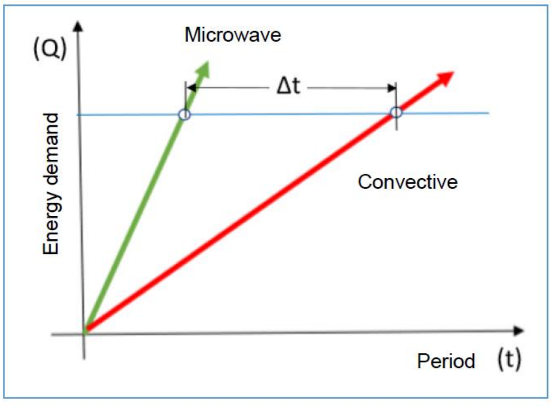

Figure 8. Microwave treatment needs less time even for identical energy input.

During dehydration using microwaves, we obtain similar velocity curves to those of convective drying, however, they show a much more intense growing trend. *Microwave drying helps the natural moisture movement within the product, which causes energy utilisation to become more efficient* (Kurják- Bessenyei, 2014), (Ludányi, 2004).

In order to protect performance measurement units, the probes give the microwave signs into the devices through fixed value absorbers. The analogue outgoing signals kept in line with measured performance reach the measurement computer through the interface.

Measured data:

$$P_d = P_h - P_v$$

Where:

P_v – performance reflecting from the material
P_d – performance dissipating in the material
P_h – input performance

From the analysis of processes, we can state that microwave drying requires roughly one magnitude less energy compared to the convective method. There are significant differences in energy consumption depending on the type of product used as material.

5. Structure of the machinery

The framework of the machinery we developed was constructed of stainless and anti-acid closed sections. This framework holds the construct, which is a tunnel-like channel (Fig. 9).

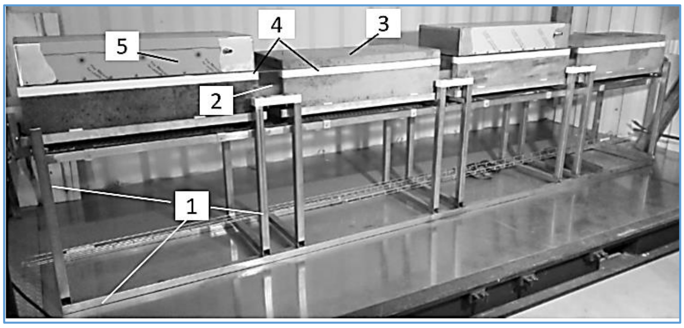

Figure 9. Side-view of the tunnel system (self-made photograph)

Explanation of abbreviations on the figure:
1. *Framework*
2. *Drying tunnel channel*
3. *High voltage / direct current panels of drying tunnel (lid)*
4. *Extension fitting (insulator)*
5. *Magnetron house*

The reflective plates under the microwave connection of magnetrons were made out of stainless and anti-acid material, and are fitted onto the lid. Therefore, in the area beneath these panels, directional plates help (increase homogeneity) the injection of radiation towards the material moving on the conveyor belt (Fig. 10).

Figure 11 shows the high voltage panel's location (in cross-section).

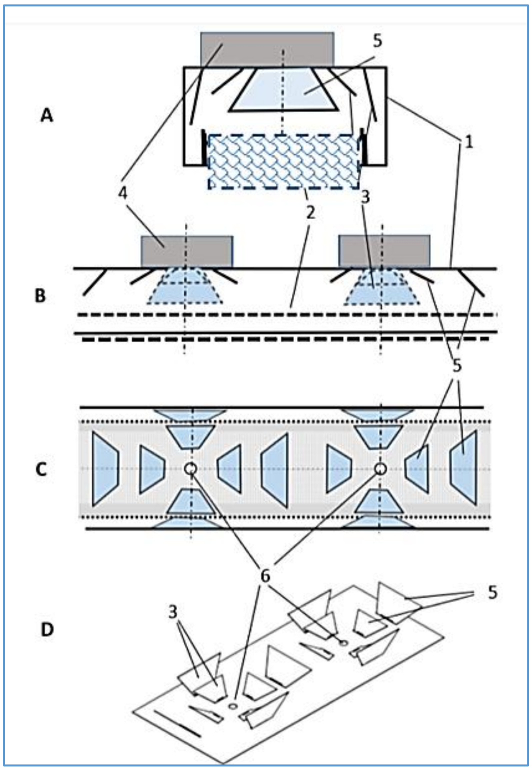

Figure 10. One part of the drying tunnel with magnetrons and reflective plates

Explanation of abbreviations on the figure:
A – cross-section,
B – longitudinal section,
C – from above,
D – axonometric sketch,
1 – internal division walls of tunnel,
2 – tunnel and perforated conveyor belt,
3 – side reflective plates to guide microwaves,
4 – magnetrons,
5 – longitudinal reflective plates,
6 – intake openings of the tunnel for magnetrons

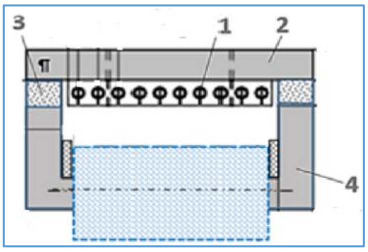

Figure 11. Cross-section of juxtalinear, alternating polarity, high-voltage unit

Explanation of abbreviations on the figure:
1- alternating polarity, high-voltage cables,
2 - lid,
3 - insulation,
4 - tunnel element.

On the top side of the tunnel, flowing air is blocked several times. These blocks tighten the bottleneck of the tunnel, and the velocity of the airflow changes. The characteristics of the airflow are shown on Figure 12, based on the ANSIS modelling.

Due to the microwave reflector, airflow increases, and air pressure decreases. Because of this phenomenon, the part below and above the perforated conveyor belt also have differing pressure levels.

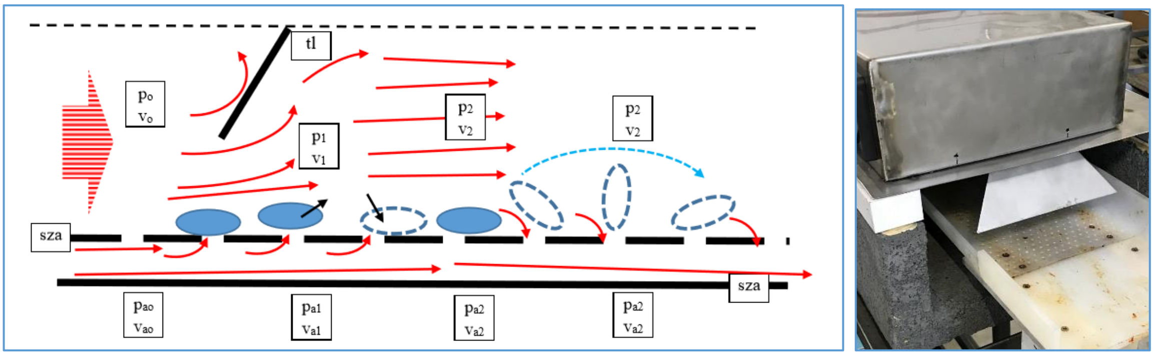

Figure 12. Changes in air pressure and velocity at the first cross-block (model and experimental device).

The figure shows (Fig. 13) the practical structure of the tunnel, where the completed material leaves the tunnel.

Explanation of abbreviations on the figure:
1 – conveyor belt,
2 – inverter motor,
3 – microwave reflector plate,
4 – Magnetron house,
5 – high voltage panel,
6 – framework structure,

Figure 13. Tunnel end, dehydrating apple

5.1. Theoretical structuring of the measurement system

The placement of the measurement units serves to determine the system's performance and energetic parameters. According to the structure seen on Figure 14, input- and output physical and energetic factors must be measured.

5.2. Pressure decrease considered for material transport

As the energy content and physical attributes of the atmosphere inside the tunnel both change, we also considered all values in linear relation, resulting in:

$$\Delta p_{v\ddot{o}} = (R_{h1} + R_{h2})Q^2$$

Calculating the resistance of the tunnel via **friction** and **shape factor** losses ($R_{h1} + R_{h2} = R_h$):

$$R_h = \frac{8\rho\lambda}{\pi^2}\frac{\Sigma 1 + \Sigma 1'}{d_e^5}$$

Meaning:

$$\Delta p_{v\ddot{o}} = R_h Q^2$$

where:

Q – intake volume flow (m^3/s)

Meaning:

$$Q = \frac{d_e^2 \pi}{4} v_1$$

v_1 – airflow velocity at intake (m/s)
d_e – equivalent flow radius (m)

When measuring for the experimental machine, $\Delta p_{v\ddot{o}}$ = 2009,88 Pa value was measured, which is almost identical to the value calculated by the flow resistance values. The smaller difference can also be caused by the significant change in vapour density expelled by the dipolar heat (but could also be due to friction resistance values). We accepted the value at 2000,0 Pa, which was validated closely by measurements (Fig. 15).

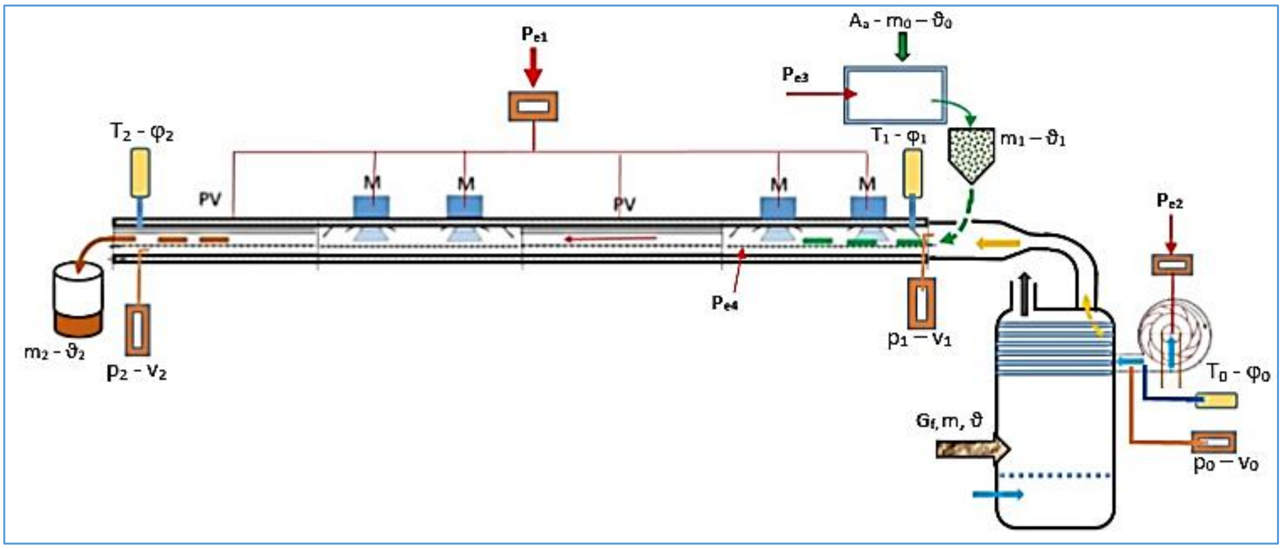

Figure 14. Structure schematics of the measurement system

Explanation of abbreviations on the figure:

Heat energy production
m – mass of wood (kg)
ϑ – its moisture content (%)
G_r – its specific energy content (MJ/kg)
P_{e2} – performance of the radial ventilator's electric engine (kW)
T_o – temperature of air intake (°C)
φ_o – its moisture content (%)
p_o – pressure (Pa)

v_o – velocity (m/s)
Intake side of the tunnel:
P_{e4} – performance of the material transport electric engine (kW)
T_1 – temperature of drying airflow (°C)
φ_1 – its moisture content (%)
p_1 – pressure (Pa)
v_1 – velocity (m/s)
v_2 – velocity (m/s)

Material to be dried
m_o – mass of input material before dicing (kg)
ϑ_o – its moisture content (%)
m_1 – its mass after dicing (kg)
ϑ_1 – its moisture content (%)

size of pieces (mm x mm)
P_{e3} – electric performance of dicer (kW)
P_{e1} – performance requirement of magnetrons and high voltage units (kW)
Dried material leaving tunnel:
m_2 – dried material's mass (kg)
ϑ_2 – its moisture content (%)

vapour-saturated air leaving tunnel:
T_2 – temperature (°C)
φ_2 – moisture content (%)
p_2 – pressure (Pa)

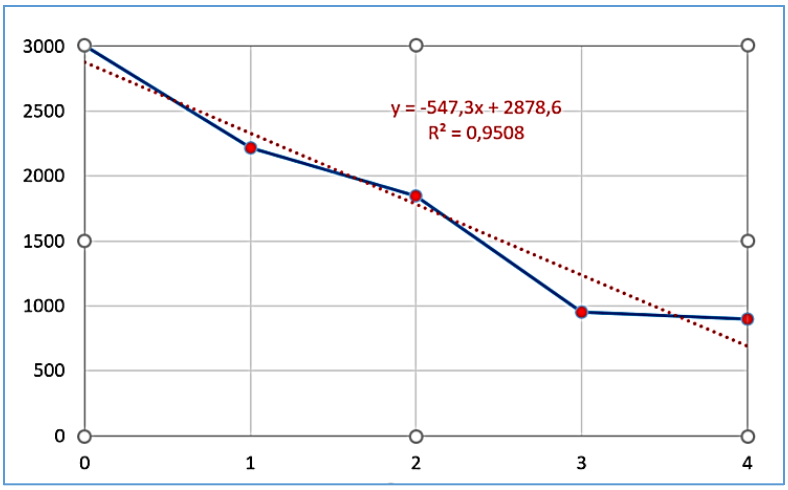

Figure 15. Pressure changes (Pa) along the length of the tunnel

It was obvious that the greatest decrease in velocity was during the part where the microwave reflection panels were placed at several different angles. In this part, the microwave changes on a scale from vertical to horizontal, due to the high frequency of reflections.

Keeping the initial velocity of the airflow constant, and merely changing load (volume passing through in time unit), a significant decrease in airflow speed was observable within the tunnel. The reason is partially the larger resistance caused by the material, and partially the more intensive evaporation of capillary water due to the microwave's effects (Fig. 16). These caused an increase in moisture content, which also caused an increase in specific density, and a decrease in temperature (Kurják. 2004).

The various dried products were analysed in the laboratory of the Institute of Horticulture, at the Hungarian University of Agriculture and Life Sciences (MATE). We determined the amount of mixtures significant for various qualities of foodstuffs (mg/100g) prior and post dehydration. Measurements were usually conducted with four repeats, in order to reduce the measurement errors, and the natural differences within the materials as much as possible. After the dehydration process, the materials were placed into inert gas environments, packed into foils, in order to dismiss any changes for the duration of the analysis (Fig. 17).

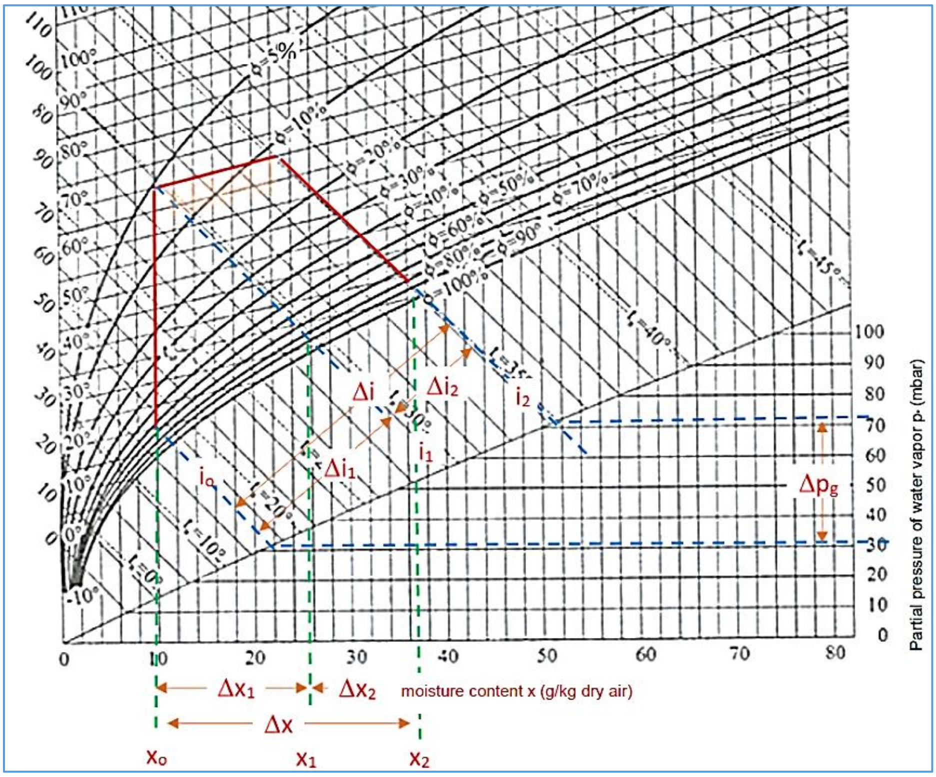

Figure 16. Edited i-x diagram, convective and microwave dehydration

Figure 17. Tomatoes prior and post dehydration process (Vertes species, top: Cukorfalat, bottom: Biborka)

Results obtained from four tomato products before (raw) and after dehydration process can be seen on Figures 18 and 19.

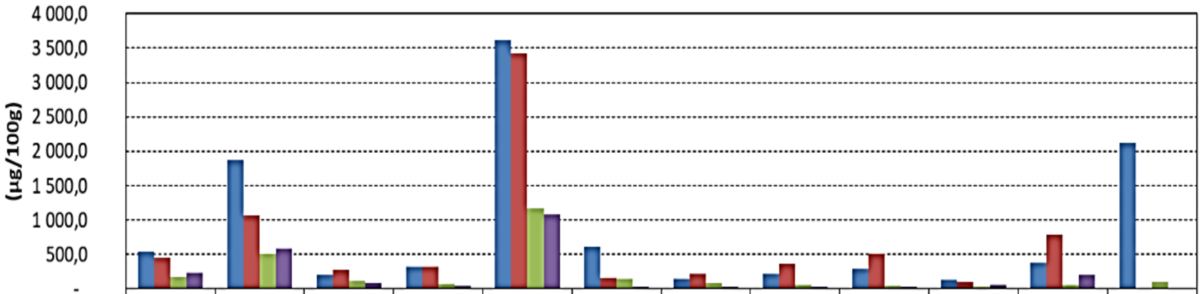

	Procyanidin B1	OH-benzoic acid	OH-cinamic acid	Procyanidin B2	Phenolic acid	Comaric acid	coffeic acid	Chlorogenic acid	Folic acid	Quercetin di-glucoside	Rutin	di-comaroyl quinic acid
BIBOR NY	543,4	1 881,2	204,1	323,7	3 616,3	616,0	142,5	218,8	297,9	130,6	374,2	2 117,5
CUK NY	451,0	1 063,6	282,0	315,8	3 419,8	163,8	218,9	369,5	512,7	109,4	791,1	-
PK NY	178,9	512,9	122,8	78,8	1 174,6	141,2	86,7	54,9	39,0	28,9	55,3	106,0
PO NY	236,9	587,0	94,7	40,3	1 079,5	35,1	35,1	32,1	24,3	52,8	197,6	-

Figure 18. Raw tomato mixtures prior to dehydration. (MATE laboratory, 2019)

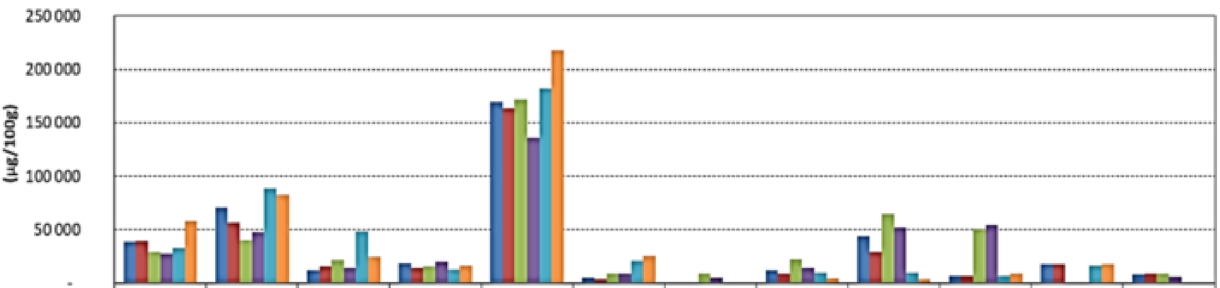

	Procyanidin B1	OH-benzoic acid	OH-cinamic acid	Procyanidin B2	Phenolic acid	Coumaric acid	coffeic acid	Chlorogenic acid	Folic acid	Quercetin di-glucoside	Rutin	di-coumaroyl quinic acid
BF ASZ	39 116	70 515	12 142	18 372	169 951	5 133	-	11 717	44 001	6 584	18 160	8 390
BKR ASZ	39 341	56 407	16 024	14 040	163 912	3 919	-	9 228	28 972	6 499	17 711	9 277
CF ASZ	29 325	40 109	21 402	15 680	171 989	9 188	9 243	22 393	64 922	50 837	-	8 858
CF ASZ	27 533	47 440	14 064	19 960	135 990	9 034	5 626	14 226	51 821	54 418	-	6 275
PK ASZ	32 865	88 244	48 645	12 764	182 016	21 257	-	9 448	10 000	7 035	16 181	-
PO ASZ	58 417	82 272	24 552	16 185	217 832	25 648	-	4 881	4 183	9 163	17 978	-

Figure 19. Mixtures of the dried tomatoes (Biborka and Cukorfalat repeat results in the top four rows, MATE laboratory, 2019)

Most important conclusions (and many more to list, but unlisted):

Among the dried tomatoes, the PO-ASZ species holds the highest lycopene concentration. The lowest concentration can be found in Cukorfalat. In spite of this, the Cukorfalat species showed a mere 4% (non-significant) loss in lycopene after processing. The loss for the PO-ASZ species was 37% during processing. The PK-ASZ species showed less degradation of lycopene at 15%. The content increased for beta-carotene – the most important source material of A-vitamin – in dried Cukorfalat and Biborka species, similarly to the first mixtures of fitoene, fitofluene and carotenoids' bio-synthesis. This proves that carotenoid's bio-synthesis continued to happen during the dehydration process of these two tomato species. The Cukorfalat and Biborka species are applicable to creating highly bioactive mixture content dried tomato products, which are important for modern and healthy diets. Price calculation: Table 1.

Table 1. Prices after dehydration, based on Auchan prices*

Name	**Euro/kg**	**Note**
Veres material (Biborka) - raw material price (Auchan)	7,71	Moisture content 88%
Energy price	0,76	Calculated
Processing price (wage, amortisation, operation)	0,55	Calculated
Total	9,03	Moisture content 20-25%
Dried (*Biborka veresi*)	36,10	Calculated

**380 HUF/Euro.*

6. Evaluation

In order to create an end product with sufficient moisture content, and keep the drying temperature between 50 and 60 centigrade at the same time, the energy amount reaching the material has to be managed. This necessitates an PLC-driven system, which optimises the energy of the microwave field, the speed of the conveyor belt, and the temperature and volume flow of the air current. Naturally, as different materials necessitate different technical parameters, experiments are necessary to determine them. The moisture content of materials to be dried has to be determined pre-dehydration, the type of material and the size of dicing also has to be accounted for. The desired end product's moisture content has to be defined. Using these data sets, the PLC controller can manage the process. The experiments validated data already present in literature, where microwave dehydration requires up to 40-70% less energy compared to conductive dehydration. The process of dehydration is significantly reduced in time.

During a gentler – low temperature – dehydration, valuable vitamins and minerals don't degrade significantly, neither in quality, nor in quantity.

The production costs and specific prices are advantageous according to calculation, much better than what was produced with traditional methods, and obtainable from the market. We may assume that final products will obtain positive reception on the market due to likeable taste and high nutrient content.

The developed small-industry and "laboratory" machinery's fundamental goal was to prove the concept of application.

Acknowledgement

The research was aided by the contract project „Megújuló energiaforrásokon alapuló és mikrohullámú anyagkezelési eljárással támogatott egyedi aszalási, szárítási berendezés kifejlesztése", ID. GINOP-2.1.2-8-1-4-16-2017-00315.

References

[1] **Aboltins A., Palabinskis J.**, (2018) Fruit Drying Process Investigation in Infrared Film Dryer. Agronomy Research 14 (1), 5–13, 2018

[2] **Beke J.**, (1997) Terményszárítás. Agroinform Budapest ISBN 983 502 646 3, 419 p

[3] **Beke, J.**, (1999) The Impact of Field Polarization on the Dewatering Process of Corn. Drying Technology, 17 (4) 687-699. p.

[4] **Beke, J., Mujumdar, A. S., Giroux M. S.**, (1997) Fundamental Attributes of Corn and Potato Drying in Microwave Fields. Drying Technology, 15 (1), 241-252.

[5] **Beke, J., Mujumdar, A.**, 1997 Hygrothermal properties of grains. In: Drying Technology in Agriculture and Food Sciences. Edited by A.S. Mujumdar. Science Publisher Inc., Enfield (NH), USA, 107-132. p.

[6] **Chen W., at al.**, (2017) Trends of spray drying: A critical review on drying of fruit and vegetable juices. Trends in Food Science & Technology Volume 65, July 2017, Pages 49-67

[7] **Dévay A.**, (2013) A gyógyszertechnológia alapjai, Pécsi Tudományegyetem Downloaded at 2016. https://www.tankonyvtar.hu/hu/tartalom/tamop412A/2011-0016_02

[8] **Moreno F.L., et al.**, (2018) Mathematical modelling of convective drying of fruits. A review Journal of Food Engineering Volume 223, April 2018, Pages 152-167

[9] **Saravacos G. D., et al.** (1999) Microwave/vacuum drying of model fruit gels. Journal of Food Engineering Volume 39, Issue 2, February 1999, Pages 117-122

[10] **Kurják Z., Bessenyei K.**, (2014) Morfológiai hatások a száradási folyamatban konvektív és mikrohullámú energiaközlés esetén, SZIE GEK Mezőgazdasági Technika, 6. sz.

[11] **Kurják Z., Barhács, A., Beke J.**, (2012) Energetic Analysis of Drying Biological Materials with High Moisture Content by Using Microwave Energy. Drying Technology 2012, 30 (3), 312-319.

[12] **Ludányi, L.**, (2004) Multimódusú mikrohullámú terek alkalmazása a szárításban. Doktori értekezés, SZIE. 153p.

[13] **Miller G., et al.**, (2012) Modeling heat and mass transfer process during convection drying of fruit. In Gu, Y T & Saha, S (Eds.) *Proceedings of the 4th International Conference on Computational Methods.* Queensland University of Technology, Australia, pp. 1-8.

[14] **Janowicz M., Lenart A.**, (2018) The impact of high pressure and drying processing on internal structure and quality of fruit. *European Food Research and Technology,* Volume 244, pages 1329–1340

[15] **Parviz A. Moghaddam, et al.**, (2016) Novel hybridized drying methods for processing of apple fruit: Energy conservation approach. Energy, Volume 103, 15 May 2016, Pages 679-687.

[16] **Radu A., et al.**, (2018) Insights in convective drying of fruit by coupled modeling of fruit drying, deformation, quality evolution and convective exchange with the airflow. Applied Thermal Engineering Volume 129, 25 January 2018, Pages 1026-1038

[17] **Szabó, G.**, (2005) Élelmiszerek minősége és a kombinált energiaközléses műveletek. Akadémiai doktori értekezés tézisei, 32p.

HUNGARIAN AGRICULTURAL ENGINEERING
No 41/2022 38-44
Published online: http://hae-journals.org/
HU ISSN 0864-7410 (Print)
HU ISSN 2415-9751(Online)
DOI: 10.17676/HAE.2022.41.38
Received: 02.05.2022 - Accepted: 26.05.2022

PERIODICAL
OF THE COMMITTEE OF AGRICULTURAL AND BIOSYSTEM ENGINEERING OF THE HUNGARIAN ACADEMY OF SCIENCES
and
HUNGARIAN UNIVERSITY OF AGRICULTURE AND LIFE SCIENCES
INSTITUTE OF TECHNOLOGY

HUNGARIAN UNIVERSITY OF AGRICULTURE AND LIFE SCIENCES
Institute of Technology

THE FINANCIAL INDICATORS OF TMR MONITORING ON DAIRY FARMS IN HUNGARY, AS PART OF QUALITY ASSURANCE TOOLS

Author(s):
G. Kövesdi[1], Sz. Orosz [1], Cs. Fogarassy [2]

Affiliation:
[1] Livestock Performance Testing Ltd., 2100 Gödöllő, Dózsa György u. 58., Hungary;
[2] Institute of Agriculture and Food Economics - Hungarian University of Agriculture and Life Sciences, 2100 Gödöllő, Páter Károly u. 1., Hungary;

Email address:
gretakovesdi@gmail.com; orosz.szilvia@atkf.hu; fogarassy.csaba@uni-mate.hu

Abstract: The TMR (total mixed ration) technology is one of the most sufficient feeding methods on the dairy farms. From a quality assurance and technological point of view, regular TMR testing is of paramount importance to reduce the risk and extent of milk production losses and animal health problems. The goal was to find out how popular the TMR monitoring in Hungary is, and find out, how much it may cost for a dairy farm in a year. In the course of our investigations, we assessed the economic indicators of TMR samples received by the NIR Forage Laboratory of Livestock Performance Testing Ltd. between 2013 and 2021, especially the distribution and size of costs per farm and per cow. Our aim was to be able to draw conclusions about the application rates, the total and relative costs of TMR analyses according to the farm size. The proportion of farms requesting TMR examinations was higher for farms with a larger number of animals (501-1000 cows inspected). Within the category, the highest TMR sample submission rate was found for the farms with 501-600 and 801-1000 cows inspected. The average monthly total TMR laboratory cost per site was extremely low in the period of 2013-2021 (HUF 3,000-10,000 /month/farm) compared to the risk and potential loss. The relative TMR cost of farms with more than 701 cows inspected was rather low (HUF 6-9 / inspected cow / month) in terms of screening for technological errors, risk of loss and quality assurance. This indicates that there is great potential for quality assurance in TMR studies at sites and that this potential is not currently being exploited.

Keywords: TMR testing, forage analytics, self control, financial indicator, quality assurance

1. Introduction

Many studies consider the total mixed ration (TMR) was the most significant advance in the worldwide dairy business in the previous 50 years [1]. It is a full diet that is prepared on a regular basis by dairy producers and originated in California in the early 1970s [2]. TMR is fed to a dairy cow to help it perform at its best [3][4][6]. The role of ruminal fermentation in dairy cow milk production has been discovered via research in dairy science. The goal is to provide the optimum possible ruminal environment for bacteria growth by combining particular nutritional amounts in the diet. The totally mixed rations (TMR) strategy addresses this demand by mixing all of the feed together and making it available for 20-22 hours a day, but several issues remain. There have been several reports of differences between theoretical and prepared TMR and successfully absorbed TMR by cows. This is accomplished by always delivering a nutritionally balanced diet, allowing cows to ingest as close to their real energy and nutrient requirements as possible while preserving the physical characteristics essential for optimum rumen function, which we now refer to as feed particle size. In order to achieve the best performance from cows good feeding management practices should be followed [7][8][9]. Examination of TMR samples would be useful in making a number of seemingly incomprehensible and 'unseen' anomalies 'visible'. Monitoring of TMR is extremely important to get a realistic picture of the composition of the mixture actually consumed by the cow, to shed light on measurement, mixing and technical problems (inaccurate measurement, inhomogeneity), to compare the measured values directly with the concentrations for a specific batch in the feed ration program (which will not be the same if the basic data are not based on specific measurement results) that may indicate intentional or negligent damage, and last, but not least, to shed light on the degree of variability / variance in the feed base and feeding system of the farm [7]. It is clear, that self-control in the aspect of TMR monitoring is cardinal. From a quality assurance and technological point of view, regular TMR testing is of paramount importance to reduce the risk and extent of milk production losses and animal health problems. This can be done by using NIR technology [8][9][10]. In this study, the goal was to find out how popular the TMR monitoring in Hungary is, and find out, how much it may cost a dairy farm. In the course of our investigations, we assessed the economic indicators of TMR samples received by the NIR Forage Laboratory of Livestock Performance Testing Ltd. between 1st April 2013 and 31st December 2021, especially the distribution and size of costs per farm and per cow. Our aim was to be able to draw conclusions about the application rates, the total and relative costs of TMR analyses according to the farm size based on the data of the samples received in the laboratory during the study period. Description of the TMR sampling frequency is important for both the farms and the laboratories, especially in the face of rising feed, raw material and fuel prices.

2. Materials and Methods

In the course of our research we used the database of the NIR Forage Laboratory of the Livestock Performance Testing Ltd., using a quantitative research model. With the help of this, we obtained data on TMR samples submitted by dairy farms between 1 April 2013 and 31 December 2021, which were inspected by Livestock Performance Testing Ltd. As the information used in the research were obtained and found by us and there were no direct connection between us and a person/ farm., the primer research model was used [11]. The basis of the quantitative approach is the quantification; we were able to retrieve data from the system using various filtering methods. With the help of these quantitative indicators, it was possible to group the answers clearly and follow regularities and draw conclusions [12][13].

2.1 Research design

All farms (152) requesting TMR examination were divided into 9 categories according to the number of cows inspected (101-200, 201-300, 301-400, 401-500, 501-600, 601-700, 701-800, 801-1000, 1001- Subsequently, the proportion of farms requesting TMR testing to the total number of farms (%), the proportion of farms requesting TMR testing to scale was calculated according to the number of cows inspected(%), the average annual total TMR laboratory testing cost (HUF thousand, 2013-2021), the average total annual TMR laboratory testing cost per farm (HUF thousand, 2013-2021), the average monthly total laboratory test cost per site (HUF thousand, 2013-2021) and the number of submitted TMR samples (pcs, 2013-2021). With the help of these calculations we were able to obtain additional information: the specific cost of TMR tests per 1 inspected cow (2013-2021, HUF / insp.cow), the specific annual cost of TMR tests per 1 inspected cow tested (2013-2021, HUF / insp.cow) and Specific monthly cost of TMR examinations per 1 inspected cow (2013-2021, HUF / insp.cow).

3. Results

In the examined period (2013-2021) a total of 6987 TMR samples were sent from 382 inspected farms (holding more than 100 inspected cows) to the Feed Analysis Laboratory of the Livestock Performance Ltd. to be tested. This means that the proportion of farms requesting a TMR test is 40%. The cost of all TMR examinations between 2013 and 2021 was HUF 111,785,000. This is an average of HUF 12,421,000 per year, while the annual average for farms is only HUF 42,000, which means a monthly TMR test cost of HUF 3,500.

The distribution of the frequency and total cost of TMR examinations by farm size is shown in Table 1.

Table 1. Distribution of frequency and total cost of TMR analyses by farm size

	101-200	201-300	301-400	401-500	501-600	601-700	701-800	801-1000	1001-
Number of farms	81	58	58	64	29	30	19	22	51
Total amount of requested TMR examinations 2013-2021, pcs	411	532	1225	1180	661	952	371	603	1052
Farms requesting TMR testing in proportion of total number of farms, %	13	14	15	16	10	9	5	7	11
Average annual TMR laboratory total cost per category (HUF thousand, 2013-2021)	731	946	2178	2098	1175	1692	660	1072	1870
Average annual TMR laboratory total cost per farm (HUF thousand, 2013-2021)	37	45	95	87	78	121	82	97	117
Average monthly TMR laboratory total cost per farm (HUF thousand, 2013-2021)	3	4	8	7	7	10	7	8	10

The cost distribution of TMR testing by farm size is shown in Table 2.

Table 2. Cost distribution of TMR analyses by farm size

	101-200	201-300	301-400	401-500	501-600	601-700	701-800	801-1000	1001-
Unit cost of TMR examinations per 1 inspected cow (2013-2021, HUF / insp.cow)	2480	1660	2332	1756	1314	1655	983	1000	612
Annual unit cost of TMR examinations per 1 inspected cow (2013-2021, HUF / insp.cow)	276	184	259	195	146	184	109	111	68

4. Discussion

Based on the data in Table 1, we found that approximately 60% of the farms requesting TMR testing were from farm with 500 or less cow populations. Farms with over 500 inspected cow farms achieved a share of 9-11% per category, of which farms with 701-800 and 801-1000 animals had the lowest rate (5 and 7%) of all farms keeping dairy cattle under control can be stated that the proportion was also weak in the case of farms counting 100-200 cows. Furthermore, we established that based on the database of ÁT Ltd. in the case of farm sizes close to the average number of cows on farms in Hungary (approx. 400 animals / farm), a higher

TMR testing requirement can be measured. This can be explained by the fact that the number of large farms is smaller than the number of dairy farms close to the average. In the category of large number of farms (81 pcs), but small sized (101-200 inspected cows), the TMR testing has a lower frequency.

The proportion of farms requesting TMR examinations per scale-based number of farms (Table 1) was higher for farms with a larger number of animals (501-1000 cows inspected), so in this case the frequency of sampling was higher. Within the category, the highest TMR sample submission rates were found for the 501-600 and 801-1000 cow counts inspected. An exception is the category of farms with more than 1000 cows, where the proportion has decreased. In the case of farms with 501-1000 inspected cows, the experts would presumably give more importance to self-control (higher risk of error, higher loss) and a larger budget is available, but the proportions are not indicated (the unit cost per cow is 2 shown in Table). In the category of farms with more than 1000 cows, international consultancy (US) is more common, in which case a different laboratory is used for the measurements due to the foreign consultant [14][15].

The average annual TMR laboratory total cost (Table 2) was the highest in the 301-400 and 401-500 cow farm categories due to the larger number of farms. This category therefore represents the potentially highest income for laboratories. However, the average monthly TMR laboratory total cost per farm proved to be extremely low (HUF 3,000-10,000 / month) compared to the risk and potential loss, indicating that there is great potential for quality assurance in TMR testing for farms and this potential is currently lacking of utilization.

For smaller farms (101-700 cows, especially 101-200 and 301-400 cows), the unit cost of TMR testing is higher. This is partly due to the lower number of cows. The unit TMR cost of farms holding more than 701 inspected cows was rather low (HUF 6-9 / inspected cow / month).

The proportion of farms requesting TMR examinations was higher for farms with a larger number of animals (501-1000 cows inspected), so in this case the frequency of sample submission was higher (Figure 1). Within the category, the highest TMR sample submission rate was found for the 501-600 and 801-1000 cows inspected. The average monthly total TMR laboratory cost per site was extremely low in the period of 2013-2021 (HUF 3,000-10,000 / month) compared to the risk and potential loss. Overall, the specific TMR cost of farms with more than 701 cows inspected was rather low (HUF 6-9 / inspected cow / month) in terms of screening for technological errors, risk of loss and quality assurance (Figure 2). This indicates that there is great potential for quality assurance in TMR studies at sites and that this potential is not currently being exploited. The reasons of such lack of monitoring can be many reasons. As checking the quality of TMR (or any other forage) is not under any kind of legal obligations in Hungary, farms tend to believe that by not sending their TMR in for quality reassuring, they are saving money.

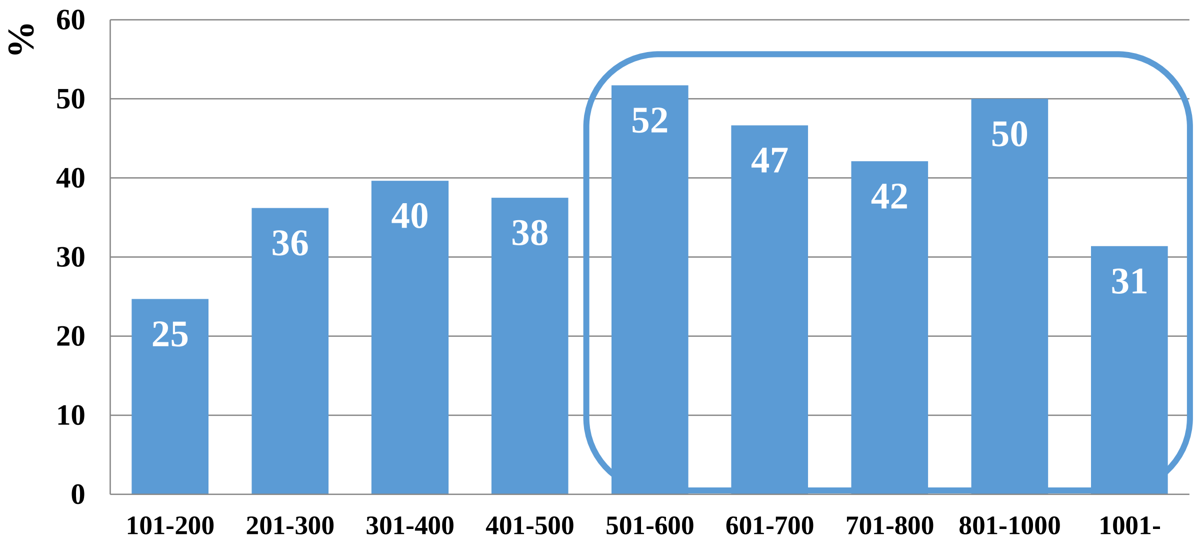

Figure 1. Farms requesting TMR testing in proportion of farm sizes, % (2013-2021, ÁT Kft. Database, %)

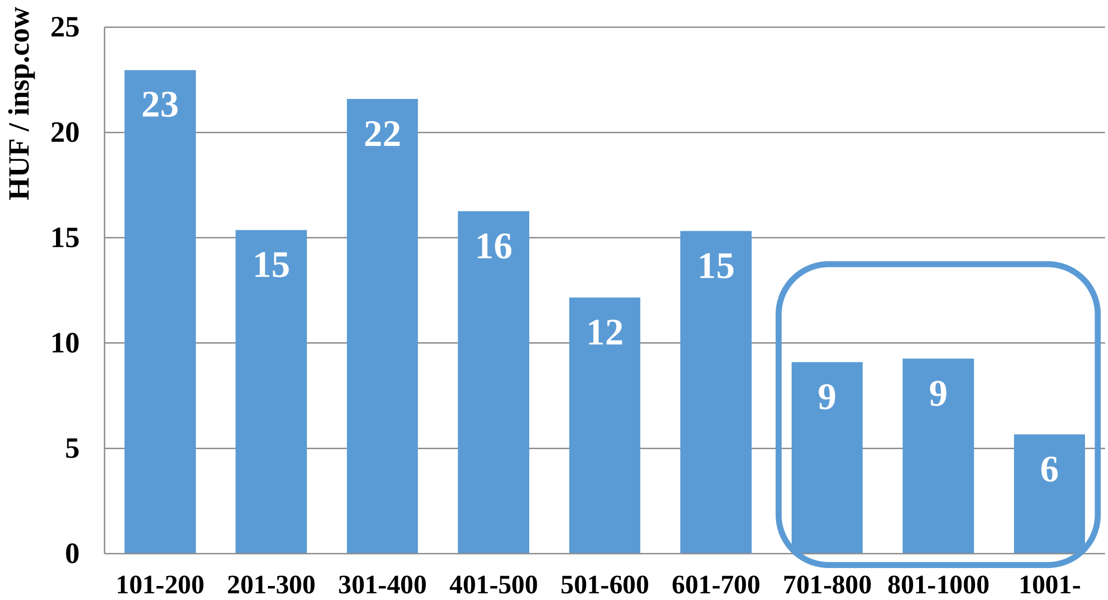

Figure 2. Monthly unit cost of TMR examinations per 1 inspected cow (2013-2021, HUF / insp.cow)

However, in case of quality assurance, these numbers are not promising. In order to understand and improve TMR quality, a lot more frequent testing is necessary. There is no method for determining the TMR's nutritional content based only on feel, texture, smell, or look. In truth, farmers have regularly bought or used TMR that has inferior nutritional content and is frequently uneconomical or counterproductive as a result of only sensory examination. Only after getting a representative sample of the forage and having that sample examined in an accredited laboratory can the forage's nutritional value be determined. It is possible to overestimate or underestimate the nutritional content of a forage lot by using tabular data from a nutritional guide. Long-term averages offer a standard by which farmers can evaluate a particular forage lot. The actual outcomes, however, will vary, sometimes greatly. This is the reason, why monthly testing is essential. Conducting a forage test is the only technique to determine the nutritional value and quality of the given TMR lot. Producers can reduce the cost of animal production and boost profitability by measuring, maintaining, and controlling the quality of the TMR and altering the diet as necessary [8].

5. Conclusions

To obtain the most performance out of cows given TMR, rations must be measured, mixed, tested, and monitored on a regular basis. Closing the loop on feed delivery to assess actual output and make modifications takes longer, but it's the only way to ensure that everything is done right. Regular, comprehensive laboratory testing of TMR samples can be costly; as a result, many farmers and consultants test only the components – but not the final TMR – to save money. With feed prices accounting for 40 to 50 percent of production expenses, this might not be the greatest place to save money [8]. The research clearly shows, that farms with a higher number of cows (501-1001-) tend to pay more attention to risk management and self controlling in terms of TMR testing. For ÁT Ltd. it is important to reach out to smaller farms and explain to them that even if TMR testing costs money, in the long run it helps with decision making and avoiding risks. Final conclusion is, in research conducted with young herds, TMR feeding minimizes feed selection, which can improve the accuracy and reliability of the test. TMR feeding of dairy cows has developed in the last half of the last 100 years. It allows for a more precise feeding of a nutritionally balanced diet, as the sorting and separation of ingredients is minimal. TMR feeding allows the incorporation of commodity by-products and special – sometimes unpleasant – ingredients into the diet. Cows suffer from less indigestion and milk fat depression and other health problems because they eat a consistently balanced nutritional diet. Feeding TMR allows feeding larger groups of cows faster and more economically than feeding forages and concentrates separately, but it comes with certain costs. In the case of larger herds, it may become economically feasible to further refine the grouping and feed ration. The increased use of robotic milking systems means new challenges and opportunities in herd feeding.

Acknowledgement

Special thanks to the National Research, Development and Innovation Office – NKFIH (Program ID: OTKA 131925).

References

[1] **Hein, T.,** (2021**)** United States: The wild and surprising history of TMR. Dairy Global. Accessed from: https://www.dairyglobal.net/health-and-nutrition/nutrition/united-states-the-wild-and-surprising-history-of-tmr/

[2] **Schingoethe, D., J.,** (2017) A 100 Year-Review: Total mixed ration feeding of dairy cows. Journal of Dairy Science, 100(12), 10143-10150. DOI:10.3168/jds.2017-12967

[3] **Drackley, J.,K., Cardoso, F.,C.,** (2014) Prepartum and postpartum nutritional management to optimize fertility in high-yielding dairy cows in confined TMR systems. Animal, 8(S1), 5-14. DOI:10.1017/S1751731114000731

[4] **Vibart R., Fellner V., Burns, J., Huntington G., Green, J.,** (2008) Performance of lactating dairy cows fed varying levels of total mixed ration and pastuer. Journal of Dairy Research, 75(4), 471-481 DOI:10.1017/S0022029908003361

[5] **Mantysaary, P., Khalili, H., Sariola, J.,** (2006) Effect of Feeding Frequency of a Total Mixed Ration on the Performance of High-Yielding Dairy Cows. Journal of Dairy Science 89(11), 4312-4320 DOI:10.3168/jds.S0022-0302(06)72478-X

[6] **Heinrich, J., Kmicikewycz, A.,** (2015) Feeding Management on TMR Systems. Dairy Herd Management. Accessed from: https://www.dairyherd.com/news/feeding-management-tmr-systems

[7] **Robinson, P. H.,** (1989) Dynamic Aspects of Feeding Management for Dairy Cows. Journal of Dairy Science 72(5), 1197-1209 DOI:10.3168/jds.S0022-0302(89)79224-9

[8] **Miller-Cushon, E.K., DeVries, T.J.,** (2017) Feed sorting in dairy cattle: Causes, consequences, and management. Journal of Dairy Science 100(5), 4172-4183 DOI:10.3168/jds.2016-11983

[9] **Coppock, C. E.,** (1977) Feeding Methods and Grouping Systems. Journal of Dairy Science 60(8), 1327-1336 DOI:10.3168/jds.S0022-0302(77)84030-7

[10] **Orosz, Sz.,** (2013) Gyenge pontunk: az önkontroll. Accessed from: http://static.atkft.hu/Cikkek/Takarmany/Onkontroll.pdf

[11] **Orosz, Sz.,** (2017) Egy fontos 'apróság'. Partnertájékoztató Hírlevél. Accessed from: http://static.atkft.hu/Cikkek/Gyep/Egyfontos_201701.pdf

[12] **Robinson, P. H., Meyer, D.,** (2010) Total Mixed Ration (TMR) Sampling Protocol. Agriculture and Natural Resources 8413

[13] **Evangelista, C., Basiricó, L., Bernabucci, U.,** (2021) An Overview on the Use of Near Infrared Spectroscopy (NIRS) on Farms for the Management of Dairy Cows. Agroiculture 2021,11,296 DOI:10.3390/agriculture11040296

[14] **Coppa, M., Martin B., Agabriel, C., Chassaing, C., Constant I., Andueza D.,** (2012) Authentication of cow feeding and geographic origin on milk using visible and near-infrared spectroscopy. Journal of Dairy Science 95, 5544-5551 DOI:10.3168/jds2011-5272

[15] **Hoffman, P. C.,** (2004) Sampling and Evaluating Total Mixed Rations. Focus on Forage 6(1)

[16] **Boncz, Im.,** (2015) Kutatásmódszertani alapismeretek. Pécsi Tudományegyetem Egészségtudományi Kar, 29-3

[17] **Watson, R.,** (2014) Quantitative Rresearch. Nursing Standard 29(31). DOI:10.7748/ns.29.31.44.e868

[18] **Bloomfield, J., Fisher, M.,J.,** (2019) Quantitative research design. Journal of the Australasian Rehabilitation Nurses Association 22(2), 27-30.

[19] Pothmann H., Nechanitzky, K., Sturmlechner F., Drillich, M., (2014) Consultancy to dairy farmers relating to animal health and herd health management on small-and medium-sized farms. Journal of Dairy Science 97(2) 851-861 DOI:10.3168/jds.2013-7364

[20] Stuth, J., Jama, A., Tolleson, D., (2003) Direct and indirect means of predicting forage quality through near infrared reflectance spectroscopy. Fiel Crops Research 84(1-2) 45-56. DOI:10.106/S0378-4290(03)00140-0

[21] Hancock, D.,W., et al. (2014) Understanding and Improving Forage Quality. UGA Extension Bulletin 1425

[22] Buckmaster, D., (2009) Optimizing Performance of TMR Mixers. Tri-State Dairy Nutrition Conference 105-117.

HUNGARIAN AGRICULTURAL ENGINEERING
No 41/2022 45-56
Published online: http://hae-journals.org/
HU ISSN 0864-7410 (Print)
HU ISSN 2415-9751(Online)
DOI: 10.17676/HAE.2022.41.45
Received: 07.05.2022 - Accepted: 31.05.2022

PERIODICAL
OF THE COMMITTEE OF AGRICULTURAL AND BIOSYSTEM ENGINEERING OF THE HUNGARIAN ACADEMY OF SCIENCES
and
HUNGARIAN UNIVERSITY OF AGRICULTURE AND LIFE SCIENCES
INSTITUTE OF TECHNOLOGY

HUNGARIAN UNIVERSITY OF AGRICULTURE AND LIFE SCIENCES
Institute of Technology

EXPERIMENTAL INVESTIGATION OF DROP-IN APPLICATION OF NATURAL REFRIGERANTS

Author(s):
P. Hermanucz[1]

Affiliation:
[1] Doctoral School of Mechanical Engineering – Hungarian University of Agriculture and Life Sciences, 2100 Gödöllő, Páter Károly u. 1., Hungary;

Email address:
hermanucz.peter@uni-mate.hu

Abstract: Cooling of raw materials and products in the food industry as well as in the whole food chain, including transportation and storage is an important task because it has a great impact to the product quality. This paper deal with the drop-in application of refrigerants in cooling systems used in the food industry. The focus of my research is to investigate the defrosting cycle of an evaporator in a cooling chamber with respect to the thermal medium used. Since during the process the temperature of the chamber can fluctuate, which can increase the deterioration of the stored food. My hypothesis is that if an environmentally or energetically beneficial change of refrigerant is implemented in a plant, the length of defrosting cycles will also change. My aim is to mathematically describe the relationship between refrigerants, chamber temperature and defrosting time. This will help to predict the effect of a possible refrigerant change on the length of the defrost cycle as a function of the chamber temperature.

Keywords: cooling system, natural refrigerant, drop-in, food storage, R290

1. Introduction

The need for refrigeration arises in different ways in different parts of the food chain: one way is to cool raw materials as quickly as possible, another is to achieve very low temperatures and, of course, to keep the temperature of the food product at a near constant level during transport and distribution. Artificial refrigeration is widely used to solve these problems.

An essential part of the refrigeration cycle is the refrigerant itself, which also poses some risks to global-environmental and human health. In many cases, the refrigeration circuit is in technically satisfactory condition, but replacing it would mean rebuilding or replacing the whole system because of the environmental impact of the refrigerant used. This is the case, for example, with the replacement of CFC or HFC refrigerants (R22, R32), which either have an ozone depleting potential or a global warming potential (GWP) that is too high [1], and where natural refrigerants with a lower GWP are available, such as R290 [2]. The solution to this problem is drop-in replacement, where no modification is required to the equipment, but only the refrigerant is replaced by a less environmentally damaging alternative.

But equally important is the risk posed by the quality of the refrigeration within each element of the cold chain, which has been investigated in several studies [3]. It has been found that the shelf life and deterioration of chilled products can be seriously affected by temperature fluctuations in the chilled compartment, as has been demonstrated by others [4]. Significant temperature fluctuations can be achieved even by opening the door of a simple household refrigerator [5]. Similar research [6] has also shown the effect of chamber temperature fluctuations on stored food products by simulation and measurement. There is a close correlation between the two, since the refrigerant used in the refrigeration circuits essentially determines the cooling capacity that can be achieved with a given piece of equipment [2] and, for equipment operating below 0°C, some characteristics of evaporator defrosting.

In industrial refrigeration system studies, it has been shown that hot gas defrosting, especially when applied with a time offset across multiple evaporators, resulted in a much more uniform internal temperature in the interior for air-to-air heat pumps compared to off-off defrosting [7]. However, this is only feasible for systems with multiple evaporators connected in parallel. In my case, the cooling chamber has only one evaporator, so this method is not applicable.

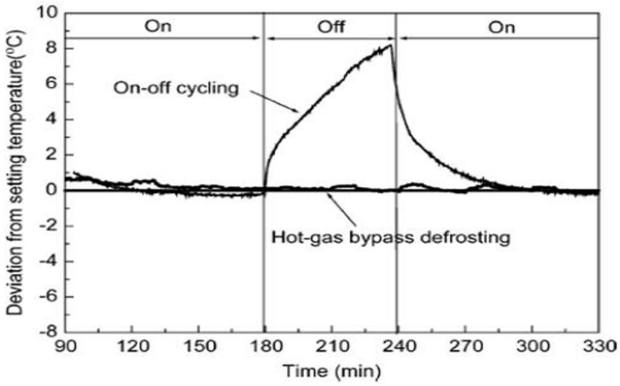

Figure 1. Comparison of on-off and hot gas defrosting [7]

For systems with a single evaporator, the temperature swing due to shut-down or hot gas defrosting is virtually identical to the "on-off cycling" shown in Figure 1, and therefore poses a serious quality risk to food stored in agricultural refrigeration equipment. The understanding of this temperature swing and the effect of refrigerant change on this phenomenon is a very important area of research, especially when considering the beneficial environmental impact of refrigerant change.

Although several evaporator designs are possible, the construction of evaporators used in industrial refrigeration is practically identical to that of simple air-to-air heat pump units. The evaporator's operation and its de-icing capabilities, and in many cases also its construction, are so similar that the evaporator of heat pumps can be used to model evaporators used in refrigeration chambers.

In this paper, I will investigate the de-icing options for evaporators, identify commonly used methods, and then measure the effect of refrigerant change on the length of defrost cycles. Finally, I will construct a simple mathematical model describing the relationship between the two, with parameters specific to the refrigerant.

2. The De-Icing Procedure

The evaporator of refrigerators and cooling chambers is an air-coolant heat exchanger consisting of finned copper tubes, the operation and modelling possibilities of which have been studied previously [8]. The refrigerant evaporates in the tubes, the heat flows through the fins from the air to the inside of the tubes. Consequently, the temperature inside the tubes is always lower than the air flowing through the evaporator. The water vapour in the air will condense on the fins to a certain extent. If the temperature of the fins reaches freezing point, they may become drier or the water that has condensed may freeze. In the case of a serpentine layer, the formation of the frozen layer occurs by the loss of the liquid phase, but in the case of refrigerated chambers, water may first condense on the fins and then freeze into ice of varying structure. I will refer to this phenomenon collectively as ice formation.

At low chamber temperatures, formation is reduced, as the absolute humidity of the air decreases significantly with decreasing air temperature. The advantage of this phenomenon is that it allows isothermal heat removal, which improves the COP of the cooling circuit, but the disadvantage is that the cross-section between the fins decreases, thus reducing the airflow. In addition, the dermal layer acts as an insulator, increasing the temperature difference between the two sides of the heat exchanger, thus reducing the evaporating temperature, and hence the evaporating pressure and ultimately the COP. In extreme cases, it makes the equipment completely inoperable, so it is necessary to guard against this phenomenon. Below are some procedures, perhaps little known, to prevent or remove the formation of a layer of dross.

2.1 Methods for avoiding and removing the ice layer

A method that can be used to avoid the formation of a layer of white frost is the hydrophobic treatment of surfaces. In this case, a hydrophobic paint is applied to the heat transfer surface, to which water droplets bind over a smaller surface area, thus improving the efficiency of the defrosting process. Some researchers have used a paint with hydrophobic properties, applied to the surface of the heat exchanger plates in a thickness of 30 μm [9]. This method is rather complementary to the others.

It is also possible to prevent ice formation using vibration, which is one of the simplest methods to prevent ice formation (frozen layer formation). Previously, the effect of vibrations has been investigated using an electrodynamic shaker with different amplitudes (40≤D≤100 mm) and frequencies (100≤f≤200 Hz) [10]. The results were encouraging, but in practice it is difficult to imagine an engineering solution where the whole evaporator is vibrated. This solution has also not been widely used in practice.

Ultrasonic ice breaking is also known. In this field, [11] experimented with high-frequency ultrasonic vibration and observed a reduction of the ice layer of about 60% using an ultrasonic source with a frequency of 37 kHz and an amplitude of 3.1 μm. The test was carried out for 90 min at an ambient temperature of 2°C and nearly 100% relative humidity on an aluminium plate. Similar studies [12] investigated the effect of ultrasonic vibration on the ice formation of a fin-tube evaporator subjected to natural convection. These test conditions cover only a small part of the cooling chamber applications.

However, very simple methods for defrosting are available. An example is the de-icing by compressor shutdown, which is analysed in detail in [13]. However, this method can only be used for chambers operating at temperatures above 0°C, which would significantly limit the applicability of the test results, and I have not dealt with this method in detail. Another very simple and widely used method is the electrically heated de-icing method investigated by [14]. In this case, an electric heating coil integrated in the evaporator performs the defrosting while the cooling circuit is not in operation. The disadvantage of this method is that temperature oscillations similar to those mentioned above are generated in the chamber. Furthermore, it is not energy efficient, as direct electric heating is always inferior to using a cooling circuit in heat pump mode.

The most common method, however, is the defrosting process by reversing the cooling cycle, which has been investigated by [15]. This method injects high-temperature refrigerant vapour from the compressor into the evaporator to accelerate the melting process. It is complex and relatively expensive to design, but the efficiency of the defrosting is better than, for example, electric filament defrosting, as the hot gas flows through the entire pipe network and can heat the entire surface of the heat exchanger. In this arrangement, the direction of the hot coolant vapour flow is the opposite of the normal operation and is therefore often referred to as reverse cycle hot gas defrosting, especially in the international literature. As this is the most common process, and the one I am investigating in my work, I will now look at the special features of this type.

2.2 The relation between defrost cycle and the refrigerant

In previous studies, measurements have been made to identify the automated defrost cycle of a cooling circuit. The results are presented in Figure 2.

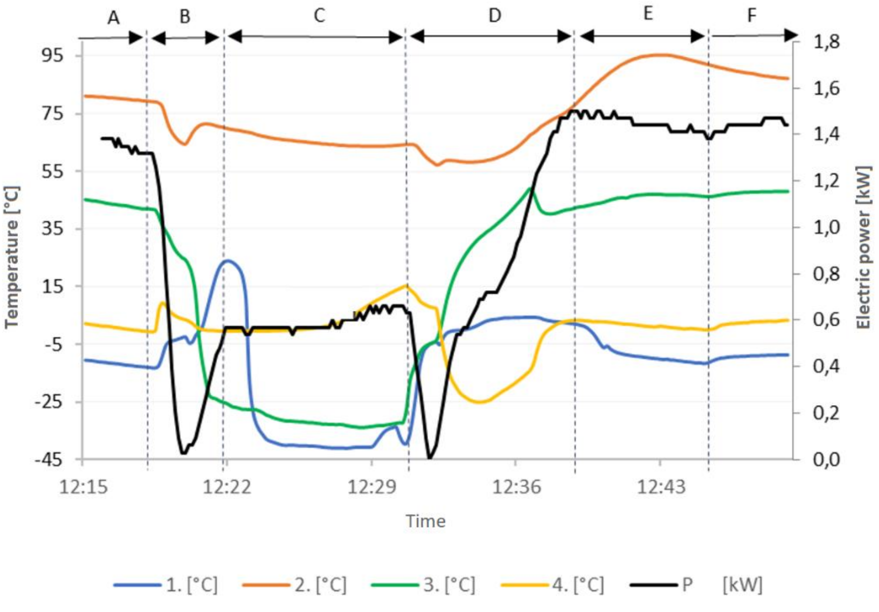

Figure 2. Temperature values measured during a typical defrost cycle

The diagram shows that at the end of stage C, the evaporator heats up to +15°C to achieve perfect defrosting. The same temperature during operation was between 0...-5°C, so a fluctuation of at least 15K can be observed. However, when the system is restarted, the evaporator can briefly cool down to -25°C, which underlines once again the importance of temperature swings and the need to avoid them or increase their periodicity. The names of the periods and the measured characteristics are shown in Tables 1 and 2.

Table 1. Parameters measured and their names in the cooling circuit

Designation	Mesured parameter
1	Compressor suction side temperature [°C]
2	Compressor discharge temperature [°C]
3	Condenser outlet temperature[°C]
4	Evaporator outlet temperature [°C]
Pel	Total electric power consumption of the system [kW]

Table 2. Designation and marking of registered periods

Period	Subrutin	Time range[s]
A	Normal operation in cooling mode	~1500
B	Decrease compressor speed and reversing the cycle	200
C	De-icing in reverse cycle	520
D	Restore the normal coolinc cycle and increase compressor speed	450
E	Warm-up the condenser	400
F	Normal operation in cooling operation	~1500

Figure 3 shows a simplified theoretical connection of the cooling circuit with the measurement points marked and the same points marked in the logp-h diagram.

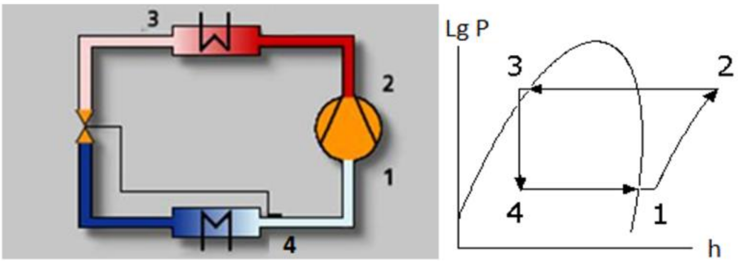

Figure 3. The measured parameters in the cooling circuit and in the logp-h diagram

From the above, it can be seen that the length of the "C" period and the period of the defrost cycle in a refrigerated chamber with an evaporator have a major influence on the temperature oscillations inside the chamber and, through this, on the quality of the stored food. In this paper, I investigate the length of the "C" period under unchanged settings when using two different refrigerants drop-in compared to the results obtained with the factory reference refrigerant.

3. Materials and Methods

In order to carry out the planned tests, I had to develop a suitable device, the outline of which is shown in Figure 4. The refrigeration circuit investigated had a nominal cooling capacity of 2.5 kW. The evaporator (labelled as ODU in the figure) was placed in a well-insulated chamber. The heat extracted from the chamber was partially covered by the heat flow entering the boundary structures, but a very large part was introduced in the form of latent heat as water vapor produced in the steam generator connected to the chamber. With this procedure, the highest possible humidity in the cooled space is achieved, which at the same time ensures the highest degree of frosting in the case of the tested evaporator.

This was necessary to ensure that the defrosting cycles were carried out as quickly as possible and under reproducible conditions. The experiments were not designed to reproduce the real operating conditions of a cold chamber, but focused on the scientific investigation of the defrosting cycles.

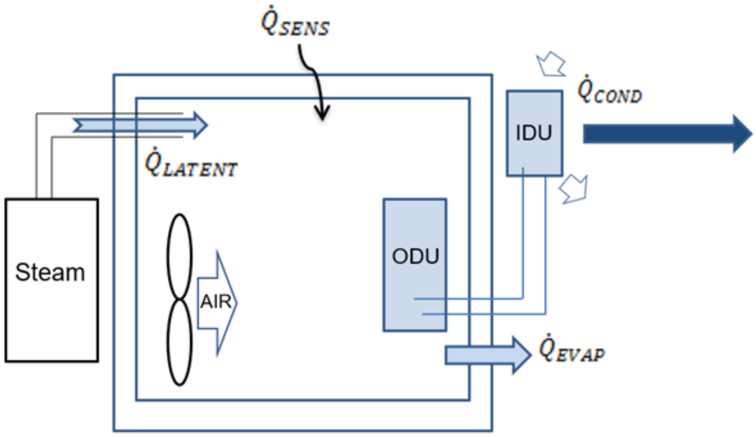

Figure 4. Schematic diagram of the measuring device

The condenser (labelled a IDU in the figure) was installed outside the chamber, so it is allowed to maintain a constant condensing temperature. The indoor temperature can be kept almost constant by changing the switching cycle time of the steam generator and by using air mixing fans. The air distribution in the tight space proved to be very even, the vertical temperature difference was not more than 1 °C. The air tightness of the chamber is adequate, as the 2 holes with 30 mm diameter, through which the electrical and refrigerant lines run, were sealed.

For the application of different refrigerants, I built new refrigerant connection points on the tested equipment, through which it was possible to drain the refrigerant, vacuum the system and drop-in the new refrigerant. With this method I was also able to perform pressure measurements for control purposes, too.

The procedure for changing the refrigerant was the same in all cases. The amount of charge was set so that the amount of material circulating in the system was constant. This meant different amounts by mass due to the different molar masses of the refrigerants. Compared to the reference R32, a larger amount of R410a was needed, while a smaller amount of R290a was needed.

3.1 Measuring devices

To study the defrosting cycles, it was necessary to analyse the transients and determine the time between them. The time was always determined in relation to a change in temperature values (the method for this is described later), so I used a 10s resolution machine recording. For my measurements, I used the so-called IMSy - Intelligent Measuring System, which has the great advantage of transmitting the measured values immediately to a server. The data can also be displayed on-line via the Internet, as shown in Figure 6. It is also possible to export the data retrospectively in .csv format for further processing. I used on-line display for the duration of the measurement, so that I could observe the unfolding of a defrost cycle in real time. The time duration of each stage was later determined using an excel spreadsheet.

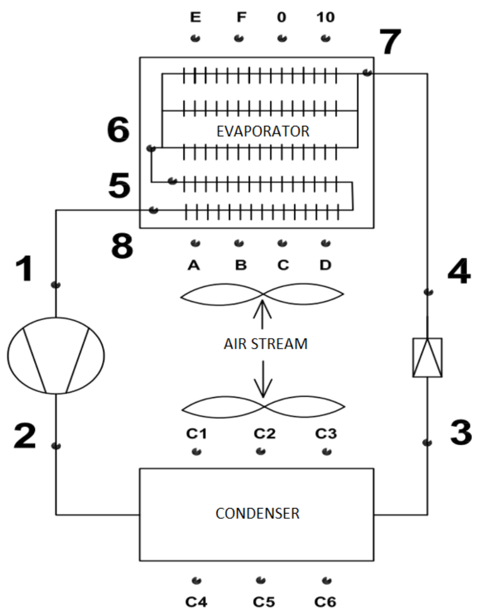

Figure 5. The measurement system and measurement locations

At each of the 24 measurement locations shown in Figure 5, measurements were taken with a Dallas DS18B20 digital thermometer with an accuracy of 0.5°C over the range -55...+125°C. The electrical power was measured using a TV0F11 device, while the relative humidity was measured using a DHT11 digital meter. The temperature sensors were fixed to the copper tubes inside the apparatus, secured with self-adhesive aluminium tape for proper heat conduction and shielded from external influences with closed-cell pipe insulation.

3.2 The investigated refrigerants

During my measurements, I used several refrigerants in the case of my defrost cycle test rig. These were R32, R290 and R410a, so I will briefly describe the properties of the refrigerants I used.

3.3 Refrigerant R410a

A blend of R32 and R125 (50/50 wt%), which is a near azeotropic blend, therefore has an extremely low temperature slip, and is almost non-fractionable during evaporation. Thus, there are less problems with leakage and no fear of the medium pair breaking up. It has an ODP of 0, a high GWP of 2088 and is therefore already being phased out of the market, which makes it interesting to investigate its substitutability. This blend is about 60% more pressurised than the cooling circuits designed for R290 and can only be used in new equipment designed for increased pressure. The use of R410a requires the use of POE (poly-olefin ester) lubricants.

3.4 Refrigerant R290

Today, hydrocarbon-based refrigerants are enjoying a renaissance because their ODP is 0 and their GWP is negligible. They were already used in refrigeration before the discovery and diffusion of Freon refrigerants, so they are not revolutionary, but their use does present a number of unprecedented challenges for both professionals and manufacturers. As hydrocarbons, they have a high flammability, which was not the case with the so-called safety refrigerants used until now. This property is problematic not only for installation but also for production, servicing and decommissioning, since these "gases", although marketed as a gas for combustion (R290 = pure propane), are not odorous in the air conditioning version, which makes it difficult to detect leaks by sensory means.

3.5 Refrigerant R32

It is the most recently used refrigerant, despite having been known for decades as a component of R410a. Its flammability and high pressure have long discouraged its use on its own, but its uptake has accelerated as climate protection goals have come to the fore. However, its combustion properties are much more favourable than those of hydrocarbon refrigerants, it is practically non-toxic, its ODP is of course 0 and its GWP is 675, which allows its wide use. The main physical properties of the refrigerants I have used are shown in Table 3.

Table 3. Physical properties of refrigerants used

Refrigerant	R290	R410A	R32
Composition	Propane 99.5% (Isobutane, n-butane)	Pentafluoro-ethane (R-125) 50% Difluoromethane (R32) 50%	100% Difluoromethane (R32)
Formula	**C_3H8** 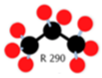	**CH2 F2, CHF2 CF3** 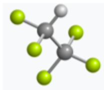 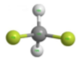	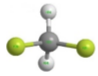 **CH_2 F_2**
Molecular weight	44.0 (g/mol)	72.6 (g/mol)	52.024 (g/mol)
Smell	Slight odor	Faint ethereal odor	Odorless
Freezing point	-185.89°C	Not determined	-136°C
Boiling temp. at 1.013 bar	-42.1°C	-51.58°C	-51.7°C
Critical temperature	96.67°C	72.13°C	78.35°C
Critical Pressure	42.50 Bar	49.26 Bar	58.16 Bar
LFL **HFL**	2.2% 9.5%	None	13.3% 29.3%
Auto-ignition temp.	480°C	>750°C	530°C
ODP	0	0	0

3.6 Settings and determination of defrost cycle times

With the help of the measuring system, the outside temperature can be set within very wide limits, however, I always kept the relative humidity at the maximum value. The setting value that best suited the purpose of my studies was determined during preliminary experiments. As a result, I decided to examine the chamber temperature between -10…+10°C in detail, and this will also be shown in the figures. My decision was based on the fact that at this temperature the air can still hold significant humidity, but it is sure to freeze on the surface of the heat exchanger. Of course, I performed several measurements in the range of -10…+2°C, but I only evaluated the length of the defrost cycles. Preliminary measurements show that this does not necessarily occur above + 2°C or only for a very long time, despite the fact that the evaporation temperature of the medium is slightly below freezing.

The settings were the same for all three refrigerants I tested, R410a, R32, and R290. The effect of the three refrigerants on the defrost cycles was investigated primarily, so I did not evaluate them from an energy point of view. The energy evaluation was performed only for the factory R32 gas charge.

In order to perform this task, it is absolutely necessary to know the time course of the temperatures reached at the characteristic points of the cooling circuit, as well as the intake and exhaust air temperatures play an important role. Correct, comparable measurements can only be made under laboratory conditions, where numerous interfering effects can be eliminated.

In the study of defrost cycles, the evaluation of transients was very important because I had to determine the beginning and end of the defrost cycle during these short periods. Given that the exact definition of the defrost cycle is not known, I will briefly describe the procedure I have used: I consider the defrost cycle to be the period during which the heat flow of the condenser is not positive. Based on this logic, I evaluated the data series in the excel spreadsheets and plotted the melting times in a graph using the method of least squares sum of deviations to judge the fit of the characteristic curves.

3.7 Mathematical background for data evaluation

I present the evaluation of the measurement data with the help of diagrams. I fitted a trend line to the data series, I gave the degree of fit (R2) and the root of the mean square error (RMSE) in the relevant cases, and I was able to draw useful conclusions from them. I used the formula presented below:

$$RMSE = \sqrt{\sum_{i=1}^{n} \frac{(\hat{y}_i - y_i)^2}{n}}, \tag{1}$$

where
$\hat{y}_i$ – the value determined by the function,
y_i – the value determined by the measurement,
n – the number of the observations.

The RMSE value shows how much the measurement results “scatter” around the fitted curve, expressed in the same dimension as the measured characteristic.

4. Results

Before the series of measurements were carried out, a test run of the measuring system was performed. According to my preliminary measurements, I cooled the chamber to -26°C without heating, which is limited by the factory protection of the cooling system. At this operating condition, the sensible heat input (Q_{sens}) entering the chamber through the walls was calculated. I calculated it to be only 19.6W/K, based on the difference in air temperature between the chamber and the laboratory. In the calculation, I assumed that the thermal power dissipated by the condenser was the combined power of the evaporator and the compressor. Since I measured the latter two, I can calculate the power absorbed by the evaporator, which is practically equal to the sensible heat flux entering the chamber. This means that for the settings I used, the maximum sensible heat flux entering the walls was 530W, which did not significantly affect the humidification efficiency. In the case I tested, the sensible heat flux entering the dampening system did not exceed 20% of the total heat flux extracted, so it did not significantly affect the measurement.

The test measurements were carried out in the chamber temperature range -26...+15°C. On this basis, I found that the best range for determining the length of defrost cycles was -10...+2°C.

I also verified the proper functioning of the data logging system and found from the recorded data that as soon as the evaporator temperature deviates significantly from the inlet air temperature, the equipment starts the defrost cycle. The cycles follow at regular intervals and, in addition to the temperature measured at 24 locations, the relative humidity inside and outside the chamber can be displayed. This means that the length of the cycles is always determined by the same algorithm set by the manufacturer. Accordingly, measurements with different refrigerants can be compared. I have documented the location and identification of the sensors, which are shown with a textual explanation in the evaluation, while the diagram shows their unique identification. Data for a typical defrost period are shown in Figure 6.

I controlled the temperature of the test chamber with the amount of introduced steam. My goal was to keep the relative humidity of the chamber at a maximum value, which gives the best result in term of the defrost cycles and is reproducible as well. As the temperature of the chamber increases, so does the amount of heat extracted, and thus the amount of steam introduced in a given time. However, this is not a problem for testing the length of the defrost cycles, as I found that the unit always starts defrosting under the same conditions, i.e. when the difference between the refrigerant leaving the evaporator and the chamber temperature increases. This could be found in the Figure 6. Thus, the length of the cycle is not affected by the degree of wetting, only the period time.

Measurements to determine the length of the defrost cycles were performed in the temperature range of -10 and + 1°C with at least 4 settings and 3 repetitions per refrigerant. The purpose of the studies was not to show the difference between the refrigerants, but to demonstrate that the trend is generally true regardless of the properties of the refrigerant. At the same time, I consider it's important from an environmental point of view to study the behaviour of R290 refrigerant in the refrigerant circuit, as it has significant environmental advantages over R410a and its COP does not lag behind it in the case of properly sized refrigerant circuits. The test for R32 refrigerant was justified by the fact that many equipment is supplied with this refrigerant today. The results are shown in Figure 7.

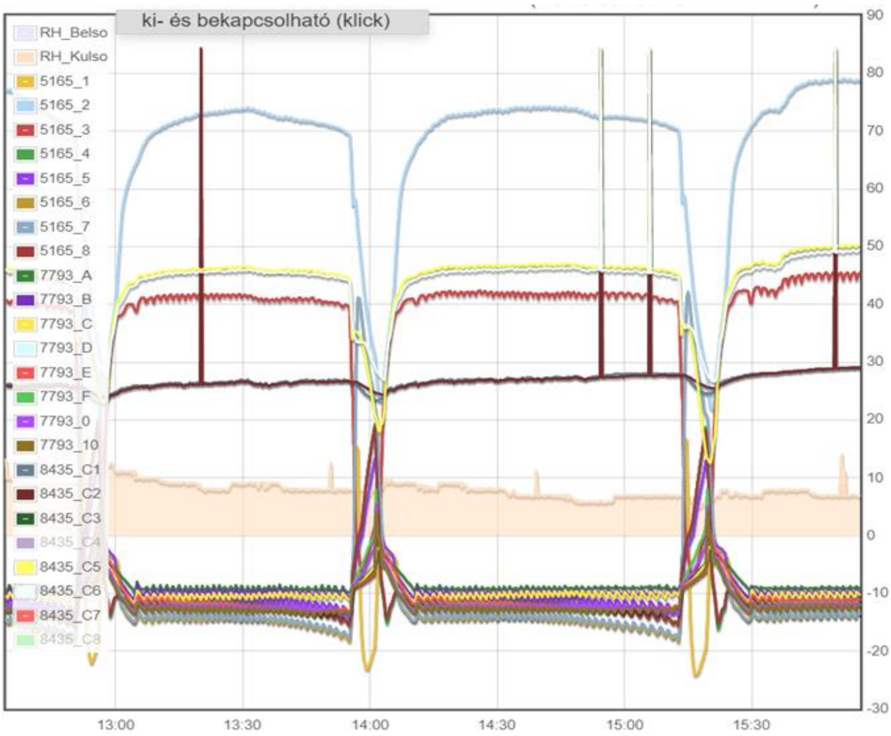

Figure 6. Data stream displayed by the measurement system in real time

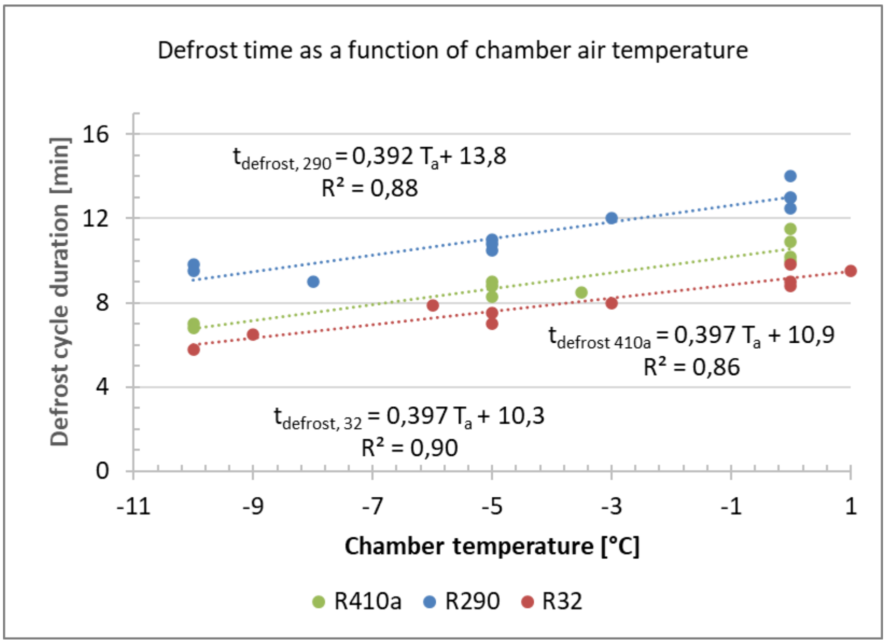

Figure 7. Defrosting time as a function of chamber temperature for three refrigerants

It can be observed that I obtained an increasing defrost time as the chamber temperature increased. This can be explained by the phenomenon that the structure of the frost layer changes at low temperatures, so condensation and freezing of smaller amounts of water already significantly impairs heat transfer. Thus, at lower chamber temperatures, less condensate must be melted, which can be achieved with less energy. In other words, with increasing chamber temperature, more condensate must freeze to reduce the same heat transfer, so more energy is needed in one cycle, resulting in a longer defrost cycle. Given that I did not find any information during the detailed literature review, I consider the above to be a new scientific result.

Defrost cycles are practically non-existent at temperatures above +2°C. Mathematically, this would mean that the plotted curves would drop sharply to 0 here, the physical content of which would be difficult to identify. The explanation for this phenomenon lies in the defrosting strategy of the cooling circuit: defrosting always starts when the temperature of the evaporator outlet line falls below the intake air temperature by a certain value, as shown in Figure 6. As this is an artificial intervention that affects the time elapsed between the defrost cycles, it is possible that a unit jump transition may occur in the behavior of the defrost cycles. This is accompanied by a change in period time. Based on the equations shown in the diagram, I conclude that there is a linear relationship between the defrost cycle time and the outside air temperature, which is

$$t_{defrost} = L \cdot T_a + E \tag{2}$$

describes a general relation, where the constants L and E for the refrigerants I tested are described in the Table 4.

Table 4. The constants I determined for each refrigerant

Refrigerant	L	E	R^2	RMSE
R32	0,397	10,3	0,9	0,97
R290	0,392	13,8	0,86	0,99
R410a	0,397	10,9	0,88	0,55

R2 characterizes the fit of the function, the value of RMSE shows the scatter of the measured values relative to the fitted function. These constants can be used to calculate, among other things, the reduction in operating time caused by defrost cycles.

My suggestion was also confirmed by the examination of the amount of condensate belonging to each cycle, because in the case of each refrigerant I was able to collect an increasing amount of condensate as the chamber temperature increased. I measured the amount of condensate per cycle using a measuring cylinder when using refrigerant R290. The results are shown in Figure 8.

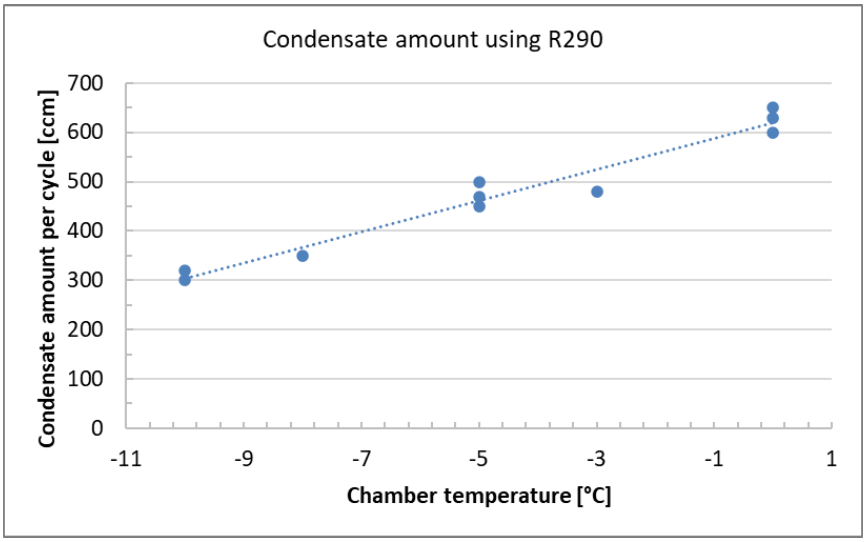

Figure 8. the amount of condensate for R290 operation

The Figure 8 shows that as the chamber temperature increased from -10°C to 0°C, the volume of the condensate increased from 310cm^3 to 630cm^3. This increase in volume justifies the increase in defrosting time over the same test temperature range.

5. Discussion

The results of my research can be used for food, energy and environmental purposes, among others. For example, the new correlations established from the experiments can be used to describe the defrosting time of the evaporator in a food refrigeration chamber if the refrigerant used in the refrigeration circuit is replaced by another refrigerant using a drop-in process. A possible solution to the problem studied in [7], or a possibility to predict the problem for several refrigerants using the same equipment, has thus been explored.

At first glance, an increasing defrost time with increasing chamber temperature may seem strange. The phenomenon is also one of the less researched topics. In investigating the reasons for this phenomenon, I found that the amount of condensate per defrost cycle increases in proportion to the chamber temperature, i.e. for higher chamber temperatures, the cycle starts at higher condensate amounts with the same defrost logic. This explains the increase in time required for defrosting.

Drop-in replacement of refrigerants can also have significant environmental benefits. Old refrigerants with high GWP can be replaced by modern alternatives with little or negligible environmental impact without any technical intervention on the equipment. An example of such a replacement is the substitution of R410a or R32 (GWP=2088...675) with R290 (GWP=3), which I have investigated.

6. Conclusions

Summarizing the results of the measurements, it can be concluded that drop-in replacement of refrigerants is feasible in the investigated thermal cycle. With R410a and R290 refrigerants used in the same quantity instead of the originally used R32 refrigerant, the refrigeration circuit remained operable without any modifications. No anomalies were observed in the experiments and the energy characteristics of the equipment did not differ significantly from those of the original refrigerant.

The experimental set-up proved to be suitable for measuring the length of defrosting cycles in a reproducible way, as the cycles followed each other with almost the same periodicity when measured at the given settings.

A correlation between the length of defrost cycles, the chamber temperature and the type of refrigerant used was found and mathematically defined. This suggests that there is a clear and inefficient relationship between defrosting time and chamber temperature. Furthermore, a relationship between the vertical offset of the function describing the defrost cycle length and the type of refrigerant can be established. By examining the amount of condensate per defrost cycle when using refrigerant R290, I found that it increases in proportion to the chamber temperature.

Acknowledgement

This work was “Supported by the ÚNKP-21-4-I-MATE/8 New National Excellence Program of the Ministry for Innovation and Technology”.

References

[1] **Cardoso, B.J., Lamas, F.B., Gaspar, A.R., Ribeiro, J.B.** (2017) Refrigerants used in the Portuguese food industry: Current status. International journal of refrigeration, vol. 83 p. 60–74

[2] **Harby, K.** (2017) Hydrocarbons and their mixtures as alternatives to environmental unfriendly halogenated refrigerants: An updated overview. Renewable and Sustainable Energy Reviews, Vol.73 p.1247-1264

[3] **Korzenszky, P., Adebayo, S.** (2018) Cooling and Storing Energetic Analysis in Food Technology In: Géczi, G., Korzenszky, P. (editor): Researched Risk Factors of Food Chain Gödöllő, Hungary, Szent István Egyetemi Kiadó p. 131-134, 4p.

[4] **Géczi, G., Korzenszky, P., Szakmár, K.** (2017) Cold chain interruption by consumers significantly reduces shelf life of vacuum-packed pork ham slices. Acta Alimentaria: An International Journal of Food Science 46: 4 p. 508-516, 9 p.

[5] **Géczi, G., Dodog, Z., Székely, L., Veres, A.** (2018) Examining the effect of door opening on the operation of domestic fridge In: Géczi, G., Korzenszky, P. (editor) Researched Risk Factors of Food Chain Gödöllő, Hungary, Szent István Egyetemi Kiadó p. 127-130, 4 p.

[6] **Ghabour, R., Kassebi, S., K., Korzenszky, P.** (2021) Simulation and Experiment of Apple Fruits in Domestic Fridge. Hungarian Agricultural Research: Environmental Management Land Use Biodiversity 30: 2 p. 11-14, 4p.

[7] **Cho, H., Kim, Y., Jang, I.** (2005) Performance of a showcase refrigeration system with multievaporator during on-off cycling and hot-gas bypass defrost. Energy, 30, p. 1915–1930.

[8] **Garbai, L., Méhes, Sz.** (2007) System Theory Models of Different Types of Heat Pumps. IASME / WSEAS International Conference on Energy & Environment, Portoroz, Slovenia, May 15-17, 2007.

[9] **Huang, L., Liu, Z., Liu, Y., Gou, Y., Wang, J.** (2009) Experimental study on frost release on fin-and-tube heat exchangers by use of a novel anti-frosting paint. Experimental Thermal Fluid Science, 33, p. 1049–1054.

[10] **Cheng, C-H., Shiu, C-C.** (2003) Oscillation effects on frost formation and liquid droplet solidification on a cold plate in atmospheric air flow. International Journal of Refrigeration, 26, p. 69–78.

[11] **Adachi, K., Saiki, K., Sato, H., Ito, T.** (2003) Ultrasonic frost suppression. Journal of Applied Physics, 42, p. 682–685.

[12] **Wang, D., Tao, T., Xu, G., Luo, A., Kang, S.** (2012) Experimental study on frosting suppression for a finned-tube evaporator using ultrasonic vibration. Experimental Thermal Fluid Science, 36, p. 1–11.

[13] **Ameen, F. R., Coney, J. E. R., Sheppard, C. G. W.** (1993) Experimental study of warm-air defrosting of heat-pump evaporators. International Journal of Refrigeration, 16, p. 13-18.

[14] **Bansal, P., Fothergill, D., Fernandes, R.** (2010) Thermal analysis of the defrost cycle in a domestic freezer. International Journal of Refrigeration, 33, p. 589-599.

[15] **Jiang, Y., Dong, J., Qu, M., Deng, S., Yao, Y.** (2013) A novel defrosting control method based on the degree of refrigerant superheat for air source heat pumps. International Journal of Refrigeration, 36, p. 2278–2288.

HUNGARIAN AGRICULTURAL ENGINEERING
No 41/2022 57-65
Published online: http://hae-journals.org/
HU ISSN 0864-7410 (Print)
HU ISSN 2415-9751(Online)
DOI: 10.17676/HAE.2022.41.57
Received: 30.05.2022 - Accepted: 20.06.2022

PERIODICAL
OF THE COMMITTEE OF AGRICULTURAL AND BIOSYSTEM ENGINEERING OF THE HUNGARIAN ACADEMY OF SCIENCES
and
HUNGARIAN UNIVERSITY OF AGRICULTURE AND LIFE SCIENCES
INSTITUTE OF TECHNOLOGY

FUZZY ARITHMETICS IN THE EVALUATION OF QUALITY CHARACTERISTICS OF HIGH-PRESSURE FOOD PRESERVATION PROCEDURES

Author(s):
Z. Sebestyén[1], I. Szabó[2], N. Schrempf[2], P. Korzenszky[2], P. Víg[1], A. Veres[1]✉

Affiliation:
[1] Institute of Mathematics and Basic Science, Hungarian University of Agriculture and Life Sciences 2100 Gödöllő, Páter Károly u. 1., Hungary.
[2] Institute of Technology, Hungarian University of Agriculture and Life Sciences, 2100 Gödöllő, Páter Károly u. 1., Hungary.

Email address:
Veres.Antal@uni-mate.hu

Abstract: In recent decades increasing consumer awareness the innovations in the very different fields of technology and changes in societal norms have led to changes in food consumption patterns. The growing demand for minimally processed natural-textured, healthy, and microbiologically safe foods has shifted processing toward high-pressure preservation rather than traditional heat treatment processes. In recent years, fuzzy control has become important in the application of technology, which is able to meet the quality expectations of consumers by dealing with the blurred boundaries of various everyday product characteristics (taste, colour, texture, etc.). The applicability of fuzzy logic has been shown to be effective in a variety of process controls, including preservation procedures. The aim of this work is to summarize the basics of fuzzy arithmetic required in the fuzzy controls used in high-pressure preservation processes.

Keywords: fuzzy logic, fuzzy arithmetic, food safety, food quality, high pressure food processing

1. Introduction

As a consequence of globalization and improved consumer awareness associated with rising living standards, the food industry turned to an innovative stage in recent decades. Consumer trends are constantly changing. It means a daily active challenge for companies in the food preservation sector to satisfy customer needs and maintain their market share. Consumers demand high quality and convenient products, with natural flavour and taste, and very much appreciate the fresh appearance of minimally processed food in addition to microbiological safety [1].

In Hungary, the economic development of the last 10 years is reflected in food consumption as well where international trends are strengthening. The increase in solvent demand has led to a wider range of products, and to an evolution in quality and a higher need for these kinds of products as well [2]. As a result of the strengthening of consumer awareness, low-income consumers are also looking for high-quality products in the appropriate price categories [3].

These shifts in demand have led the international food market suppliers to search for and apply new methods, combine older ones to merge production processes that ensure the high quality with the efficiency of mass-production. Preservation technology plays a key role in quality improvement. Traditional heat treatment-based processes are only partially able to meet requirements such as preserving the appearance and taste of the product due to the harmful effects of heat. In present the usage of modern control processes in food production is fundamental to guarantee efficiency in production both for costs and quality.

Based on international literature for the past 30 years, the appearance of fuzzy control in high-pressure preservation processes is relatively new, but it offers a promising solution to the challenges of modern food quality requirements.

Preservation of food under high pressure dates to the 20th century. Although the technology was available at the beginning of the 19th century [4, 5], wide-range industrial application had not progressed for nearly 100 years. The development of high-pressure equipment started in the early 1990s, particularly with respect to pressure tolerance testing of microorganisms [6]. The technology is known in the industry by several names such as HPP (High Pressure Processing) or HHP (High Hydrostatic Processing), and at the end of the last century it was marked by Knorr [7] in 1993 and by Hoover [8] in 1997 as one of the most promising non-thermal food preservation processes. Its main advantage is the negligible effect on the organoleptic properties and intrinsic values of the treated products.

Nowadays, products that are preserved under high pressure, such as juices, purees, yoghurts, eggs and meat products, account for an increasing share of the market worldwide. In the last 30 years, numerous researches have studied the safety of food processing and the compliance of the customers with the quality requirements. Based on these studies it can be stated that technological developments need to be implemented on regional, company and most of all on the product level. Examination of food ingredients alone is not sufficient to predict their interactions in the products.

2. The role of fuzzy logic

Basic food quality aspects (taste, texture, etc.) are usually described in the words of everyday language: excellent, good, average, acceptable, unsatisfactory. It is easy to see that the bounds of these categories are not sharp enough to handle them with the usage of classic logic. The same is true if we want to characterize how important a particular quality characteristic (such as color) is in the terms of the „image” of the product: very important, fairly important, less important, and so on.

To be able to process these uncertain data (performing operations, make rankings, statistical evaluation), they need to be quantified. Fuzzy numbers are generalizations of crisp numbers that also carry the numerical uncertainty of the qualitative (linguistic) categories.

Fuzzy sets were introduced independently by Zadeh [9] in 1965 and Dieter Klaua [10, 11] in 1965 and 1966 as an extension of the classical notion of set. In the years that followed, fuzzy theory developed slowly, and the first successful technical and industrial adaptation was unpredictable.

Zadeh proposed the concept of linguistic variables in the models describing highly complex systems. Here, instead of an exact numerical value, generalized fuzzy intervals, kernel values and fuzzy membership functions take over the role. The advantage of this approach is that the values in the intermediate regions can be given by convex combinations of membership functions. Although the Zadeh’s method resulted reduction in complexity compared to the previous symbolic approach, the number of state variables remained exponential. Computational demands were reduced by Mamdani, and he was the first who also successfully implemented the control to a non-linear model of a steam boiler system.

In our research numerous case studies were reviewed of the industrial implementation of fuzzy controlled high pressure preservation technologies, especially in the term of the connection with food quality characteristics. Víg et al. [12] in 2021 examined several case studies in high pressure preservation, particularly in terms of applicability and process control implementation. In the recent works of Chutia et al. [13] in 2020 and Kausik et al. [14] in 2015 two implementations were presented of fuzzy controlled high-pressure preservation of fruit juices, which technology is proved to be more satisfying in quality and shelf live compared to heat treatment processes. In these works, and generally in the theory of fuzzy control including the process of evaluating data fuzzy arithmetic plays an important role, and understanding this theoretical background is essential to be able to improve methods and algorithms.

Foundation and different types of approaches toward fuzzy set theory has a wide range of literature in mathematics. Gottwald [15] in 2008 classified these approaches in 40-years backward highlighting in conclusion the importance of the classic way presented by Zadeh. The main aim of the present work is to briefly summarize the mathematical background of fuzzy arithmetic.

3. Fuzzy arithmetic

3.1. Fuzzy sets

In this section we summarize those concepts and results of the theory of fuzzy sets which play important role in various applications based on the works of Fodor et al. [16] and Grzegorzewski et al. [17].

The word „fuzzy" has different meanings in suitable contexts. In scientific and technical fields the term „fuzzy" refers to any uncertain, inaccurate object having no clear boundary.

According to the well-known axiom of the classical set theory, for any object x and any set A, it is uniquely decided whether x belongs to A or not. Assuming that A is a subset of a fixed set X, A can be identified with its characteristic function:

$$\chi_A(x) := \begin{cases} 1, if\ x \in A, \\ 0, if\ x \notin A. \end{cases}$$

Elements of X belonging to A and those not belonging to A can be distinguished from each other by means of the characteristic function of A.

In case of fuzzy sets, on the other hand, some transitions are allowed. A fuzzy set A can be given by its membership function, a generalization of the characteristic function. A mapping $\mu: X \to [0,1]$, that is, a function μ defined on X with values between 0 and 1, is called a membership function. For a given $x \in X$, the number $\mu_A(x)$ expresses how much x is compatible with the notion described by the fuzzy set A. The higher this function value is, the more x belongs to the mentioned set.

In addition to numerous classic literary examples of the need and usage of fuzzy sets, food industry applications appear widely in recent research. Korzenszky et al. [18] investigated the connection between the apple (species: Golden Delicious) ripeness and skin coloration based on the CIELAB color space system, which is based on the opponent color model of human vision, where the pairs red and green, and blue and yellow form an opponent pair. In the research ripeness is defined by three categories: unripe, ripe and overripe based on the green-red skin color transition (a^* value in CIELAB). The apples between the a^* values -6 and 10 are regarded as ripe, then the corresponding a^* values belong to the interval [-6,10], the characteristic function of which is shown on Figure 1.

According to the classical set theory, an apple with $a^* = 7$ regarded as unripe suddenly becomes ripe at -6. Instead, it is more reasonable to say that an apple is ripe at $a^* = 2$. It does not mean that any apple with $a*$ value between -6 and 10 is not ripe, but rather that, the farther the value from 2 is, the less the apple is regarded as ripe. Furthermore, for example any apple is not ripe if $a^* < -6$ or $a^* > 10$.

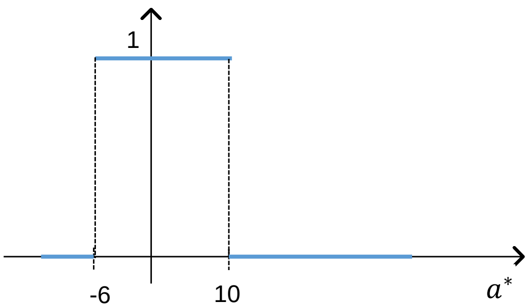

Figure 1. The characteristic function of ripeness (Golden Delicious apple)

Figure 2. represents a possible membership function of the ripe property. The grade (membership value) decreases linearly from 1 to 0 towards the endpoints of the interval [-6, 10].

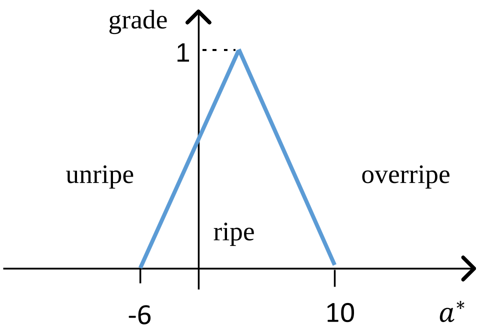

Figure 2. A possible membership function of ripeness (Golden Delicious apple).

Any fuzzy subset of X is identified with its membership function. Since every characteristic function is also a membership function, every traditional subset of X is also a fuzzy subset of X, due to this identification.

The following concepts related to fuzzy sets will be formulated by means of the membership functions so that they will be compatible with the corresponding classical definitions in case of ordinary sets. Thus, two fuzzy sets are equal if and only if their membership functions are identical.

Similarly, the fuzzy set A is a subset of the fuzzy set B, if the membership function of A is smaller than or equal to that of B at any point:

$$A \subset B \text{ if and only if } \mu_A(x) \leq \mu_B(x) \text{ for all } x \in X.$$

Let $\alpha \in]0,1]$, we define the α-cuts of A as

$$A_\alpha := \{x \in X \,|\mu_A(a) \geq \alpha\}.$$

That is, A_α contains all elements of X, which are compatible with A at least at level α. The α-cuts are monotonous in the following sense:

$$0 < \alpha \leq \beta < 1 \text{ implies } A_\alpha \supseteq A_\beta.$$

The *core* of a fuzzy set A consists of those elements in X, which are completely compatible with A:

$$core\ A := \{x \in X \,|\mu_A(x) = 1\} = A_1.$$

The *support* of a fuzzy set A consists of those elements in X, for which the membership function values are positive, i.e.,

$$supp\ A := \{x \in X \,|\mu_A(x) > 0\}.$$

3.2. Operations on fuzzy sets

Let X be a given set, A be a fuzzy subset of X, whose membership function is $\mu_A: X \to [0,1]$. The *complement* of A is the fuzzy set $\overline{A}$, whose membership function is defined as

$$\mu_{\overline{A}}(x) := 1 - \mu_A(x).$$

For example, if A is the fuzzy set of the ripe apples, then $\overline{A}$ denotes that of the non-ripe ones. Using the previous example, the membership function of $\overline{A}$ is the following:

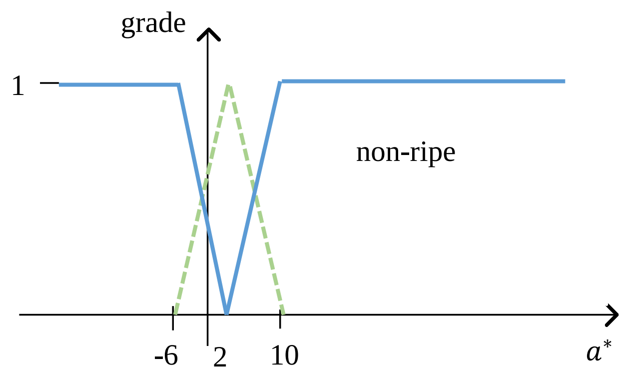

Figure 3. Membership function of non-ripe apples (Golden Delicious apple).

Let A and B be fuzzy subsets of X with membership functions μ_A and μ_B, respectively. The union of A and B is the fuzzy set $A \cup B$, whose membership function is the maximum of those of A and B, that is,

$$\mu_{A\cup B}(x) := \max\{\mu_A(x), \mu_B(x)\} \text{ for all } x \in X.$$

Similarly, the *intersection* of A and B is the fuzzy set $A \cap B$, whose membership function is the minimum of those of A and B, that is,

$$\mu_{A\cap B}(x) := \min\{\mu_A(x), \mu_B(x)\} \text{ for all } x \in X.$$

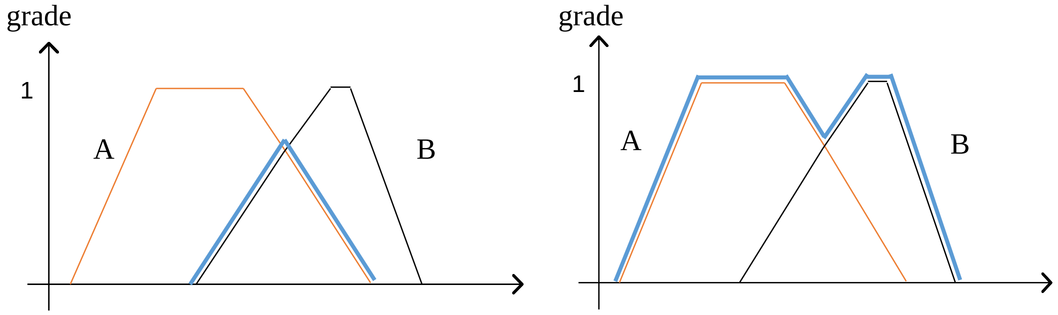

Figure 4. Union and intersection of fuzzy sets.

3.3. Fuzzy numbers

Fuzzy numbers play a central role in the fuzzy modelling of uncertainty.

Let A be a fuzzy subset of $\mathbb{R}$ (the set of real numbers) with membership function μ_A. Then A is called a *fuzzy number* if

1. $supp\ A \coloneqq \{x \in \mathbb{R}\ |\mu_A(x) > 0\}$ is a bounded interval,
2. there exists $x_0 \in \mathbb{R}$, such that $\mu_A(x_0) = 1$,
3. The α-cut $A_\alpha \coloneqq \{x \in \mathbb{R}\ |\mu_A(x) \geq \alpha\}$ is convex for all $\alpha \in]0,1]$.

Fuzzy numbers defined by these properties can be of various types. Here we present one important special type, the fuzzy numbers of trapezoid shape.

3.4. Fuzzy numbers of trapezoid shape

Let $a \leq b$ be arbitrary real numbers, and α, β be positive numbers. The fuzzy number denoted by $A = (a, b, \alpha, \beta)$ is called of trapezoid shape, if its membership function is given in the following form:

$$\mu_A \coloneqq \begin{cases} 1-(a-x)/\alpha, & if\ a-\alpha\ \leq x < a, \\ 1, & if\ a \leq x \leq b, \\ 1-(x-b)/\beta, & if\ a < x \leq b+\ \beta, \\ 0, & if\ x < a-\alpha\ or\ x > b+\beta. \end{cases}$$

That means the interval $[a, b]$ is the core of the fuzzy number A, while the open interval $]a-\alpha, b+\beta[$ is the support of A. The parameters α and β are called the left and right width of the fuzzy number A, respectively. The membership function is linear between the mentioned points, hence its shape in fact is trapezoid (Figure 5.).

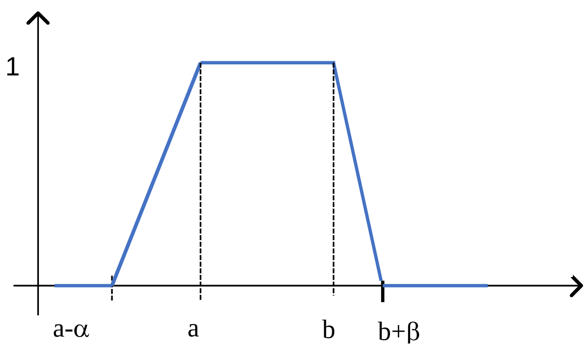

Figure 5. Core and support of a fuzzy number.

Fuzzy numbers of triangular shape are obtained in the special case $a = b$.

In case of some arithmetic operations (e.g., division) it is essential to exclude zero from the possible values of a fuzzy number. Therefore, we introduce the concept of a positive and negative fuzzy number.

A fuzzy number (of trapezoid shape) $A = (a, b, \alpha, \beta)$ is called positive if $a - \alpha > 0$, negative if $b + \beta < 0$.

3.5. Arithmetic operations with fuzzy numbers of trapezoid shape

The main objective when defining arithmetic operations with fuzzy numbers is to ensure their compatibility with the operations with ordinary real numbers. This is called the principle of extension.

Let $A_1 = (a_1, b_1, \alpha_1, \beta_1)$ and $A_2 = (a_2, b_2, \alpha_2, \beta_2)$ be fuzzy numbers of trapezoid shape. Applying the principle of extension, we obtain the following exact form for the sum of A_1 and A_2:

$$A_1 + A_2 = (a_1 + a_2, b_1 + b_2, \alpha_1 + \alpha_2, \beta_1 + \beta_2).$$

This means that the intervals defining the cores, together with the left and right widths are added. Thus, the uncertainty of the sum, as expected, is at least as much as that of the terms of the sum.

If $A = (a, b, \alpha, \beta)$ and λ is a given real number, based on the principle of extension, we have

$$\lambda \cdot A = \begin{cases} (\lambda a, \lambda b, \lambda \alpha, \lambda \beta), & if\ \lambda \geq 0, \\ (\lambda b, \lambda a, |\lambda|\beta, |\lambda|\alpha), & if\ \lambda < 0. \end{cases}$$

That means the length of the core and the support is multiplied by λ if λ is nonnegative. If λ is negative, then the λ-multiples of the original endpoints of the core should be interchanged, while the $|\lambda||$-multiples of the left and right widths are also interchanged with each other.

For $\lambda = -1$ we have

$$-A = (-b, -a, \beta, \alpha).$$

The difference of the fuzzy numbers A_1 and A_2 is defined as $A_1 - A_2 = A_1 + (-A_2)$, that is

$$A_1 - A_2 = (a_1 - b_2, b_1 - a_2, \alpha_1 + \beta_2, \alpha_2 + \beta_1).$$

Our goal is to define the reciprocal of a fuzzy number $A = (a, b, \alpha, \beta)$ of trapezoid shape. As a generalization of the ordinary concept, the reciprocal of a fuzzy number makes sense only if zero is not among the possible values of it. Hence the reciprocal is defined for either positive or negative fuzzy numbers.

The following formula provides an approximative result for the reciprocal of A:

$$\frac{1}{A} = \left(\frac{1}{b}, \frac{1}{a}, \frac{\beta}{b(b + \beta)}, \frac{\alpha}{a(a - \alpha)}\right).$$

If $A_1 = (a_1, b_1, \alpha_1, \beta_1)$ and $A_2 = (a_2, b_2, \alpha_2, \beta_2)$ are fuzzy numbers of trapezoid shape, then their product is not exactly of this type. Hence an approximative formula is applied for the product, where the side functions are approximated linearly, while the endpoints of the core and support are accurate. The „sharper" the fuzzy numbers are, the more accurate approximation is obtained. Let

$$x_m \coloneqq \min\{(a_1 - \alpha_1)(a_2 - \alpha_2), (a_1 - \alpha_1)(b_2 + \beta_2), (b_1 + \beta_1)(a_2 - \alpha_2), (b_1 + \beta_1)(b_2 + \beta_2)\},$$

$$x_M \coloneqq \max\{(a_1 - \alpha_1)(a_2 - \alpha_2), (a_1 - \alpha_1)(b_2 + \beta_2), (b_1 + \beta_1)(a_2 - \alpha_2), (b_1 + \beta_1)(b_2 + \beta_2)\},$$

$$y_m \coloneqq \min\{a_1 a_2, a_1 b_2, a_2 b_1, b_1 b_2\},$$

$$y_M \coloneqq \max\{a_1 a_2, a_1 b_2, a_2 b_1, b_1 b_2\},$$

then

$$A_1 \cdot A_2 = (y_m, y_M, y_m - x_m, x_M - y_M).$$

Let $A_1 = (a_1, b_1, \alpha_1, \beta_1)$ be arbitrary and $A_2 = (a_2, b_2, \alpha_2, \beta_2)$ be either a positive or negative fuzzy number. Their ratio is obviously defined as

$$\frac{A_1}{A_2} = A_1 \cdot \frac{1}{A_2}$$

3.6. Defuzzification

When carrying out analyses involving fuzzy data, it may be important to represent the resulting fuzzy numbers as classical – so called crisp – real numbers. A procedure of converting fuzzy numbers to crisp ones is called defuzzification. Various methods are known and widely applied, from among which the following are mentioned.

3.6.1. Center of gravity (COG)

If A is a fuzzy number (identified with its membership function), then the crisp number a_0 represented by A is given by

$$a_0 = \frac{\int zA(z)dz}{\int A(z)dz}$$

where the integral is taken over the (bounded) support of A. This is in fact the (x-coordinate of) the center of gravity of the region below the graph of A.
For a fuzzy number $A = (a, b, \alpha, \beta)$ of trapezoid shape the formula gives the following:

$$a_0 = \frac{3b^2 - aa^2 - \alpha^2 + \beta^2 + 3a\alpha + 3b\beta}{6b - 6a + 3\alpha + 3\beta}.$$

In case of a symmetric trapezoid, a_0 is the center of the support of A.

3.6.2. Area (COA)

Let $a_1 \in [a - \alpha, b + \beta]$ be the point, for which the vertical line $x = a_1$ divides the region below A into two parts of equal area. To determine a_1, we distinguish 3 cases.

- Case 1: $|\alpha - \beta| \leq 2(b - a)$. This is equivalent to $a \leq a_1 \leq b_1$, and then
$$a_1 = \frac{a + b}{2} + \frac{\beta - \alpha}{4}.$$
- Case 2: $\alpha - \beta > 2(b - a)$. This is equivalent to $a - \alpha < a_1 < a$, and then
$$a_1 = a - \alpha + \sqrt{\alpha \left(b - a + \frac{\alpha + \beta}{2}\right)}.$$
- Case 3: $\beta - \alpha > 2(b - a)$. That means $b < a_1 < b + \beta$, in this case
$$a_1 = b + \beta - \sqrt{\beta \left(b - a + \frac{\alpha + \beta}{2}\right)}.$$

3.7. Ordering of fuzzy numbers

For the extension of certain mathematical statistical methods, it is necessary to order the fuzzy numbers (of trapezoid shape). Since there can be considerable overlapping between the supports and cores, that is, they are not disjoint, we introduce the concept of the index of a fuzzy number. For a given $A = (a, b, \alpha, \beta)$ we define

$$I(A) := \frac{a + b}{2} + \frac{\beta - \alpha}{4}.$$

Then, a total order relation can be defined on the fuzzy numbers in the following way: If A and B are fuzzy numbers of trapezoid shape, then A is said to be smaller than or equal to B, if $I(A)$ is smaller than or equal to $I(B)$.

4. Conclusions

The integration of technological innovations that have taken and are just taking place in food industry can be of decisive importance for small and medium-sized companies in Hungary to enlarge their market share. High pressure preservation and fuzzy control of these processes are also known and implemented in some cases in Hungary. However, the region-specific consumption patterns and the microbiological and biochemical speciality of local raw materials demand company and region level adaptation of technologies to improve efficiency of preservation processes in terms of safety, economy and environmental impact. Based on our review we conclude that the importance of high-pressure processing is increasing in quality food preservation, where fuzzy control is particularly useful to apply. The theory of Fuzzy arithmetic supplies a wide spectrum of tools to improve the efficiency the control processes of high-pressure food processing.

Acknowledgments

Project no. 2020-1.1.2-PIACI-KFI-2020-000151 has been implemented with the support provided by the Ministry of Innovation and Technology of Hungary from the National Research, Development and Innovation Fund, financed under the 2020-1.1.2-PIACI KFI funding scheme.

References

[1] **Hugas, M., Garriga, M., Monfort, J.M.** (2002), New mild technologies in meat processing: high pressure as a model technology, Meat Science, 62, Issue 3, 359-371.

[2] **Huszka, P., Polereczki, Zs.** (2009), A fizetőképes kereslet és az árak hatása a magyar lakosság élelmiszerfogyasztására, Élelmezési Ipar Szakfolyóirat, 63 (8), pp. 241-247.

[3] **Szabó D.** (2017): Determining the target groups of Hungarian short food supply chains based on consumer attitude and socio-demographic factors, Studies in Agricultural Economics, 119: 115-122.

[4] **Hite, B. H.** (1899): The effects of pressure in the preservation of milk, West Virginia AgricExp. Sta. Bull., 58, 15-35.

[5] **Hite, B. H., Giddings, N. J., Weakley, C. E.** (1914): The effect of pressure on certain microorganisms encountered in the preservation of fruits and vegetables, West Virginia AgricExp. Sta. Bull., 146., 2-46.

[6] **Patterson, M. F.** (2005): Microbiology of pressure treated foods, J. Appl. Microbiol., 98(6): 1400-1409.

[7] **Knorr, D.** (1993): Effects of high hydrostatic pressure processes on food safety and quality, Food Technol., 47, 156-161.

[8] **Hoover, D. G.** (1997): Minimally processed fruits and vegetables: reducing microbial loan by non-thermal physical treatments, Food Technol., 51, 66-71 p.

[9] **Zadeh L. A.** (1964): Fuzzy sets, Information and Control, Volume 8, Issue 3, June 1965, Pages 338-353.

[10] **Klaua, D.** (1965): Über einen Ansatz zur mehrwertigen Mengenlehre, Monats-berichte der Deutschen Akademie der Wissenschaften Berlin 7, 859–867.

[11] **Klaua, D.** (1966): Über einen zweiten Ansatz zur mehrwertigen Mengenlehre, Monatsberichte der Deutschen Akademie der Wiss enschaften Berlin 8, 161-177.

[12] **Víg P., Szabó I., Schrempf N., Veres A., Sebestyén Z., Korzenszky P.** (2021): Fuzzy control and its applications, Mechanical Engineering Letters, Vol. 21. Issn 2060-3789 MATE, pp. 142-149.

[13] **Chutia H., Mahanta C. L., Ojah N., Choudhury A. J.** (2020): Fuzzy logic approach for optimization of blended beverage of cold plasma treated TCW and orange juice, Journal of Food Measurement and Characterization 14, 1926–1938.

[14] **Kaushik N., Reddy G. A., Rana R., Rao P. S.** (2015), Application of fuzzy logic technique for sensory evaluation of high pressure processed mango pulp and litchi juice and its comparison to thermal treatment, Innovative Food Science and Emerging Technologies 32 (2015) 70–78.

[15] **Gottwald S.** (2008): Foundations of a theory for fuzzy sets: 40 years of development, Int. J. Gen. Syst. 2008. 37:69–82. 17.

[16] **Fodor J., Roubens M.** (1994): Fuzzy Preference Modelling and Multicriteria Decision Support, Kluwer Academic Publishers, Dordrecht, 1994.

[17] **Grzegorzewski P., Mrówka E.** (2005): Trapezoidal approximations of fuzzy numbers, Fuzzy Sets and Systems, 153 (2005), 115-135.

[18] **Korzenszky P., Kassebi S.** (2021), Changes in physicochemical properties of golden delicious apples during storage, In: 4th International Conference on Biosystems and Food Engineering: Book of Abstracts, Budapest, Paper: E418, 1 p.

HUNGARIAN AGRICULTURAL ENGINEERING
No 41/2022 66-71
Published online: http://hae-journals.org/
HU ISSN 0864-7410 (Print)
HU ISSN 2415-9751(Online)
DOI: 10.17676/HAE.2022.41.66
Received: 01.06.2022 - Accepted: 25.06.2022

PERIODICAL
OF THE COMMITTEE OF AGRICULTURAL AND BIOSYSTEM ENGINEERING OF THE HUNGARIAN ACADEMY OF SCIENCES
and
HUNGARIAN UNIVERSITY OF AGRICULTURE AND LIFE SCIENCES
INSTITUTE OF TECHNOLOGY

ANALYSIS OF LOGISTICAL AND MACHINE WORK COSTS OF THE CULTIVATION OF SWEET SORGHUM AS RAW MATERIAL FOR RENEWABLE ENERGY PRODUCTION

Author(s):
L. Magó[1]

Affiliation:
[1] Institute of Technology – Hungarian University of Agriculture and Life Sciences, 2100 Gödöllő, Páter Károly u. 1., Hungary;

Email address:
Mago.Laszlo@uni-mate.hu

Abstract: This work is a comprehensive examination that analyses the machine fleet formation and machine use of plant production farms that grow sweet sorghum too by using computer aided modelling. It considers the characteristics of machines used at the production technologies of different plants and it especially focuses on the appliance of machines with the convenient capacity and level from the side of costs at different farm sizes. The survey was based on the work tasks of a "classical" crop production farm. By the technical-economical analysis of the production-technology of sweet sorghum it has been determined that the total production cost of this plant per hectare in case of small-scale farm size is minimum 965 EUR. Examining the large-scale production, the costs are decreasing, but they cannot be reduced under the 860 EUR/hectare level.

Keywords: plant production, farm size, machine fleet planning, machine utilisation, low-cost machine fleet

1. Introduction

The goal of the research is the technical-economical analysis of the production-technology system of the sweet sorghum that is known as energy plant and nowadays as a promising base material of biotechnological industries [1].

Work done *by an efficiently developed machine system* is a significant condition of the fruitfulness of farming [2]. The machine prices and the cost of their utilization are extremely high and all these result in extraordinarily high production costs. *Rational machine utilization* is a definitive factor of the efficiency of venture-farming [3].

We have accomplished the examinations by taking power-machines from different quality and cost levels as base. Through this we have showed that not only the size of the farms effects the amount of the operational costs, but the standard of mechanization too [4].

2. Materials and Method

2.1 The sweet sorghum (Sorghum vulgare saccharatum)

The sweet sorghum is one of Hungary's plants that is capable to produce the greatest amount of biomass and it's production can be fitted in the conventional alternation of the cereals and industrial plants and the outstanding yields can be ensured at lower costs than other cultures. From the point of view of energetic use, the component of the sweet sorghum that is classed as secondary product, the high sugar content solution that can be pressed from the spears, that is a suitable base material for bioconversion methods. The amount of the productable sugar reaches or exceeds the amount of the glucose that can be produced from cereals grown on a land with the same size. The complex use of the components that can be obtained from the sweet sorghum can significantly increase the reachable profitableness of agriculture [5].

The plant is subtropical, needs hot weather and takes drought significantly. It is also called durra or sweet-cane. It was grown in a higher amount between the two world wars. After the II. World War, until the start of the sugar production, the sugar containing syrup pressed and condensed from the plant was used instead of sugar. Nowadays it is mainly used to produce silage fodder, planted with silage corn. The growing conditions are very advantageous, because the sweet sorghum gives a stable yield even in case of poor water supply (60-70 tons/hectare) [6].

2.2 The surveyed crops

The surveys can be conducted by *modelling* the machine working processes of agricultural production. On the base of field crop production, a crop plan including cereal plants for human consumption, *sweet sorghum* for animal breeding and for *energy* production purposes and oil seeds – as sunflower and the nowadays very popular crucifer - appropriate for human consumption and energy production as well and reflecting the special features of production in Hungary has been applied. Depending on venture size the proportion of the crop area of the individual plants has been stipulated in view of the agronomical and production technological conditions.

2.3 The significance of machine utilization, the machine families applied, the parameters of model calculations

In the utilization costs of the more and more up-to-date and expensive power machines the proportion of *fixed costs*, especially amortization and maintenance is very high [7]. This expense can be decreased by increasing *utilization*. If the applied means are coupled to the individual field work operations at their effective operation cost – i.e., taking the rate of utilization into account – the effect of *working-hour performance* on costs will become measurable [8].

Basically, the cheapest power machine families used in Hungary on the one hand, and the ones with the highest possible investment cost demand available on the market of agricultural machinery on the other have been the subject of the survey [9, 10].

The basic figures of machine utilization have been determined with the help of the data base of the Hungarian Institute of Agricultural Engineering [11, 12].

The *model-calculations* have affected the farm size points of machine stock development in a farm size of 30 and 1000 ha. On this basis we can come to statements affecting a wider segment of the agricultural property structure, resp. To conclusions concerning mechanization and machine utilization [13].

3. Results

3.1 The constitution of the machine system in case of the examined operating sizes

The power-machine system that can be ordered to serve the examined operating size of 30 hectares to finish the soil preparation in a good quality consists of the minimal 40 kW output piece and the attachable soil tilling, nutritive spreading and insecticide process machines. In case of the 1000 hectare farm size that is the base of the large-scale examination, the minimum is the tractors with 60-120 kW of output that can be the base of the machine works. The different output-categories are represented by two power-machines in each case. The easier nutritive supply and insecticide tasks are done by the machines with smaller output and the heavier tasks are done by the machines with higher output. The *materials handling to the depot* can also be done by these tractors by using tow-cars to increase the exploitage of the machines.

In case of farm size of 30 hectares, the finishing of the harvesting works as wagework is the most efficient. According to the calculations, on a 1000 hectare sized farm, to reach the acceptable capacity-utilization, one *cereal combine-harvester machine* can be operated as the property of the farm. The appliance of the self-propelled silo harvester that does the gathering of the sorghum as a property, highly increases the machine costs of the farm, therefore it can be seen in the chapter *results* in details that it is more advantage out to use a self-propelled silo harvester for commission work.

3.2 The number of the executed working-hours in function of the power-machine category, the mechanical level and the farm size

The number of the executable working-hours of the power-machines in case of different farm sizes determines the composition to each category of the power-machine system;

In case of the examined *smaller sized farm* (30 hectares) based on our calculations *low exploitage* can be reached to the tractors: maximum 435 working-hours/year.

In case of large estate sizes (1000 hectares) the executed machine working-hours of the farms power-machine fleet, based on our model calculations is 6650 working-hours, from which the tractors represent a major (1100 working-hours/year (power-machine with 60 kW output) and 1700 working-hours/year (power-machine with 120 kW output)) part.

With a clever-chosen cereal harvesting machine at *one thousand hectare* farm size executing about 450-500 working-hours it reaches *significant* exploitage, that results in *acceptable* operational cost. The annual capacity exploitage of the self-propelled silo combine in case of own property is only 150 working-hours, that makes the idea of purchasing the machine as property to think it over.

In case of a 30 hectare sized farm the machine work demand of sweet sorghum that's production is fitted in the rotation of crops is 120 working-hours, that is 14,8 working-hours/hectare. This value is slightly higher than the economic average. In case of a 1000 hectare sized farm the machine work demand of sweet sorghum that's production is fitted in the rotation of crops is 1675 working-hours, that is 6,7 working-hours/hectare. This marks well that the production of sweet sorghum is a labour-intensive activity, because this value is also higher than the value that is specific to the whole farm. By using *modern machines*, the shown working-hour execution parameters will decrease with 4-5 % [14, 15].

In case of small-scale production, the significant number of shift-hours increases the living work outlay, thereby *increases the employment*. In the farms with this size the use of small output machines is reasonable. However, the proper usage of the small capacity machines is not ensured either, so the significant constant costs induce *higher operational costs* [16].

3.3 The analysis of the machine usage costs

Applying *low-level* power-machine fleet, the annual machine use cost of a 30 hectare farm that produces sweet sorghum too is 11.785 EUR, that is 393 EUR per hectare. The specific machine cost of the produced crops is the following: wheat 365 EUR/hectare, sunflower 375 EUR/hectare, rape 395 EUR/hectare, sweet sorghum 440 EUR/hectare. In the sowing plan the ratio of the plants is the following: wheat 40%, sunflower 25%, sweet sorghum 25%, rape 10%.

Applying *modern power-machines* the annual machine use cost is 14.645 EUR, that is 491 EUR per hectare. In case of the produced plants the machine costs are the following: wheat 460 EUR/hectare, sunflower 475 EUR/hectare, rape 500 EUR/hectare, sweet sorghum 540 EUR/hectare.

Those who work on small sized farm can count with low power-machine utilization, that also has effects on the use costs per working-hour of the tractors. This value is 19 EUR/working-hours in case of the 40 kW tractors that are usually used in small works. At this production size, the calculated cost of the borrowed used cereal harvester and self-propelled silo combine is 52,5 EUR/working-hours and 72,7 EUR/working-hours. In case of *modern machines*, the specific cost of the mentioned tractor to a time unit is 24 EUR. The cost of the cereal combine is 73,6 EUR/working-hours. In case of an ensilage cutter, we can also count with the given values, because in the database that we used for the calculations we haven't found two different technical levels from the harvesting machines with these functions.

Considering a 1000 hectare sized farm in case of *low level* mechanization, taking the above mentioned sowing plan ratios the annual use cost of the machines is 303,5 thousand EUR, that is 303,5 EUR/hectare. The machine cultivation cost per hectare to each of the plants: wheat: 240 EUR, sunflower 270 EUR, rape 245 EUR, sweet sorghum 465 EUR.

If the use of the self-propelled ensilage cutter machine is not as an own property, than it is *leased work*, the machine use cost of the whole farm is 267,8 thousand EUR. The specific value for a hectare is 267,8 EUR. And the specific machine cost of the sweet sorghum production is the advantageous level of *320 EUR/hectare*.

With the appliance of *high-level* power-machines the annual machine use cost projected to the whole farm is 339 thousand EUR, specifically 339 EUR/hectare. In case of wheat, it is 275 EUR/hectare, sunflower 305 EUR/hectare, rape 275 EUR/hectare and sweet sorghum 505 EUR.

It can be observed that the machine cost of sweet sorghum is the highest in every case, compared to the other plant cultures. This is mostly because great volume of the harvesting and crop transporting tasks: at least 60-80 t/hectare of crop has to be harvested and transported to the processing plant.

If the ensilage cutter machine does it's tasks as *leased work*, the costs decrease. As a result of the calculations, the total machine use cost of the whole farm is 303,5 thousand EUR. Specifically it is 303,5 EUR/hectare. The machine work cost of the sweet sorghum production is *365 EUR/hectare*.

The Figure 1 also shows the previously introduced things, where the upper and lower limit of the machine use costs are shown in function of the farm size, that are determined considering the use of low-level power-machines and implements and the expensive power-machines that represent the modern machine technologies.

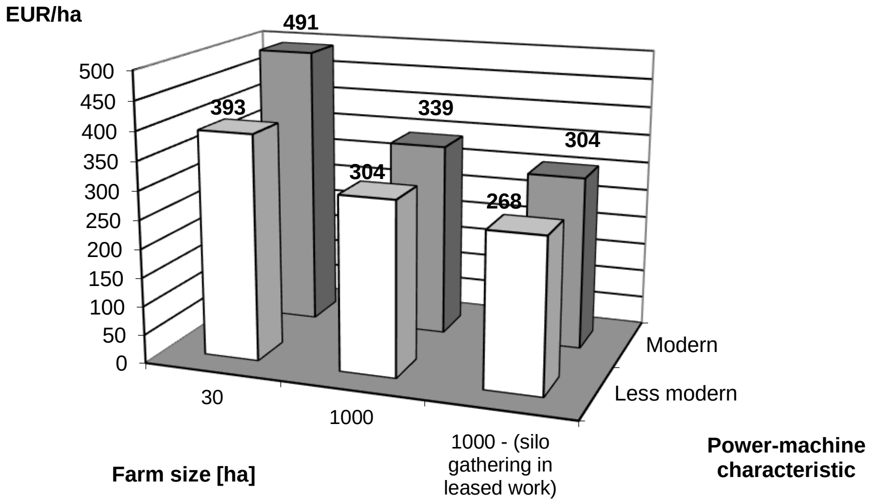

Figure 1. The specific machine utilisation costs in case of different mechanization levels at farms with the investigated sizes

In large-scale production the exploitage of the power-machines is more advantageous. The tractor with 60 kW output works 1100 working-hours and the medium sized universal power-machine with 120 kW output works 1750 working-hours annually. The use cost of them to one working-hour is 15,7 EUR, and 27,3 EUR. According to our calculations the use cost of the cereal harvester and self-propelled silo combine as own property is 83 EUR/working-hour, and 243,2 EUR/working-hour. If we borrow the ensilage cutter for work, the cost reduces significantly to 97,4 EUR/working-hour. In case of *modern power-machines* the specific cost of the mentioned tractors to a time unit are 19,7 EUR and 31,4 EUR. The cost of the cereal combine is 93,4 EUR/working-hours. In case of an ensilage cutter as we have mentioned, we can calculate with the above given values.

The operational costs of the work processes of the sweet sorghum production calculated after the computer modelling can be seen on Table 1.

The marked costs in the chart show the direct costs of the machine operation, plus the accessory costs (farm level costs) that increase the discussed values with almost 20%.

The difference between the costs of the small and the large-scale farm size is well-marked. This all can be explained with the efficiency of the machine exploitage. In the field of costs there is also a difference between the use of modern and less modern machines. In case of small-scale farm size, with using less modern power-machines a more advantageous cost level can be reached, although the quality of the work and the circumstances of the working must be considered. In case of large-scale farm size, the difference between the operational costs of the less modern and modern machines decrease significantly, because the operation of the less modern machines is more expensive at larger strain and the high level constant costs of the modern machines significantly decrease, according to their better exploitage, considering one unit of work.

The values in brackets show the first-cost of the leased work.

Table 1. The direct machine operation costs of the work processes of the sweet sorghum production

	In case of using low-cost power-machine		**In case of applying modern power-machines**	
Farm size	**30 ha**	**1000 ha**	**30 ha**	**1000 ha**
Dimensional unit	EUR/ha	EUR /ha	EUR /ha	EUR /ha
Stubble ploughing	23	15,4	28,6	17,6
Fertilizer distribution	11,8	8	14,8	8,3
Muck-spreading		34,9		39,8
Stubble care	23	15,4	28,6	17,6
Deep ploughing	69,4	33,8	78,9	37,5
Plough levelling	23	15,4	28,6	17,6
Herbicide spraying	10,9	7	13,4	7,8
Chemical pouring	15,5	10,6	19,2	12,1
Preparation of seedbed	15,5	10,6	19,2	12,1
Sowing	22,3	18	25,9	19,8
Chemical plant protection	10,9	7,0	13,4	7,8
Within-the-row cultivation	19,6	7,7	23,8	9
Harvesting	*(65,2)*	171 *(64,1)*	*(65,2)*	171 *(64,1)*
Crop transportation to depot	*(57,1)*	32,9	*(65,3)*	38,5

4. Conclusions

Besides the introduced machine costs, we must count with the prices of the input materials of the sweet sorghum production to know the whole cost of the production of the plant. Adding all the cost of the nutrient supply, the seeds and the cost of the pesticide, we face that a minimal input material cost is 500 EUR/hectare. Beside this we must not forget about the cost of the insurance and other supplemental expenses that is connected to the production.

Adding everything, the total production cost of the studied plant per hectare in case of small-scale farm size is minimum 965 EUR. Examining the large-scale industrial production the costs reduce, but they can not be reduced under the 860 EUR/hectare level.

The aim of our research work and the exposition of its results is the professional support of the machine investment decisions and the machine utilization practice of the different size ventures promoting hereby the creation of the conditions of fruitful farming and rational machine investment decisions.

References

[1] **Erdeiné Késmárki-Gally Sz., Szabó I.**: (2012) A magyarországi cukortartalmú növények (termesztésének) gazdasági elemzése - Beszámoló Jelentés, VM Mezőgazdasági Gépesítési Intézet, Költségvetési kutatási téma. 12. p.

[2] **Magó L.**: (2020) Smart Control on Agricultural Machines, Hungarian Agricultural Engineering, Periodical of the Committee of Agricultural and Biosystem Engineering of the Hungarian Academy of Sciences, Vol. 37/2020. p. 41 - 47. DOI: 10.17676/HAE.2020.37.41

[3] **Husti I., Kovács I.**: (2009) Adaptation of Integrated Enterprise Management Systems for Farm Machinery Management, Abstracts of the International Conference “Synergy and Technical Development in the Agricultural Engineering”, Gödöllő, Hungary, 31. August - 3. September 2009. p. 101.

[4] **Magó L.**: (2008a) The Comparison of the Technical-economical Parameters of Machine Utilization under Different Level of Mechanization Subject to Farm Size, Agricultural Engineering Research – Bulletin of the Hungarian Institute of Agricultural Engineering, Gödöllő, 39 p.

[5] **Erdeiné Késmárki-Gally Sz., Barabás N.**: (2012) A cukorcirok termesztési vizsgálata Halmajon, Mezőgazdasági Technika, tudományos, műszaki fejlesztési és kereskedelmi folyóirat, Vol. LIII, No 12., p. 34-36.

[6] **Kocsis L.**: (2009) A cukorcirok betakarításának lehetőségei a feldolgozási folyamat gazdaságosságának figyelembevételével. Mezőgazdasági Technika. Vol. L., No. 7. p. 12-14.

[7] **Daróczi M.**: (2007) Basic Tasks of the Agricultural Investment Process, Hungarian Agricultural Engineering. No. 20., p. 65-66.

[8] **Magó L.**: (2008b) Improving the Efficiency of Machine Utilization by Rationalization of Shift-hour Performance of Power Machines Considering the Farm Size, Towards Environmental Technologies, International Conference on Agricultural Engineering, AgEng2010, Clermont-Ferrand - France, 6-8 September 2010. Book of Abstracts p. 268. Full paper in Conference CD issue.

[9] **Magó L.**: (2007) Low Cost Mechanisation Solutions for Effective Farming on Small and Middle-sized Arable Farms, Hungarian Agricultural Engineering, Periodical of the Committee of Agricultural Engineering of the Hungarian Academy of Sciences, Vol. 20/2007. p. 61-64.

[10] **Fenyvesi L., Gockler L., Hajdú J., Husti I.**: (2003) A mezőgazdaság műszaki fejlesztésének lehetséges megoldásai. Gazdálkodás, No. 5. 1-15 p.

[11] **Gockler L.**: (2015) Mezőgazdasági gépi munkák költsége 2015-ben., NAIK MGI. Gödöllő. 32 p.

[12] **Erdeiné Késmárki-Gally Sz., Rák R.:** (2020): Mezőgazdasági gépi munkák költsége 2020-ban. NAIK MGI. 32 p.

[13] **Bártfai Z., Lágymányosi A, Szabó I., Tímár T.**: (2019a) Development of a Digital Database for Supporting Precision Technologies, Mechanical Engineering Letters, Vol. 19. p. 195. - 201.

[14] **Magó L., Cvetanovski A.**: (2019) Smart Attached Working Equipment in Precision Agriculture, Hungarian Agricultural Engineering, Periodical of the Committee of Agricultural and Biosystem Engineering of the Hungarian Academy of Sciences, Vol. 35/2019. p. 5-12., DOI: 10.17676/HAE.2019.35.5,

[15] **Bártfai Z., Blahunka Z., Kátai L., Szabó I.**: (2019b) Synergy of Robotics and ICT in the Smart Farming, Hungarian Agricultural Engineering, Periodical of the Committee of Agricultural and Biosystem Engineering of the Hungarian Academy of Sciences, Vol. 36/2019. p. 22. - 28., DOI: 10.17676/HAE.2019.36.22,

[16] **Takács I., Baranyai Zs., Takács E., Takács-György K.**: (2008) Change of Labour Productivity on Field Crop Farms in the EU Countries from 1989 to 2005, Cereal Research Communications, Akadémiai Kiadó, Vol. 36: p. 51-54.

HUNGARIAN AGRICULTURAL ENGINEERING
No 41/2022 72-78
Published online: http://hae-journals.org/
HU ISSN 0864-7410 (Print)
HU ISSN 2415-9751(Online)
DOI: 10.17676/HAE.2022.41.72
Received: 01.06.2022 - Accepted: 30.06.2022

PERIODICAL
OF THE COMMITTEE OF AGRICULTURAL AND BIOSYSTEM ENGINEERING OF THE HUNGARIAN ACADEMY OF SCIENCES
and
HUNGARIAN UNIVERSITY OF AGRICULTURE AND LIFE SCIENCES
INSTITUTE OF TECHNOLOGY

FEASIBILITY STUDY OF USING SOLAR THERMAL ENERGY FOR HEATING SWIMMING POOLS IN CENTRAL EUROPEAN CLIMATE (HUNGARY AS A CASE STUDY)

Author(s):
R. Ghabour [1], S. Hossain [2], P. Korzenszky [2]

Affiliation:
[1] Doctoral School of Mechanical Engineering – Hungarian University of Agriculture and Life Sciences, 2100 Gödöllő, Páter Károly u. 1., Hungary;
[2] Institute of Technology - Hungarian University of Agriculture and Life Sciences, 2100 Gödöllő, Páter Károly u. 1., Hungary;

Email address:
Ghabour.Rajab@phd.uni-mate.hu; Gtu.sazzad@gmail.com; Korzenszky.Peter.Emod@uni-mate.hu

Abstract: Heating swimming pools using electrical elements is costly and causes environmental impact by producing CO_2 emissions. While renewable energy, such as solar energy, proves a viable alternative source for swimming pool heating. This article aims to simulate various Solar Domestic Hot Water (SDHW) systems in cold climates like Central European countries to define the best system for swimming pool heating. Three different systems were compared: a solar heating system without auxiliary heating or heat exchanger (B6), with a heat exchanger (B6.1) and with a heat exchanger and an auxiliary heating source (B6.2). Also, five crucial variables were chosen, along with the variation of the other parameters using the response surface method (RSM). This system optimisation aims to define an optimal system with less financial expenditure. It was found that the best system is B6, represented by Experiment No 25, which indicates the Collector type: flat plate collector (FPC), pool depth: 1 m, pool temperature: 26 °C, pool covers, and windshield are actively operated. We used the T*SOL Valentine Software-2018 (kWh) to measure the solar contribution for each case. For each vector, our coded values range from [-1, +1]. The formula 2^k (2^5=32 experiments) defines the number of experiments, where k is a vector number. In addition, two more experiments were done to define second-degree non-linear coefficients with a pool depth (B) of 1.5 m and 28 °C pool temperature. These two additional experiments, however, had no impact on our results. Finally, the swimming pool heating systems suitable for this weather were compared. This experiment can help the locals to find the optimal swimming pool heating system for their pools.

Keywords: solar heating; pool heating; auxiliary heating; T*sol; R-script

1. Introduction

In cold climates (such as Budapest), approximately 15% of its consumed energy is for water heating. Moreover, these applications require less than 100 °C, easily achievable by renewable energy, for example, solar domestic water heating (SDWH) technology [1]. Conventional water heating systems using fossil fuels or electric heaters cause a greenhouse effect, high maintenance costs, and are expensive [2]. Hence, the future of solar water heating system technology is promising for its eco-friendly nature and renewable energy usage. Hence, by the end of 2018, Solar water heating collectors' total capacity was 482 GW (where the glazed type was 452 GW, and the rest 30 GW was unglazed type collector) worldwide [3]. Meanwhile, European countries such as Germany, Poland, Spain, Denmark, Italy, Austria, and Switzerland aggregate 27.1 GW [4]. According to the European Solar Thermal Industry Federation (ESTIF), Europe can save up to 5,600 tonnes of crude oil in 2020 by solar thermal energy [5]. By the end of 2050, the European Union will provide a solar thermal capacity of 1200 GW overall. The total solar collector area is 200,000 m^2, whereas there are 19 million m^2 glazed collectors in Europe. A solar collector area of 1000 m^2 can save up to 170 tons of CO_2

emissions, have a natural gas savings of 85000 m3, and have a return on investment (ROI) period of fewer than three years [6].

SDWH can be divided into two parts such as design and operation. The collectors can be designed in many ways. Flat plate collectors (FPC) and Evacuated tube collectors (ETC) are two primary types of solar collectors. The Temperature can reach up to 65 ℃, and efficiency can be achieved at 80% in Evacuated tube collectors [7]. However, this varies from meteorological, design, and load profile situations. The temperature variation can freeze water inside the flow channel at night and burst it for its volumetric expansion. So, in this system, 30% Glycol is mixed with water to prevent it from freezing.

It should be noted that evaporation causes the highest energy losses, which can be prevented partially if the cover is adequately used [8]. In this experiment, windshields are also considered to prevent heat loss [9]. In SDWH, energy is converted to thermal energy by solar radiation inside a solar collector. Sometimes, a conventional gas-fired boiler (an electric heater can also be used) is called an auxiliary heater. The auxiliary heater is connected to the heat exchanger, located in the highest part of the storage tank, where solar energy is insufficient [10]. An insulating layer is needed to reduce heat losses in the tank. Solar fraction is the ratio of solar energy sent to the standby tank to the total energy sent to the tank from the solar system and auxiliary heating [11]. Solar or system efficiency is the ratio of energy provided to energy irradiated onto the collector array's active solar surface. The coverage ratio defines how long we get the desired Temperature in a day [12,13].

There was no actual study on using solar thermal energy in central Europe in the literature. Also, the approach using RSM and linear modelling is still missing from the database. The utilisation of solar thermal energy is getting bigger and bigger every day, especially in central Europe in Austria, for example, which is considered the best country to produce solar thermal energy per 1000 capita in 2020 globally. This motivates researchers from other central European countries to investigate the potential of using solar thermal energy for domestic, industrial, and other functions

2. Experimental concepts

The swimming pool in Gödöllő, Hungary, is the actual case swimming pool, and the data are validated through the swimming pool owner. Some fixed parameters have been considered for this experiment, as in Table 1.

Table 1. Main system parameters

Metrological Location	Budapest Ferihegy
Collector area	6 m^2 (1 x 6)
Pool area	33.5 x 11.5 m^2
Solar Collector Inclination	24 °
Pool cover	90%
Cover type	Bubble sheet type
Cover time	7pm - 7am
Working days	15th May - 15th September
Glycol	30%
Daily freshwater requirements	50 l
volume flow rate	40 l/h/m^2 (per collector)
Annual irradiation on each collector	1370.9 kWh/m^2

The B6 system is a swimming pool without auxiliary heating or HX (Heat exchanger). Solar collectors convert direct solar energy to heat energy, mainly heating the domestic water and swimming pool. There are a few types of solar collectors. This article used only Flat plate and Evacuated tube type collectors, as shown in Figure 1. The variables are collector type, pool depth, pool temperature, cover, and windshield. Our desired pool temperature is 26 ℃ or above, and the pool depth must be 1 m or more as listed in Table 2.

Figure 1. Actual pictures of the studied case

Table 2. Case study variables

Variables		Values	Denoted by
Collector type	Flat Plate Collector (FPC)	Negative	A
	Evacuated Tube Collector (ETC)	Positive	
Pool depth	1 m	Negative	B
	2 m	Positive	
Pool temperature	26 °C	Negative	C
	30 °C	Positive	
Cover	Without Cover	Negative	D
	With Cover	Positive	
Windshield	Without windshield	Negative	E
	With windshield	Positive	

The schematics of the three analysed systems can be seen in Figure 2.

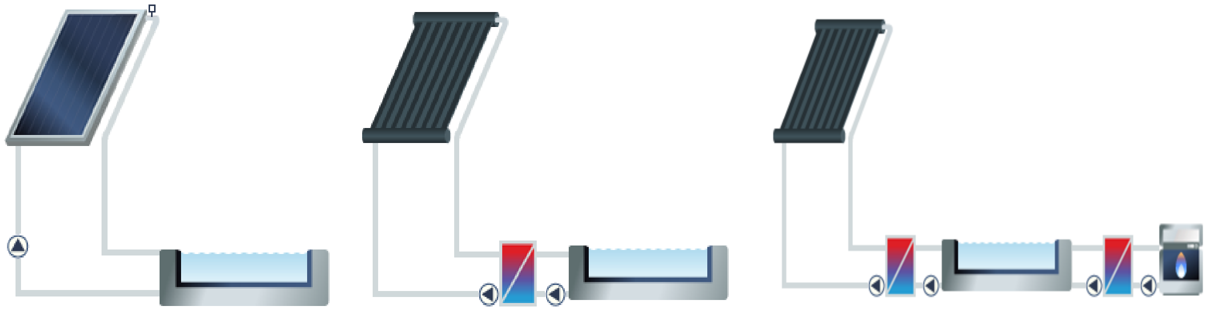

Figure 2. (a) No HX or auxiliary heater, (b) With HX, no auxiliary heater, and (c) With HX and auxiliary heater.

The simulation was conducted using T*SOL software to get the solar contribution ratio which refers to how much solar energy (in kWh) has been contributed to heat our swimming pool. In contrast, linear modelling was conducted using R scripts software using coded values for defining optimal values using the response surface method (RSM). The least-squares approach is used in the programming phase to provide a general rationale for the line's best match position among the data points under consideration.

3. Results and Discussion

Solar contribution refers to how much solar energy (in kWh) has contributed to heating our swimming pool water. From the Figure 3 Pareto plot chart, it is seen that factor A (collector type) has the most significant positive impact, with around 90 kWh annual magnitude. Since A is positive, we get 90 kWh annual magnitude as extra while using ETC. Therefore, we will choose an Evacuated Tube type solar collector instead of a flat plate collector. The following two highest single factors are E and D, having 40 kWh and 30 kWh annual magnitude, respectively. However, these factors are negative; hence choosing the windshield and cover off gives us an additional solar energy contribution of 40 kWh and 30 kWh annually. Apart from single factors, two interacting factors are AE and AD, with a positive magnitude of 10 and 8 kWh annually. The third double factor is DE, with an annual negative magnitude of 5 kWh. From Figure 3 also, it is clearly shown that single Factor C has the highest negative impact of 4.75 (%) magnitude. If we choose 26 °C, we have a higher magnitude. The following two single factors are E and D, with a positive magnitude of 3.9 (%) and 2.8 (%) magnitude. Since they are positive, we will choose the windshield and cover. Besides, the first three highest two interacting factors are CE, CD, and DE, where CE and CD are negatives and DE is positive.

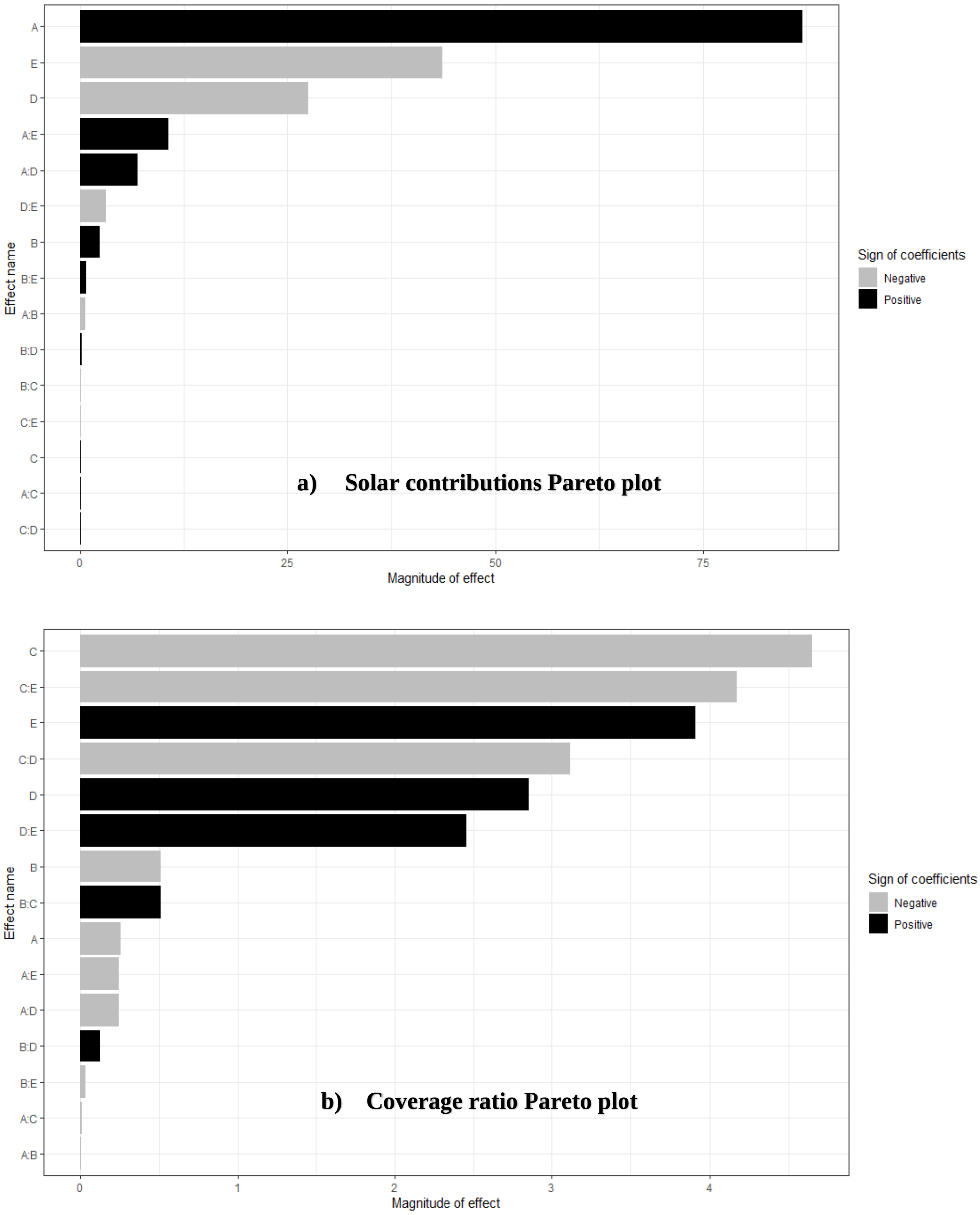

Figure 3. Pareto plot of a) solar contribution and b) coverage ratio

The two factors' interactions are illustrated in Figure 4: AE: we see that for the best efficiency, E is negative, and A is positive. That means the windshield should be off, and an Evacuated Tube collector should be used. AD: if D is negative and A is positive, we get the maximum solar contribution. So, the cover should be off, and we should use an evacuated Tube collector. DE: the system efficiency increases if both factors are negative individually. Both cover and windshield should be off for the highest solar contribution. After considering the solar contribution requirement, coverage ratio and financial perspective, we will choose to experiment no 25 (Collector type: FPC, Pool depth: 1m, Pool temperature: 26 °c, with cover and windshield, are active) for Budapest in the B6 swimming pool heating system as in Table 3.

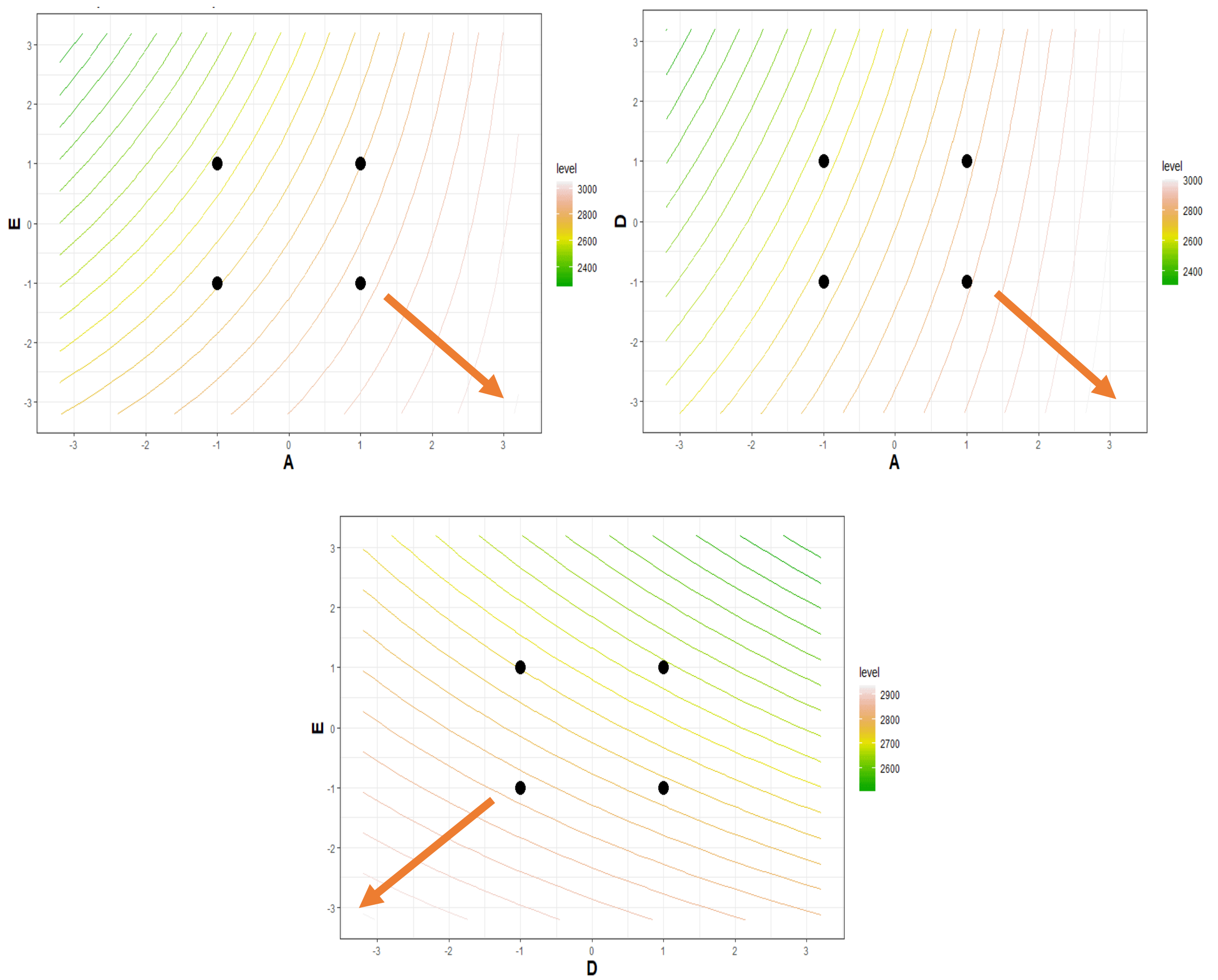

Figure 4. Two factors interaction

4. Conclusions

We used TSOL Valentine Software-2018 and collaborated with MeteoSyn to get the solar contribution (kWh) and coverage ratio (%). For modelling purposes, we used an R-script program where we considered the top five impacting variables: collector type, pool depth, pool temperature, cover, and windshield. Our coded values vary between [-1, +1] for each variable. The number of experiments is determined by the formula 2^k, where k is a variable number. As each variable has two values [-1, +1], the total experiment number was $2^5 = 32$. In addition to these 32 experiments, we conducted two more experiments considering that pool depth (B) is 1.5 m to identify second-degree non-linear coefficients. So, the total number of experiments was 34. However, these two experiments did not affect our measurement as the heating system with auxiliary heating or heat exchanger is costlier, and the solar contribution among them is insignificant. We compare the heating system without a heat exchanger or external heating source (B6). After considering the solar contribution, coverage ratio, pool temperature and financial aspect, we have chosen the best systems in swimming pool heating for Budapest. The best system indicates that the collector type is FPC, pool depth is 1 meter, pool temperature is 26 ℃, and has a windshield and cover during closing time. As the government tries to reduce carbon emissions and search for an alternative energy source, this solar heating system can be used widely in central European countries.

Table 3. Optimisation results

	Collector type	SP Dimension	Pool temp	Cover	Windshield	y 1	y 2	y 3
No	[FPC, ETC]	[1,1.5,2]	[26,28,30]	[No, Yes]	[No, Yes]	Solar contribution [kWh]	Coverage ratio%	Ava Pool Temp
1	FPC	1	26	No	No	2740	33.3	20.19
2	ETC	1	26	No	No	2881	35	20.18
3	FPC	2	26	No	No	2744	33.4	20.27
4	ETC	2	26	No	No	**2884**	**35.1**	20.27
5	FPC	1	30	No	No	2740	33.3	20.19
6	ETC	1	30	No	No	2881	35	20.18
7	FPC	2	30	No	No	2744	33.4	20.27
8	ETC	2	30	No	No	**2884**	**35.1**	20.27
9	FPC	1	26	Yes	No	2679	32.6	21.6
10	ETC	1	26	Yes	No	2844	34.6	21.59
11	FPC	2	26	Yes	No	2683	32.6	21.71
12	ETC	2	26	Yes	No	2847	34.6	21.7
13	FPC	1	30	Yes	No	2679	32.6	21.6
14	ETC	1	30	Yes	No	2845	34.6	21.59
15	FPC	2	30	Yes	No	2683	32.6	21.71
16	ETC	2	30	Yes	No	2847	34.6	21.7
17	FPC	1	26	No	Yes	2638	32.1	22.57
18	ETC	1	26	No	Yes	2819	34.3	22.56
19	FPC	2	26	No	Yes	2645	32.2	22.66
20	ETC	2	26	No	Yes	2823	34.3	22.65
21	FPC	1	30	No	Yes	2638	32.1	22.57
22	ETC	1	30	No	Yes	2819	34.3	22.56
23	FPC	2	30	No	Yes	2645	32.2	22.66
24	ETC	2	30	No	Yes	2823	34.3	22.65
25	FPC	1	26	Yes	Yes	2550	31.1	24.42
26	ETC	1	26	Yes	Yes	2773	33.7	24.41
27	FPC	2	26	Yes	Yes	2569	31.2	**24.49**
28	ETC	2	26	Yes	Yes	2778	33.8	**24.49**
29	FPC	1	30	Yes	Yes	2560	31.1	24.42
30	ETC	1	30	Yes	Yes	2773	33.7	24.41
31	FPC	2	30	Yes	Yes	2569	31.2	**24.49**
32	ETC	2	30	Yes	Yes	2778	33.8	**24.49**
33	FPC	1.5	28	No	No	2742	33.3	20.24
34	ETC	1.5	28	Yes	Yes	2775	33.7	**24.49**

Acknowledgements

This work was supported by the Stipendium Hungaricum Programme and the Mechanical Engineering Doctoral School, The Hungarian University of agriculture and life sciences, Gödöllő, Hungary.

References

[1] **Alva, G., Liu, L, Huang, X., Fang, G.,** (2017) Thermal Energy Storage Materials and Systems for Solar Energy Applications. Renewable and Sustainable Energy Reviews, 68, 693–706. doi: 10.1016/j.rser.2017.09.043.

[2] **Aste, N., Pero, C. Del, and Leonforte, F.,** (2012) Optimisation of Solar Thermal Fraction in PVT Systems. Energy Procedia, 30, 8–18. doi: 10.1016/j.egypro.2012.11.003.

[3] **Dalenbäc, J.,** (2008) Large-Scale Solar Heating and Cooling Systems in Europe. Proceedings of ISES World Congress 2007 (Vol. I – Vol. V), 799-803. doi: 10.1007/978-3-540-75997-3_151.

[4] **Ghabour, R., Korzensky, P.,** (2019) Mathematical modelling and experimentation of soy wax PCM solar tank using response surface method. Analecta Technica Szegedinensia, 14, 35-42. doi: 10.14232/analecta.2020.2.35-42.

[5] **Ghabour, R., Korzenszky, P.,** (2022). Linear Model of DHW System Using Response Surface Method Approach. Tehnicki vjesnik - Technical Gazette, 29, 201–205. doi: 10.17559/tv-20201128095138.

[6] **Ghabour, R., Korzenszky, P.,** (2021). Technical and Non-Technical Difficulties in Solar Heat for Industrial Process. Acta Technica Corviniensis – Bulletin of Engineering, 3, 11–18.

[7] **Hang, Y., Qu, M., Zhao, F.,** (2012) Economic and Environmental Life Cycle Analysis of Solar Hot Water Systems in the United States. Energy & Buildings, 45, 181–188. doi: 10.1016/j.enbuild.2011.10.057.

[8] **Iparraguirre, I., Huidobro, A., Fernández-García, A., Valenzuela, L., Horta, P., Sallaberry, F., Osório, T., Sanz, A.,** (2016) Solar Thermal Collectors for Medium Temperature Applications: A Comprehensive Review and Updated Database. Energy Procedia, 91, 64–71. doi: 10.1016/j.egypro.2016.06.173.

[9] **Kylili, A., Fokaides, P. A., Ioannides, A., Kalogirou, S.,** (2018). Environmental Assessment of Solar Thermal Systems for the Industrial Sector. Journal of Cleaner Production, 176, 99–109. doi: 10.1016/j.jclepro.2017.12.150.

[10] **Lugo, S., Morales, L. I., Best, R., Gómez, V. H., García-valladares, O.,** (2019) Numerical Simulation and Experimental Validation of an Outdoor-Swimming- Pool Solar Heating System in Warm Climates. Solar Energy, 189, 45–56. doi: 10.1016/j.solener.2019.07.041.

[11] **Renaldi, R., Friedrich, D.,** (2019) Techno-Economic Analysis of a Solar District Heating System with Seasonal Thermal Storage in the UK. Applied Energy, 236, 388–400. doi: 10.1016/j.apenergy.2018.11.030.

[12] **Ruiz, E., Martı, P. J.,** (2010) Analysis of an Open-Air Swimming Pool Solar Heating System by Using an Experimentally Validated TRNSYS Model. Solar Energy, 84, 116–123. doi: 10.1016/j.solener.2009.10.015.

[13] **Taibi, E., Gielen, D., Bazilian, M.,** (2012) The Potential for Renewable Energy in Industrial Applications. Renewable and Sustainable Energy Reviews, 16, 735–744. doi: 10.1016/j.rser.2011.08.039.

[14] **Zhou, F., Ji, J., Yuan, W., Zhao, X., Huang, S.,** (2019) Study on the PCM Flat-Plate Solar Collector System with Antifreeze Characteristics. International Journal of Heat and Mass Transfer, 129, 357–366. doi: 10.1016/j.ijheatmasstransfer.2018.09.114.

HUNGARIAN AGRICULTURAL ENGINEERING
No 41/2022 79-86
Published online: http://hae-journals.org/
HU ISSN 0864-7410 (Print)
HU ISSN 2415-9751(Online)
DOI: 10.17676/HAE.2022.41.79
Received: 05.06.2022 - Accepted: 30.06.2022

PERIODICAL
OF THE COMMITTEE OF AGRICULTURAL AND BIOSYSTEM ENGINEERING OF THE HUNGARIAN ACADEMY OF SCIENCES
and
HUNGARIAN UNIVERSITY OF AGRICULTURE AND LIFE SCIENCES
INSTITUTE OF TECHNOLOGY

THE ROLE OF MILL MACHINERY IN REDUCING DON-TOXIN

Author(s):
E. Kecskésné-Nagy [1], J. Nagy [2]

Affiliation:
[1] Faculty of Horticulture and Rural Development – John von Neumann University, 6000 Kecskemét, Izsáki u. 10., Hungary;
[2] Institute of Technology - Hungarian University of Agriculture and Life Sciences, 2100 Gödöllő, Páter K. u. 1., Hungary.

Email address:
nagy.nori@kvk.uni-neumann.hu; nagy.jozsef@uni-mate.hu

Abstract: In recent years the fusarium infection and accompanying DON–toxin contamination caused serious losses in the wheat growing and processing. Besides decrease of average yield it was serious problem that not a small part of the growned and harvested crop was unsuitable for food and forage production or the usage was limited. This phenomena caused problem in many countries all over the world according to data of scientific literature. There is a statement in the literature also that DON-toxin content can be decreased efficiently and safely only during the cultivation of plant and the possibilities for that are very limited during processing. We wanted to prove with our experiment that it is possible to decrease DON-toxin level of wheat items by application modern equipment and machineries, wherewith the losses and the food safety risks can be minimized. During our experiment we studied the effect of two milling machine on DON toxin content. (Sortex Z color sorter and Scule Verticone intensive surface cleaner). Both modern machine can be built-in the cleaning process in the mills. In our investigation we took samples from harvested wheat items during processing in the year of the experiment. The data were subjected to complex investigation and we evaluated them with different statistical methods. On this basis we can unequivocally state both machines are effective in reducing toxin level of basic material. In the year of the experiment the regression analysis showed that the Schule surface cleaner was more effective than the color sorting machine.

Keywords: effectivity of color sorting, effectivity of grain-surface cleaning, milling wheat, effectivity of toxin reduction

1. Introduction

Among the various fungal diseases that occur during the rainy season in wheat crops the Fusarium spp. fungal species are very significant, the infection of which appear the fusariotoxins [1], [2]. The fungus attacks among others the wheatear and the toxins produced by these microorganisms pose a serious food safety risk [3]. DON-toxin is one of the most significant representative of fusariotoxins [4].

Trichotercles - DON-toxin is the member of this group - are strong cellular poisons that have cytostatic and protein synthesis inhibitory effects, they damage the nervous system and also have an immunotoxic effect [5]. Acute DON toxicity may cause headache, dizziness, nausea, vomiting and diarrhea in humans. DON initially inhibits protein synthesis, upsets the cytokine regulation, the end result of which may be cell death. Presumably the digestive system complaints and also the immune inhibitory effect are due to this mechanism [6]. Indicates their danger that these compounds may be allowed in foodstuffs for human consumption up to 1 mg/kg while the maximum concentration in feedstuffs may be 5- 10 mg/kg [7]. In the case of unprocessed durum wheat used as food raw material the maximum allowable DON-toxin content is 1,75 ppm and in unprocessed edible wheat or otherwise in aestivum wheat this value is 1,25 ppm [8].

DON-toxin is water-soluble, but it is very stable during storage and processing of infected cereals. It is resistant to production processes and does not decomposes on heating [9], so it can go through the entire food chain. Mézes's [10] studies showed that after more than one year of storage of grains when temperature and humidity conditions allowed, owing to bacterial processes some detoxification was observable.

Degree of wheat grain formation disturbances depends on the time of infection. If the weather is favourable for the infection of fusarium fungi after fertilization, at the beginning of grain development, then the proportion of grains in which the fungus is present in the core (endosperm) is higher in the given wheat item. The color of the grains changes in this case. It may be lighter, it may be mainly greyish white, but light lilac or pink discoloration may occur. Color change is of great importance to my experiments. In early infection, some of the eyes, besides the above mentioned, may be smaller, softer, with lighter weight. If the weather becomes wet in the advanced state of the wheat grains, that is at the beginning of the whole ripening, then the fungus infection reaches the nucleus only in a small percentage, the infection centre develops in the layers of the grain shell. In such a case, the color change of the grains is less typical and the size of the grain will not be significantly smaller. But the healthy grains will be softer than the infected ones. At the end of full ripening diseased grains barely deviate from the healthy ones, the core interior remains intact. Occasionally there may be mycelium or mild discoloration on the surface of wheat, which may indicate infection, but in fact it is difficult to distinguish these grains from the healthy ones. The phenomenon described above has been proved by experimentation. Veres [11] did not find close correlation between the external and internal contamination of the grain, that is he proved, that they were developed due to independent phenomena.

The literature generally assumes that during the processing there is no or very limited and uncertain possibility of reducing the degree of mycotoxin, that is the level of food safety risk for each wheat item. [4], [12], [13]. Sándor and workers [14] and Frank [15] carried out model experiments to reduce DON-toxin, in which they studied equipment developed and constructed in laboratories, similar to surface cleaning procedures used in mill processing. They started out from the assumption most of the toxins are concentrated in the germ and shell of wheat grains. They evaluated a relatively small number of samples taken from a given wheat item. The results are important from the point of view that they have demonstrated certain surface cleaning methods can be applied to reduce the toxin content of wheat item, although here the results are not always convincing. But we must not ignore that the degree and nature of the fusarium infection depends on the fungus in which phenophase attacks the wheat. This determines that only the seed, the germ, or the endosperm of the wheat is affected by the infection. It should not be ignored also under mill processing conditions, cleaning and its efficiency can show other results than under laboratory conditions due to the mixing of raw material items, the nature and modernity of the process as well as many other factors. From the point view of of food safety, however, it is important not only to obtain correct information on the theoretical possibilities but also on the effectiveness of the actual process.

From the point of view of our experiment the pre-grinding operations have an important role in the milling process. According to our assumption in the case of infected wheat items the degree of toxin reduction depends on what kind of equipment and technical tools are operated during the production process. The first phase of these operations is the cluster cleaning followed by surface cleaning. During the cluster cleaning in several stages equipment select those components that are unsuitable for milling or wastes from wheat. During surface cleaning the outer surface of wheat grains is removed together with contaminations [16], [17].

Sortex Z+ color sorter was not designed to reduce DON-toxin content. In the food sector and outside also there are very many areas where it is possible to use this machine. In mill processing during cluster cleaning it provides a new, more precise, faster and less wasteful cleaning option.

It offers an opportunity to select components from cereal items the size of which is the same as intact, healthy seeds, but optically different. This is relevant to our experiment. The previously used sorting equipment could not efficiently isolate the quality detrimental components. From the wheat basically the physical contaminations and broken, weird seeds are selected by the machine due to their different color properties [17], [18]. In our experiment, we wanted to prove that the selection of seeds infected by fusarium and resulting in discoloration in the early stage of crop formation becomes possible with the use of this modern machine. As a result, the concentration of DON-toxin in the raw material decreases.

The Schule Verticone VPC 480 is an intensive surface cleaning machine used to shell cereals, legumes and spices. (Figure 1.) In the milling industry, the primary reason for the application is to clean the outer surface of wheat grains from contaminated pollutants and microorganisms [19].

By using it the final product quality will be better and it has a positive effect on the capacity of the mill will also. During the experiment we wanted to demonstrate that the toxin level of seeds infected at a later stage of the crop formation period can be reduced by using this machine and thus achieving a reduction in the toxin concentration of the raw material.

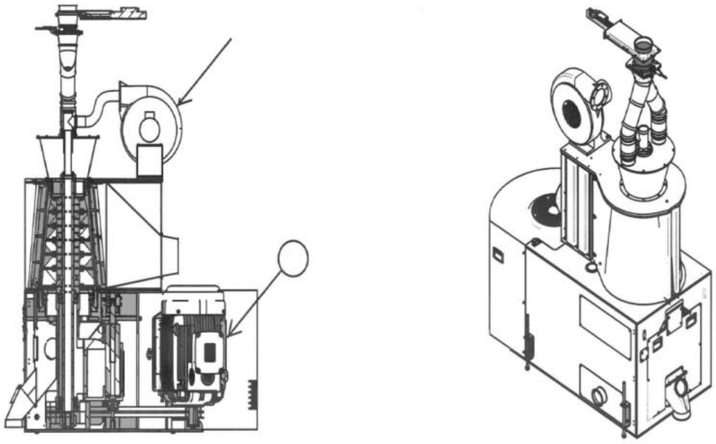

Figure 1. Schule Verticone VPC 480

2. Materials and Methods

2.1. The place of experiment, method of investigation

During our research work we investigated, whether high DON-toxin content can be decreased in the milling process by application adequate technological conditions. The goal is to enable a part of wheat items which was excluded from the food industrial or forage production to get back into the food chain, and it do should'not mean risk. It is important question also, how can the rate of toxin reduction.

For the sake of the practical usability of results it was important to set the experiment in production circumstances. Research in the case of investigation of food safety technological conditions that is reduction of risks should be achieved in production circumstances in order to prove it is possible to decrease the DON toxin content of wheat and to reduce food safety risks.

We carried out research work at Júlia Malom Ltd. The company started the production and the distribution of mill products in 2005. Later it performed developments in several steps and nowadays it operates three milling production lines. The site is in Kiskunszállás, which is 18 km from Kecskemét.

Owing to modern technology milling of the products happens in a closed system, starting from the mill-loading-hopper to the storage of flour in silo and packaging.

When we selected the place for research it was important aspect that the experiments should be completed in controlled circumstances, the whole mechanism of the process and its surroundings should be transparent, mappable and measurable. Besides the conditions, experimental settings should be changeable and repeatable [20].

2.2. Sampling method

During our research work the subject of investigation was the analysis of wheat items harvested in different years. In this article we summarized the evaluation results of samples of wheat items harvested in the year of the experiment. The sampling system was elaborated according to the technological phases because of nonstop operation. The goal is to follow up the change of toxin content of wheat items during the production process. We took five samples from a given wheat item on different spots. First three sampling spot was before Sortex color sorting machine (fraction V_1) and after the machine. After color sorting there were two fractions: from the purified milling wheat (fraction V_2), and from the remaining, selected so called by-products (fraction V_3). We created two sampling spots before Schule machine (fraction V_4) and after the machine (fraction V_5) (Figure 2.).

The samples of fractions V_4 and V_5 can be taken 12,5 hours the color sorting. The time lag was determined by the duration of technological phases. We sampled one wheat item on one day, and we took four sub-samples from each sampling spot. That is we tested DON toxin content of 20 wheat sub-sample from one wheat item. Sub-samples were taken in equal intervals, that is in every 10 minutes. (We started 0. minute and finished 30. minutes)

Figure 2. The place of sampling (Fraction V_5)

20 wheat items were investigated from the wheat harvested in the year of the experiment. That means we tested DON-toxin content of 400 sub-sample.

2.3. Statistical methods to evaluate datas

During experiment we would like to examine how change the toxin content the color sorting machine respectively the surface cleaner as well as joint use of two machines. We adjust the statistical analysis to this, and we compare samples as follows:

1. before Sortex color sorting (fraction V_1) and after (fraction V_2),
2. before Schule machine (fraction V_4) and after (fraction V_5), and
3. before Sortex color sorting (fraction V_1) and after Schule machine (fraction V_5).

The statistical method was elaborated that away we could make analysis with statistically really related samples. Thus we had to determine a given item and the related samples which best describes the changes taking place during the process. That we could reach by averaging four sub-sample which was taken on the same day from the given sampling spot. Statistical analysis was performed with averages.

As a first step we examine the distribution of samples. Generally known, in case of samples with normal or approximately normal distribution the range of statistical procedures available is wider and more accurate results can be obtained than with using non-normal distribution samples. We help approximate to normality a bit by averaging the sub-samples also based on the central boundary distribution thesis. Although in our case the thesis is not fulfilled completely, still usage of averages gives us a wider opportunity.

We used two of the fit testing procedures to determine normality: Kolmogorov–Szirnov-test amended version proposed by Stephens [21], [22] and Wilk–Shapiro-test [23]. The Kolmogorov–Szirnov-test with Stephens's amendment is user-friendly, because the same critical value can be used for different sample sizes, but it can not be said to be too strong test. Opposite Wilk–Shapiro-test, which is one of the strongest normality tests. We submit our data to both tests so we can create a clear picture whether the more permissive or stricter conditions are fulfilled. After the normality test the DON-toxin level change is investigated.

For this a comparison of four related sample (V_1; V_2; V_4; V_5) is performed. In addition to normality in this experiment we have to examine the sphericity of samples also, that is, whether the standard deviation of related samples is equal, which will be checked with Mauchly-test [24].

In case if the distribution of data is not normal or the sphericity is not met, then for a related samples the Friedman test is the most frequently used nonparametric statistical procedure. However, if normality and at the same time sphericity are met then repeated measurement variance analysis should be used for full data analysis. For variance analysis, we consider that statistical literature qualifies as a robust process, which means that if the conditions are not fully met, the procedure can be safely applied [25].

If we do not want to make a complete data test, we only want to investigate two related samples, then we need to use a difference-sample created from sample pairs. The parametric procedure is the even t-test, which precondition is normality also, in turn the nonparametric equivalent is Wilcoxon signed rank test. This test can be used for symmetric distribution difference-samples. That is this procedure has also preconditional. The presence of symmetry can be checked by a Pearson index.

Thereafter, we are also looking for whether it can be predicted based on the measured data how much toxin reduction can be achieved upon completion of the cleaning (fraction V_1 and V_5). For this we perform regression analysis [26]. In case of normal distribution from regression functions the linear gives the best estimate

3. Results and discussion

First we sought statistical verification to determine data analysis and evaluation methods. That is, we checked whether the averaging samples could be considered as normal distributions. During which the four samples were tested (V_1, V_2, V_4, és V_5) with version of Kolmogorov–Szirnov test recommended and with Stephens and Wilk–Shapiro method. Our H0 hypothesis in this case is that the sample is derived from a normal distribution. Using the modified version of the Kolmogorov-Smirnov test, recommended by Stephens, the test statistic and the critical value were as follows:

V_1	0,96	
V_2	0,85	critical value α=0,05: 0,895
V_4	0,84	
V_5	0,69	

The data show that, with the exception of the V_1 sample, our samples have normal distribution according to this statistical procedure.

When the Wilk–Shapiro-test was applied the test statistic and the critical values were as follows:

V_1	0,82	
V_2	0,84	critical value α=0,05: 0,98
V_4	0,85	
V_5	0,93	

In this case, the strongest normality test rejects normality for all four samples.

The two normality tests had different results. Therefore, in order to reach an exact conclusion, we also subject our data to the evaluation of both the statistical methods assuming normality and statistical methods that do not require normality. If we are strict in terms of normality, the four related samples should be examined using the Friedman-probe. The null hypothesis H_0 of the Friedman-probe is that the distribution of all four samples is the same. For our related samples the value of the probe is 54.78, the critical value at the significance level $\alpha = 0.05$ is 7.815. Since the test statistic is much higher than the critical value, we reject the null hypothesis, distribution of our samples is different. That is the reduction in toxin content of starting wheat items can be attributed to the cleaning process.

If we are less strict about the normality test then based on the Kolmogorov-Smirnov test it can be said that normality was only damaged at one sample. As discussed earlier, sphericity should be investigated in this case as well. On the basis of the corrected empirical deviations, the deviations were the same except for the last sample.

V_1	0,27
V_2	0,27
V_4	0,27
V_5	0,21

Although this is convincing at first sight, but for the sake of statistical accuracy we used the Mauchly-test, which has the H_0 null hypothesis that the standard deviations are the same. The value of test statistic in this case is 3.12 $*10^{-6}$. Here, the critical value for the significance level $\alpha = 0.05$ is 0.38. We accept H_0 null hypothesis if the test statistic value is lower than the critical value. The results clearly indicate that we can consider the deviations as the same, so the sphericity was fulfilled.

Because of the damage to normality, we applied variance analysis referring to robustness. The null hypothesis of the variance analysis is same as the null hypothesis of the Friedman-probe, but in this case the test conditions are stricter. So, due to the conditions, this null hypothesis is actually equivalent to the correspondence of the expected values. If these conditions - normality and sphericity - are fulfilled only the expected values should correspond to distributions. The test statistic in our case was 63.66 for related samples. The critical value for the significance level $\alpha = 0,05$ is 2,766. Since the test statistic is also much higher than the critical value, we reject the null hypothesis again, distribution of our samples is different. The test confirmed the previous finding that the direct cleaning process prior to milling has an effect on reducing the DON-toxin content of the raw material. So both statistical analysis show that the distribution of DON-toxin levels varies during selecting and cleaning, and based on variance analysis, we can say that the average value of this level has changed.

Then we were wondering if there was any difference in efficiency between the two cleaning processes. For this we have tested the sample pairs. In this case we also followed the principle that we tested the data with both the statistical methods assuming normality and statistical methods that do not require normality.

Wilcoxon's Signal rank-probe can be used independently of normality. Its condition is symmetry which was determined by the Pearson index. The index for difference samples derived from sample-pairs are as follows:

V_1 and V_2 difference sample	-0,63
V_4 and V_5 difference sample	0,12
V_1 and V_5 difference sample	0,55

If this skew indicator number is in absolute value greater than 1, then we are talking about a strong asymmetry of distribution, otherwise the distribution is considered almost symmetric. This means that symmetry can be assumed for all three samples, so the test was applicable. The null hypothesis of Wilcoxon's sign-on rank-test is that the distributions are the same. The statistic values and the critical value of the test are as follows:

V_1 and V_2 difference sample	3,92	
V_4 and V_5 difference sample	3,92	critical value α=0,05: 1,64
V_1 and V_5 difference sample	3,92	

Since the test statistic value is greater than the critical value, therefore we reject the null hypothesis, thus statistically it can be demonstrated that DON-toxin concentration decreased for each sample pair. Hereinafter we used even t-test supposing normality. The H_0 null hypothesis of the even t-test is that the mean of the difference sample formed from two samples is zero. The test statistic values and critical value are as follows:

V_1 and V_2 difference sample	8,46	
V_4 and V_5 difference sample	6,01	critical value α=0,05: 1,73
V_1 and V_5 difference sample	11,29	

As the test statistic values are higher than the critical value, we also rejected the null hypothesis, which means that all three sample pairs cause change. That is to say, with the even t-test we could prove the efficiency of cleaning of the two machines to reduce the concentration of DON-toxin in wheat crops.

Finally, we've been looking for the answer whether the decrease of DON-toxin level of the raw material can be deduced from the knowing the starting value. The practical significance of this is that the mixing rates of known toxin-contaminated lots can be determined by milling experts in such a way so that the mixture can not cause a food safety problem. In the case of each sample pair regression analysis was used to estimate the rate of reduction of DON-toxin level examining the color sorting separately, then after the surface cleaning and the combined effect of sorting and cleaning. First we determined the regression analysis of the samples taken before and after the Sortex color sorting. The equation of the line that matches the V_1 and V_2 pairs:

$$y=-0,04+0,96x,$$

The function demonstrates that the output DON-toxin level can be estimated based on the initial toxin content by taking its 0.96 portion and then reducing the resulting value by 0.04. The explanatory value of the model is $r^2 = 0,98$, which means what proportion of variance we can give of the variable y with the estimated value y, that is with the model. The standard error of the match is 0.04. The practical expert so exactly can determine to what extent the cleaning process can reduce the toxin concentration of the starting raw material. The margin of error we will also get an answer how much this value can be within that range. Knowing the function by mixing the wheat lots, the starting toxin level can be set precisely which makes it possible to produce a safe end product even in the most infected years.

We have also done the regression analysis for samples taken at the Schule machine. The equation of the line that matches the V_4 and V_5 pairs:

$$y=0,76x,$$

The output DON-toxin level can also be calculated based on the function. The explanatory value of the model is $r^2= 0,91$. Standard error of matching 0,06.

We examined the results of the joint operation of the color sorting and the surface cleaner machines. To this we have determined the equation the line that matches the V_1 and V_5 pairs:

$$y=-0,07+0,76x,$$

The explanatory value of the model is $r^2= 0,93$. Standard error of matching 0,04. In accordance with the description detailed above for the V_1 and V_2 sample pairs, in order to minimize losses and achieve maximum yield, milling experts can estimate the DON-toxin content after cleaning of wheat items based on these values.

4. Conclusions

Summing it up it can be stated that by statistical analysis of the sample pairs we have proved that using the Sortex and Schule machines the DON-toxin level decreased as a result of the cleaning process. When comparing the three regression functions, it can be seen that in this year the Schule machine could produce a greater proportion of the decrease in DON-toxin levels and, in essence, resulted in a total decrease. All this means that our research goal is fulfilled. It is verifiable that with the use of modern equipment we can achieve a significant reduction in the level of toxin in the mill processing technology, which is also indicated by r values. This is extremely important in rainy and heavily fusarium infected years. Due to the experimental results, we can minimize serious economic damage, since by using the calculations described above the mixing ratios can be set appropriately and it may also be possible to use wheat crops that were previously considered to be higher risk and excluded from production. We also presented a basis for milling experts who can determine, optimize the mixing rate of wheat lots and can plan the purchasing even more deliberately. The results of the regression analysis can be used to estimate the toxin level of wheat to be milled based on the DON-toxin content of the starting lot.

Other side approaching this issue, the use of the results is also important for the health protection of the population. It is necessary to encourage the milling enterprises to develop technology and to apply modern equipment in the production process in order to keep the toxin contamination as low as possible even in wheat crops within the allowable limit. As wheat flour is a raw material of basic foodstuffs, this is of great importance for the health protection of the population.

References

[1] **Muthomi, J.W., Musyimi, S. L., Wagacha, J.M., Narla, R. D.** (2012): Occurrence of Fusarium species and associated T2-toxin in Kenyan wheat. Agric. Sci. 3. 24-34.

[2] **Njeru, N.K., Muthomi, J.W., Mutegi C.K., Wagacha, J.M.** (2016): Effect of Cropping Systems on Accumulation of Fusarium Head Blight of Wheat Inocula in Crop Residues and Soils. Journal of Plant Sciences 11: (1-3) 12-21. ISSN 1816-4951, DOI: 10.3923/jps.2016.12.21
[3] **Lipps, P. E.** (2002): Head blight or scab of small grains. Word Mycotoxin J. 4. 429-435.
[4] **Szabó Hevér, Á**. (2013): A kalászfuzárium rezisztencia molekuláris hátterének vizsgálata frontana eredetű térképező búzapopulációkban. Doktori értekezés, Gödöllő. 141.
[5] **Kovács, F. Bíró, G.** (2002): Élelmiszerbiztonság az EU szabályozás tükrében. Agroinform Kiadó. Budapest. 242.
[6] **Echling, G., Cockburn, A., Snowdown, P., Buschhaus, H.** (1997): The significance of the Fusarium toxin deoxinivalenol (DON) for human and animal helth. Cereal Research Communications (25) 3, Proceedings of the 5TH European Fusarium Seminar Szeged, Hungary 527-532.
[7] **Deák, T.**, (szerk.) (2011): Élelmiszer-mikrobiológia. Mezőgazdasági Kiadó. 382. p
[8] **Commission Regulation (EC) No 1881/2006** of 19 December 2006 setting maximum levels for certain contaminants in foodstuffs, Official Journal of the European Union https://eur-lex.europa.eu/legal-content/EN/TXT/PDF/?uri=CELEX:32006R1881&qid=1642087533401&from=HU
[9] **Sohár, P-Né**. (2007): Mikotoxinok az élelmiszerláncban. Élelmiszervizsgálati közlemények. Különszám. 53. 60-68.
[10] **Mézes, M.** (2009): Takarmánytoxikológia. Egyetemi jegyzet, Gödöllő. 99.
[11] **Veres, E. – Borbély, M.** (2007): Az őszi búza felhasználhatósága a vizuális és mikrobiológiai Fusarium fertőzöttség-, valamint a toxin vizsgálatok alapján. Agrártudományi közlemények. (12) 26-34.
[12] **Szeitzné Szabó M**. (szerk.) (2009): Gabonaalapú élelmiszerek fuzárium toxin szennyezettségének csökkentési lehetőségei. Magyar Élelmiszerbiztonsági Hivatal, Budapest, 33.
[13] **Commission Regulation (EC) No 2006/583** of 17 August on the prevention and reduction of Fusarium toxins in cereals and cereal products, Official Journal of the European Union https://eur-lex.europa.eu/legal-content/EN/TXT/PDF/?uri=CELEX:32006H0583&qid=1642087354928&from=EN
[14] **Sándor M., Győri Z., Sípos P.** (2010): Malomipari lehetőségek értékelése az őszi búza mikotoxin szennyezettségének csökkentésében. Élelmiszer Tudomány Technológia. LXIV. (2) 4-9.
[15] **Frank P.** (2010): Technológiai kísérletek a búza fuzárium toxin szennyezettségének csökkentésére. Élelmiszer Tudomány Technológia LXIV. (2) különszám. 16-20.
[16] **Kihlberg, I., Johansson, L., Kohler, A., Risvik, E.** (2004): Sensory qualities of whole wheat pan bread – influence of farming system, milling, and baking technique. J. Cereal Sci. 39, 67-84.
[17] **Inamdar, A. A., Suresh, D. S**. (2014): Application of color sorter in wheat milling. International Food Research Journal 21(6) 2083-2089.
[18] **Dowell, F.E., Boratynski, T.N., Ykema, R.E., Dowdy, A.K. Staten, R.T.** (2002): Use of optical sorting to detect wheat kernels infected with Tilletia indica. Plant Disease (86) 9., 1011-1013.
[19] **Szabó P. B. - Véha A.** (2015): Sütőipari, malomipari technológia gyakorlatok. Gyakorlati tananyag. TÁMOP-4.1.1.F-14/1/KONV-2015-0009. 124
[20] **Gőcze, I.** (2010): A tudományelmélet és kutatásmódszertana alapjai. A tudományos kutatás és publikálás. Tanulmány. Budapest: ZMNE. 108.
[21] **Kolmogorov, A.** (1933): Sulla determinazione empirica di una legge di distribuzione. Giornale del Istituto Italiano degli Attuari, 4., 83-91.
[22] **Stephens, M., A.** (1974): Edf statistics for goodness of t and some comparisons. Journal of the American Statistical Association, 69. 730-737.
[23] **Shapiro, S., Wilk, M**. (1965): An analysis of variance test for normality (complete samples). Biometrika, 52. 591-611.
[24] **Mauchly, John W.** (1940): Significance Test for Sphericity of a Normal n-Variate Distribution. Ann. Math. Statist. (11) 2.,
[25] **Fidy J., Makara G.** (2005): Biostatisztika. Informed 2000 Kft. http://www.tankonyvtar.hu/hu/tartalom/tkt/biostatisztika-1/ch11s03.html
[26] **Reiczigel, J., Harnos, A., Solymosi, N**. (2014): Biostatisztika. Nem statisztikusoknak. Pars Kft. Nagykovácsi. 462.

HUNGARIAN AGRICULTURAL ENGINEERING
No 41/2022 87-93
Published online: http://hae-journals.org/
HU ISSN 0864-7410 (Print)
HU ISSN 2415-9751(Online)
DOI: 10.17676/HAE.2022.41.87
Received: 01.09.2022 - Accepted: 25.09.2022

PERIODICAL
OF THE COMMITTEE OF AGRICULTURAL AND BIOSYSTEM ENGINEERING OF THE HUNGARIAN ACADEMY OF SCIENCES
and
HUNGARIAN UNIVERSITY OF AGRICULTURE
AND LIFE SCIENCES
INSTITUTE OF TECHNOLOGY

DESIGN OF POSITIONING EQUIPMENT FOR WELDING GAS PIPES OF DIFFERENT DIAMETERS

Author(s):
Z. Szakal[1], I. Oldal [1], L. Zsidai[1]

Affiliation:
[1] Institute of Technology - Hungarian University of Agriculture and Life Sciences, 2100 Gödöllő, Páter Károly u. 1., Hungary;

Email address:
szakal.zoltan@uni-mate.hu; oldal.istvan@uni-mate.hu; zsidai.laszlo@uni-mate.hu

Abstract: The research involved the design of pipe positioning equipment for the repair of natural gas and oil pipelines. This paper presents the research results of the design of the hydraulic pipe positioning and straightening device and its practical implementation. Several concept calculations and design analyses were carried out during the design. The final design and layout was selected from several possible solutions.

Keywords: natural oil, natural gas, welding, positioning, hydraulic system

1. Introduction

We are designing a gripping device to replace damage to natural gas pipelines due to natural failure. A natural gas pipeline is a steel pipe placed at a depth appropriate to the soil conditions [1]. The failure of the steel pipes used can be caused by three main factors: corrosion, mechanical action, and soil movement [2]. Steel pipes are elastic, and over the years the subsidence of the soil can cause stresses in the pipe [3, 4]. Ageing and thermal expansion of the pipes also cause difficulties in cutting and welding [5]. When cutting tubes, previously stored stresses are released and the tube will snap during cutting [6]. Steel tubes are made of carbon steel [7], so welding is not a problem [8, 9], but the deviation of the joined tube ends should be less than 0.5mm [10]. Various pipe positioning devices are available on the market, and their design can be either internally or externally fixed [11]. In the present work, we plan to design an externally fixed structure, as it is required to be applied in the field. In the soil the pipes deform, for welding deformation must be compensated, the deviation from circularity of the pipe must be less than 0.5mm. Precision cutting equipment that cannot be attached to commercially available pipe positioning devices is only a diamond wire saw [12] or a pipe saw [13]. Pipe gripping devices can be single-arm or double-arm per side [14], but the double-arm design results in a more stable grip and provides more options for positioning [15]. The pipe positioning device we have designed can be used for pipes with diameters of 500-750mm, which are common in the industry.

The structure designed in the project shall be capable of correcting any deformation of the joint surfaces of the pipeline sections joined during the repair.

In field work, the time window available is limited by weather and process time, but this should not be at the expense of quality parameters. The quality factor is a particularly strong constraint, as in a project it is no longer possible to allow for a time margin where several hours of pipe section straightening or re-cutting and the re-design of the weld ends are required. In addition, in many cases these will hold up further work on the pipelines.

Factors to be considered when designing a pipe positioning device with regard to the design of the gripping structure:

- the pipe positioning device must hold the two pipe sections to be welded together in the correct position, so the gripping structure must be robust,
- the right and left pipe clamps should be connected by a common rigid bridge,
- the design of the bridge should take into account the space requirements for additional equipment,

- the bridge structure should be designed to allow the safe installation of hydraulic and electronic lines,
- provide a stable grip up to a pipe diameter of 300 - 650 mm,
- adjustable prismatic top supports should be provided for pipes of different sizes to facilitate installation,
- the gripping device should be openable and releasable,
- when the grips are in the closed position, mechanical locking should be used to prevent any possible pipe bounce,
- the mechanical safety lock should be fitted with an electronic signalling and electrical locking system,
- dual-acting hydraulic cylinders should be used,
- work rollers should be fitted with anti-fall devices,
- the structure must be capable of being lifted, so it should be equipped with lifting points.

2. The concept

The different concepts for the hydraulic unit for the positioning of the pipe ends were developed after several rounds of discussions. During the discussions the following designs were reviewed.

Possibilities of pipe gripping in terms of force application:
- manually driven, spindle design,
- hydraulically operated belt clamp,
- with circularly arranged hydraulic work rollers.

In terms of force application to eliminate tube deformation, the structure can be:
- wedge spindle design,
- wedge type, with direct hydraulic movement,
- wedge design, with indirect hydraulic movement,
- with radially mounted hydraulic cylinders,
- axially mounted hydraulic cylinders and a lifting device.

In terms of power supply, the structure can be:
- a structure with its own hydraulic system from an external power source,
- a structure with its own hydraulic system powered by a diesel engine,
- a structure connected to the hydraulic system of an implement,
- hybrid system (electrohydraulic drive),

Opening-closing of the structure in terms of design of the structure can be:
- self-steering,
- with its own hydraulic actuator,
- mechanical spindle design,
- a system with a self-locking mechanism,
- a hybrid system (hydraulically operated with gravity control).

2.1. Planning

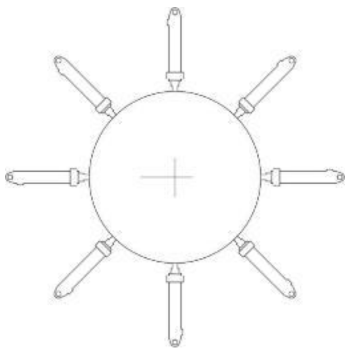

Figure 1. Fingers for pipe positioning and pipe repair

From the literature review and analysis of the tools available on the market, it was found that hydraulic working cylinders are the most commonly used to repair potential circular defects in gas and oil pipelines. These cylinders are directly connected to the section of pipe under investigation. Hydraulic cylinders are attached to a stable and rigid belt section with a centre line of axis coinciding with the theoretical centre line of the complex pipe repair structure to be designed. The hydraulic work rollers are stably bolted to the belt section, and the length of the stems of the work rollers is designed to accommodate the dimensions of the gas and oil pipelines in Hungary (300 -600 mm) as specified in the project. The theoretical design agreed in the joint discussions is illustrated in the Figure 1.

The structure consists of a laser-cut, bolted and welded belt of 20-thick boiler plate, hydraulic working cylinders, piping and valves.

2.1.1. The device and its parts

Figures 2., and 3. show the most important parts of the device.

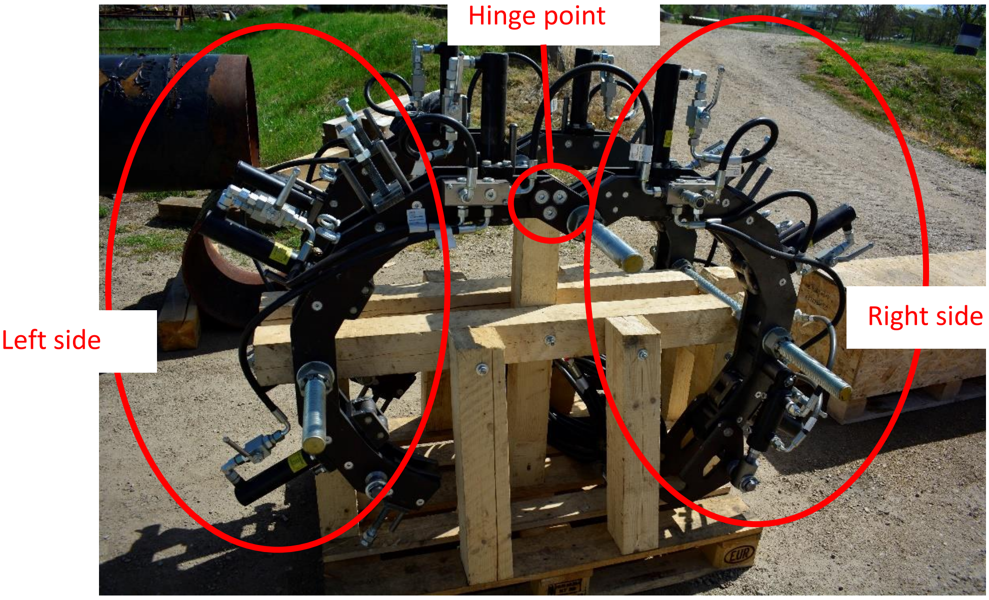

Figure 2. Front view of the structure with 6 hydraulic cylinders

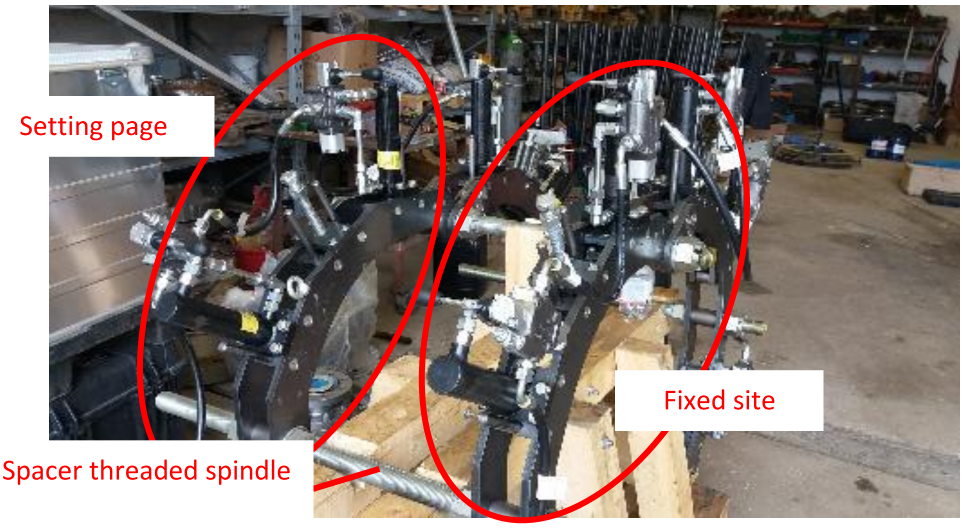

Figure 3. Side view of the pipe clamp positioner

2.2. Positioning of the pipe clamping rollers

Different pipe diameters also have different circumferences, so the device should be designed for the smallest and largest pipes still in use. Due to the varying circumferences of the pipe sizes, the distances between the working cylinder connections also vary. In the case of smaller tubes, the working cylinder stems are closer together, so that they can do a better job of improving circularity. When repairing larger diameter pipes, the attachment points of the working cylinder stems fall further apart, so the pipe shape may be statistically closer to the theoretical circle during the work, but it will be a polygon. To solve this problem, two things can be done, one is to increase the supporting surface by fitting a slipper on the stems of the working rollers to match the pipe size, the other is to increase the number of working rollers.

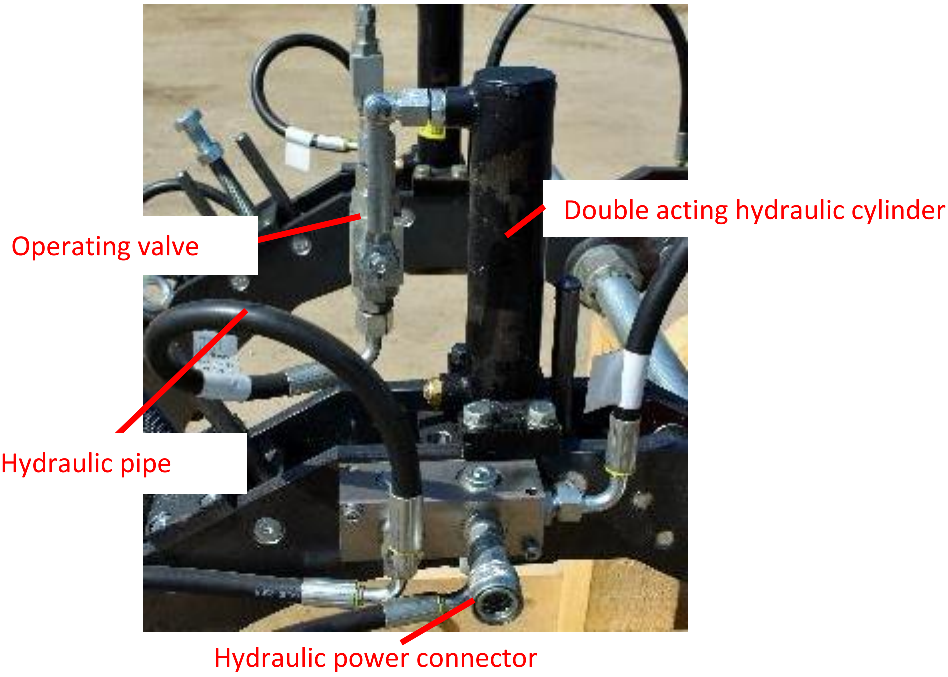

Figure 4. Positioning the hydraulic cylinder on the belt section

The double-acting working rollers are bolted to the belt section and connected by flexible piping for flexible operation. 2 hydraulic quick couplings are mounted on the belt section to ensure the hydraulic fluid inlet and outlet. Figure 4. shows the hydraulic system on the device.

2.3. Connection of hydraulic power cylinders to tubes

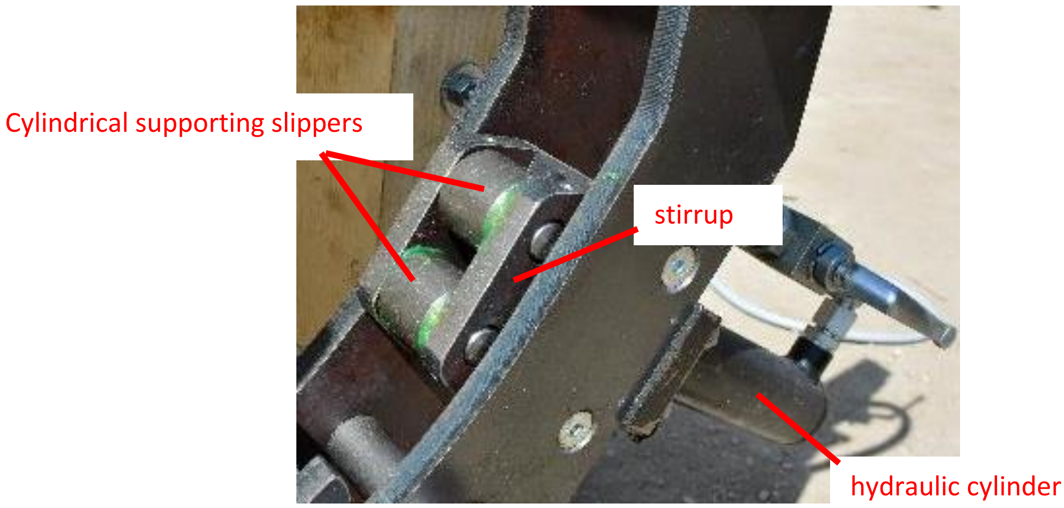

Figure 5. Cylindrical slippers mounted on the end of the working cylinder

The pipe positioning and straightening structure designed for this work is intended to cover a significant size range of gas and oil pipelines in use in Hungary, so the end-mounted slippers on the work rollers are designed to be roller-mounted, which is well suited to the pipe sizes in use.

A "U" shaped stirrup is threadedly attached to the shank of the working cylinder, which holds the cylindrical support shoes on pins. The cylindrical pins allow the support shoes to rotate, which helps in any possible device adjustment. The Figure 5. illustrates the cylindrical support cylinders.

3. Disassembly of the appliance installation on the gas pipe

The part of the belt to be fitted to the section of pipe to be repaired, containing the working rollers, shall be designed to be openable. The structure shall be provided with a sliding pin to allow opening. The hinge point is a threaded stem of size M24 (Figure 6.), on which a bushing is mounted and held in place by two crown nuts. The hydraulic circuit used to power the hydraulic working cylinders on both sides is connected by rubber bushings for opening. The Figure 7. shows the device in the open state.

Figure 6. The pipe positioning and pipe shapes repair structure hinge point

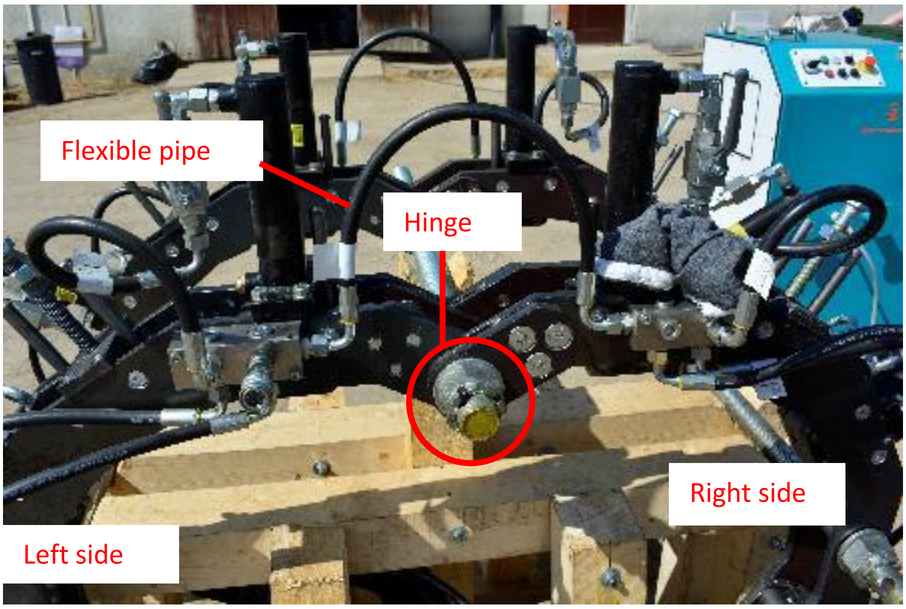

Figure 7. The pipe positioning and pipe repair structure in the open position

The structure of the weight load brakes open and close. It opens automatically when the structure is lifted by gripping the right and left sides of the structure via a lanyard and closes when the structure is placed on the tube.

Figure 8. Installing the pipe positioning device

4. Conclusions

In the course of the work a complex field pipe cutting, gripping and positioning structure was developed, as part of which a hydraulic pipe gripping, positioning and straightening device was designed. Based on the literature research and market demand analysis, a construction design was formulated to be implemented in the POC phase of the project. The Figure 8. shows when the device was tested in practice. During the research, a number of solutions were investigated for positioning pipe ends for welding during the repair of gas and oil pipelines, and for the correct geometry (root voids and circularity). During the research, it became clear that the working conditions (mud, temperature, time to repair) of the repairs were to be considered in order to design a structure that was as simple and robust as possible.

The research led to the production of a structure capable of:

- hold the pipe to be cut firmly,
- to hold the complex system in a central position on the pipeline,
- adjust the circularity of the pipe section if it is defective,
- it is capable of holding the required root gap in a stable manner.

The hydraulic pipe gripping, positioning and straightening device consists of two belt sections whose distance can be adjusted by means of threaded spindles. On the belt sections are mounted the hydraulic working cylinders, which have a double function, on the one hand to position the complex device centrally and on the other hand to repair the pipe end, which may have been damaged in terms of circularity, to the correct shape. The hydraulic working cylinders are connected to a stable and rigid belt section with an axial centre line coinciding with the theoretical centre line of the complex pipe repair device. The hydraulic work rollers are stably bolted to the belt section, and the length of the stems of the work rollers is designed to accommodate the dimensions of the gas and oil pipelines in Hungary (300 -600 mm) as specified in the project.

Acknowledgements

The research was funded by the project "Development of mobile mechatronic industrial applications using laser and structural stress measurement technologies" and "KFI 16-1-2017-0216".

References

[1] **Liang Guangchuan, Yu Yuhang, Peng Xingyu** (2016): Standardized surface engineering design of shale gas reservoirs, Natural Gas Industry B 3 (2016) 90e98

[2] **Folga S. M.** (2017): Natural Gas Pipeline Technology overview; Decision and Information Sciences Division Argonne National Laboratpry 2007 november

[3] **Richard P, Fuerest P. E.** (2013): Methode for Predictionof flexible Pipe Deflection, Bureau of reclmation M-25 Second Edition, 12. 18.

[4] **Daniel Vasilikis, Spyros A. Karamanos** (2012): Mechanical behavior and wrinkling of lined pipes;

International Journal of Solids and Structures 49. 3432–3446

[5] **Schmidt L.C., Lu J. P. and Morgan P.R.** (1989): The Influence on steel tubular strut load capacity of strain aging and Bauschinger effect. Journal of Construction Steel Research, Vol.14, No2 pp.107-119,

[6] **Hilberink, A., Gresnigt, A. M., Sluys, L. J.** (2011): Mechanical behavior of lined pipe during bending, numerical and experimental results compared. In: Proceedings of International Conference on Ocean, Offshore and Arctic Engineering (OMAE), Rotterdam, The Netherlands.

[7] **EN 10204 Metallic products** (2004): Types of inspection documents 10.p.

[8] **ISO 3690 Welding** (2012); Determination of hydrogen in deposited weld metal arising from the use of covered electrodes for welding mild and low alloy steels, 23.p.

[9] **EN 719 Welding coordination** (2006): Task and responsibilities 8.p.

[10] **Sánchez Sánchez Héctor, Cortés Salas Carlos** (2008): Deformation of Steel Pipes with Internal Pressure Under Axial Compression and Bending Load Under Seismic Action; The 14thWorld Conference on Earthquake Engineering October 12-17, 2008, Beijing, China

[11] **Wang Liquan at. al.** (2016): Research and development of a self-centering clamping device for deep-water multifunctional pipeline repair machinery; Natural Gas Industry B 3 (2016) 82-89

[12] **Zhang Yongrui, Wang Liquan, Yang Yang, Zhang Lan** (2015): Experiment on cutting efficiency of diamond wire saw in Seabed oil pipes. J Harbin Eng Univ;36(1):119e22.

[13] **Gong Haixia, Zhao Jie, Zhang Lan, Li Peng** (2009): Design of hydraulic pressure guillotine pipe saw. Mach Tool Hydraul;37(3):71e2.

[14] **Wang Liquan, Dong Jinbo, Zhang Lan (**2012): Design of facilities for deep sea pipeline connection. Nat Gas Ind; 32(4):75e8

[15] **Wang Liquan, Dong Jinbo, Zhang Lan, Wang Chunbo** (2012): Design and simulation of deep-sea pipeline axial force and alignment tool. J Harbin Eng Univ; 33(10):1295e9.

CONTENT OF No 41/2022

CONTENT OF No 41/2022